Development of Drop-on-Demand Sample Injection System by Inkjet technology and Its Application to Analytical Chemistry

Fengming Chen

September, 2013

Tokyo Metropolitan University

Contents

Chapter 1

Introduction

1.1 Introduction of inkjet technology

Inkjet technology that can precisely control specific velocity and volume at defined microarray spots. It is also a power tool has the ability of generating pico-liter levels of liquid on the surface of a wide variety of substrates.

Inkjet printing technology is one of the most important forms of information transfer and expression method since it has many advantages such as environmentally friendly process and low-cost manufacturing [1-2]. Inkjet printing technology has been widely utilized in word processing as in personal computers in the workplace home or office printing operations. In the age of information, information is mainly presented and passed through the graphics and characters. The development of inkjet technology started off in the late 1950s. Since then, many inkjet devices have seen the light of today and the technology has been implemented in many different designs and the technology has been widely used of potential applications [3-19]. Nowadays, the commercial inkjet printer has been widely used and played an essential role especially in the printing manufacture areas. At the same time, as the development of micro-fabrication technology, scientists noticed that inkjet technology was an ideal method for micro-scale machining. When we used inkjet technology to fabricate devices, the design was very simple and visual, and the method has the advantages of easy operation and high resolution.

1.2 Inkjet Printing Process

1.2.1 Continuous inkjet technology and drop-on-demand inkjet printing

Fundamentally, there are two different mechanisms by which inkjet printers generate droplets, namely continuous inkjet (CIJ) and the drop-on-demand (DOD) inkjet methods [20-21]. The main development towards modern inkjet printing technology concepts is shown in Figure 1.

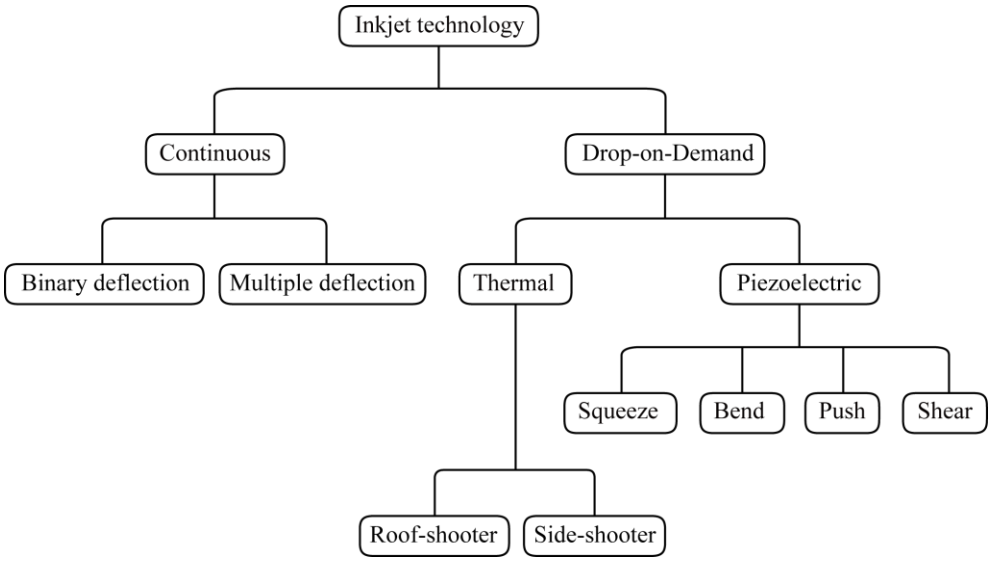

Figure 1. Classification of the inkjet printing technologies [20].

Both methods of droplet generation can produce fluid droplets with diameters in the range of 10 to 150 μm. CIJ printing is used mostly for coding and marking applications with a droplet diameter of approximately 100 μm; DOD printing is dominant in graphics and text printing with a smaller drop diameter, typically 20–50 μm. The DOD inkjet method included two types: bubble-jet technology and piezoelectric inkjet technology were shown in Figure 2 [22].

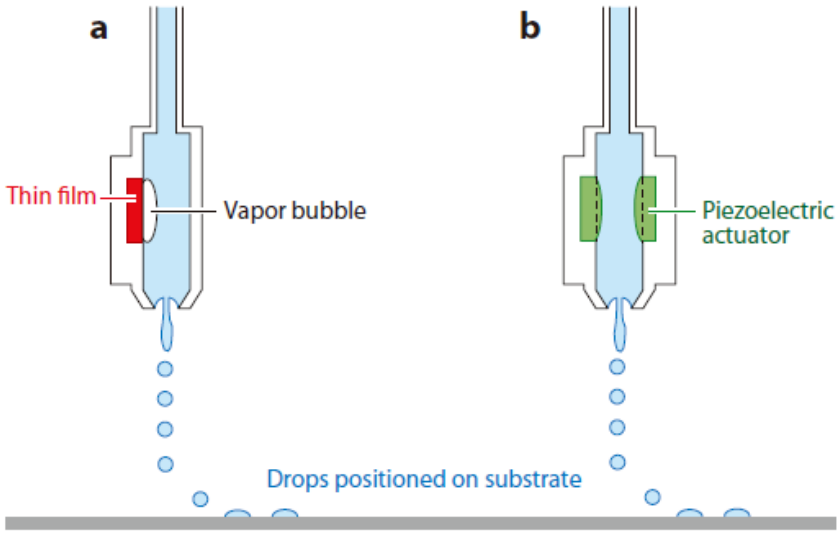

Figure 2. bubble-jet technology and piezoelectric inkjet technology [22].

Continuous inkjet printing technology emerged in the 1960s [23]. In CIJ printing, a small droplet jet from a small nozzle through pressure wave. The droplet jet could be break-off into uniform size and spacing were described mathematically by vibrating the ink within the nozzle cavity at a fixed ultrasonic frequency through Lord Rayleigh for inviscous jets [24], and Weber for viscous and surface tension jets of diameter perturbations [25]. The droplet formation can be controlled by the droplet deflection methodology. The continuous inkjet can be designed as a binary or multiple deflection system.

In a binary deflection system, conductive ink forms a small droplet jet from a small nozzle through pressure wave. A droplet breaks off from the jet in the presence of a varying electric field [26]. And thus the droplets could be charged selectively and are either charged or unchanged as they emerged out of the continuous jet. The charged electrode droplets are allowed to deflect towards several positions when passing through an electric field applied onto the high voltage deflection plate, while the uncharged droplets were captured by the gutter and re-circulated in the system, continuous inkjet system is shown in Figure 3.

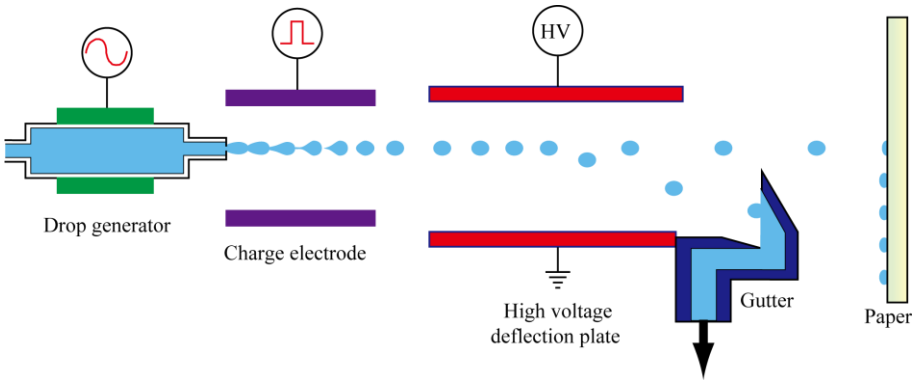

Figure 3. Continuous ink-jet: A binary-deflection system

In a multiple defelction system shown in Figure 4 [27], the stream of drops passes through an electrostatic field formed by a fixed high voltage across a pair of horizontal deflection plates. Because the charge on each drop is controlled individually, a droplet can be deflected vertically a desired amount. The droplets are

charged and deflected to the media at different levels, the uncharged droplets fly straight to a gutter to be recirculated.

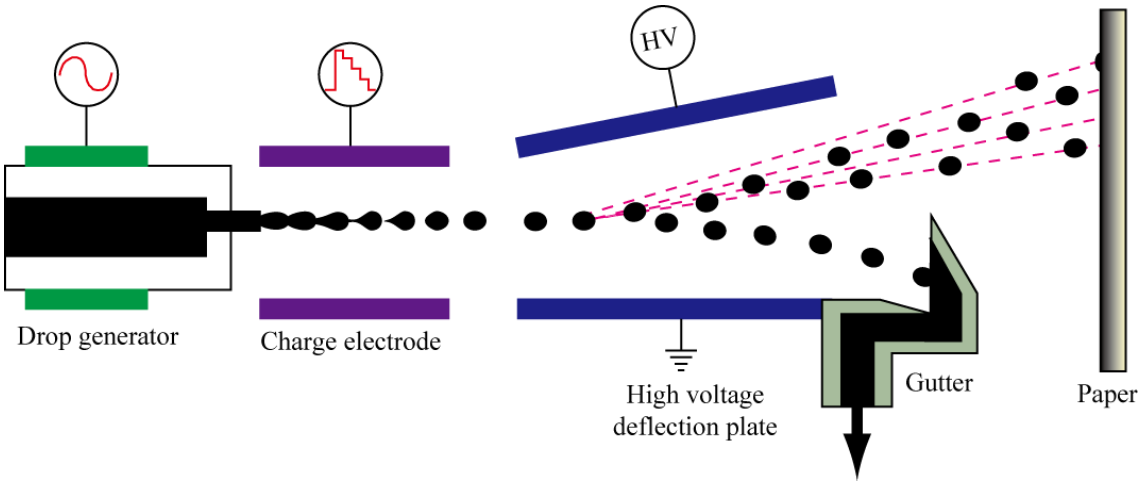

Figure 4. Continuous ink-jet: A multiple-deflection system.

Instead of continuously inkjet printing， Drop-on-Demand inkjet technology produces droplets only when an actuation pulse is provided and a small liquid droplet is ejected from a nozzle and dispensed onto a substrate at desired locations by the additive process. Major advantages of DOD printers over continuously inkjet printers include the fact that there is no need for a charge electrodes, high voltage deflection plate, guttering, and recirculation systems. The majority of activity in inkjet printing today is in the DOD methods. Depending on the mechanism used in the droplet formation process, the technology can be categorized into four major methods: thermal, piezoelectric, electrostatic, and acoustic inkjet. Most, if not all, of the DOD inkjet printers on the market today are based on thermal inkjet printing (also known as bubble-jet technology) and based on piezoelectric inkjet printing according to the two different ways in which ink were forced from the printer nozzle used.

The working principle of thermal inkjet technology is based on the generation of vapor bubbles by heating the liquid, as vapor bubbles expand, the liquid is pushed away and droplet was ejected in a perpendicular direction away from the evaporating bubble from the nozzle (shown in Figure 5).

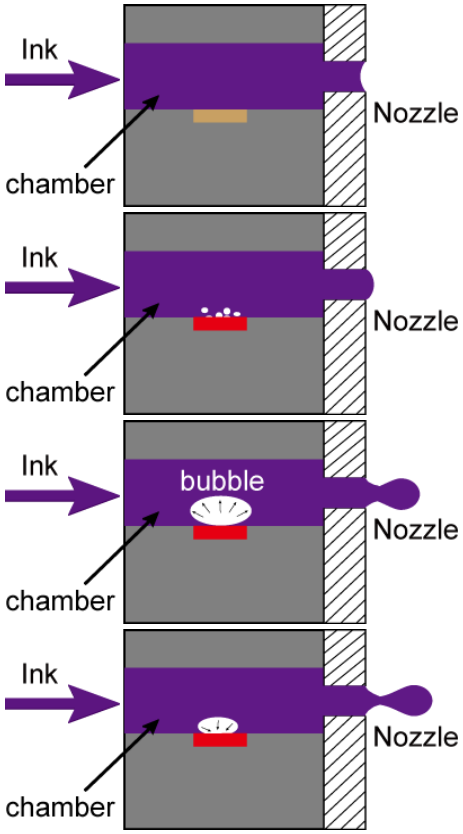

Figure 5. The side-shooter of thermal inkjet printing

Because of the heating required and the difficulty in aspiration, the thermal inkjet mode is not suitable in many applications such as high throughput biomedical screening. Piezoelectric inkjet technology is favored over thermal printing as it does not need the high temperatures required for thermal printing (200–300℃), which can potentially lead to thermal degradation of the ink, particularly when it contains materials such as organics or biological materials [28-31]. In piezoelectric inkjet printing, piezoceramic material changes its shapes under electronic pulses, which causes ink chamber volume change generating a pressure wave that propagates toward the nozzle. This pressure wave overcomes the viscous pressure loss in a small nozzle and the surface tension pressure rises from ink meniscus so that an ink droplet can begin to form at the nozzle [3, 32]. The basic pressure requirement is shown in Figure 6. According the piezoelectric deformation mode [33], the technology can be categorized into four main types: squeeze, bend, push, and shear. But the mostly

popular piezoelectric deformation technology is bend mode.

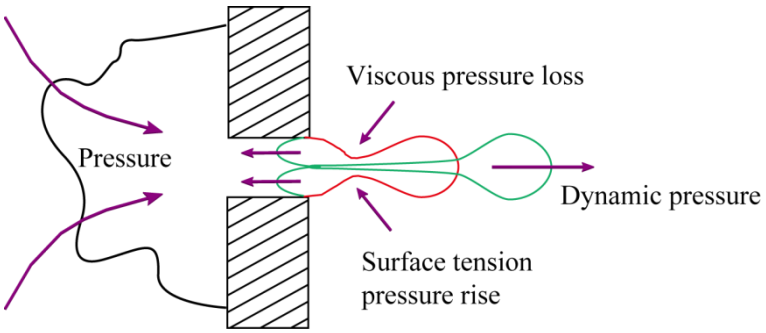

Figure 6. The basic pressure requirement for ejecting an inkjet droplet [11].

In a typical bend-mode design (shown in Figure 7), the piezoelectric plate is bonded to the diaphragm (for example: ITO glass) electromechanical transducers, forming the ink chamber that is used to eject the ink droplets. Therefore, when a driving voltage is applied to the piezoelectric material, the ink chamber is deformed and a droplet is forced out of the nozzle. When a driving voltage is applied to the piezoelectric material, the piezoelectric ceramic changes its shapes due to piezoelectric effect. The deformation of piezoelectric ceramics presses the ink chamber and a droplet is forced out of the nozzle.

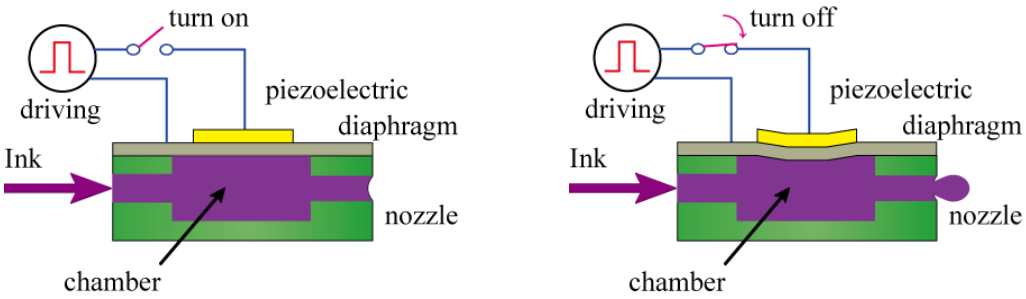

Figure 7. DOD System: A bend-mode piezoelectric inkjet technology.

1.2.2 Printable Fluids

The generation of droplets in a DOD printer is a very complex process [34] and numerous reviews have discussed this issue in details [33-37]. Hence, I briefly describe some basic and important criteria for printable fluids. The behavior of

liquid droplets can be characterized by a number of dimensionless physical constants, including Reynolds (Re), Weber (We) and Ohnesorge (Oh) numbers:

$$\mathrm{Re} = {va\rho}/{\eta}$$

$$We = {v^2 a\rho}/{\gamma}$$

$$Oh = \frac{\sqrt{We}}{\mathrm{Re}} = \frac{\eta}{\sqrt{d\rho\gamma}}$$

Where ρ, η, γ are the density, dynamic viscosity and surface tension of the fluid respectively, *v* is the velocity of the droplet, and *a* is a characteristic length.

Fromm firstly proposed that the Ohnesorge number (Oh), can be used to characterize droplet formation [38]. The parameter Z, which is defined as 1/Oh, is proposed that Z>2 are the preconditions for stable droplet generation. Reis and Derby further propose the following range, 10>Z>1, for stable droplet formation with numerical simulation of drop formation [39]. The fluid/air surface tension at the nozzle is also a limiting factor for droplet generation. A droplet must have sufficient energy to overcome this barrier for ejection. Duineveld et.al suggested that a minimum velocity for droplet ejection can be calculated as follows [40];

$$V_{\min} = \left(\frac{4\gamma}{\rho d_{\mathrm{n}}} \right)^{1/2}$$

Where d_n is the nozzle diameter.

Finally, for the stable deposition of droplets onto the substrate, we should also consider the impact of the ejected droplets on a substrate. Basically, the droplet should not be splashed when the impact on the substrate. Stow & Hadfield firstly proposed that the threshold for the onset of splashing can be calculated by following equations [41]:

$$We^{1/2}\mathrm{Re}^{1/4} \geq \mathrm{f}(R)$$

Where *f(R)* is a function of surface roughness and for a typical flat, smooth surface, *f(R)* ≈ 50 [42]. Through the above equations and the limiting values of Z, it is possible to construct a map in a parameter space, with coordinates Re and We, that can be used

to define fluid properties that are unable in DOD inkjet system, as shown in Figure 8 [35]. The validity of this predicted regime of printability has been explored for a large range of fluid properties with particle-filled systems, and the map offers a useful guide for fluid properties selection [43].

In the above discussion, we have assumed that the fluid behaves in a linear Newtonian manner. However, in material science when polymer solutions are usually printed, the rheological properties of such fluids can be highly nonlinear. Therefore, we need to modify the printability characteristics of a fluid displayed in Figure 8. Haskal et al. reported that for solutions of poly (p-phenylene vinylene) (PPV), the characteristic fluid tail that forms during DOD printing becomes longer and more stable [44]. Other polymer solutions also have similar behaviors, with extended and stable ligaments found with increasing polymer molecular weight and concentration. Xu et al. explored the effect of concentration and molecular weight on printed drop behavior and concluded that the transition from a nearly Newtonian behavior to one dominated by fluid extensional elasticity can be explained in terms of conventional models of polymer solution behavior [45]. The action of small concentrations of polymers can stabilize the tail so that it retracts into the main drop during flight through surface tension, resulting in a single drop on impact.

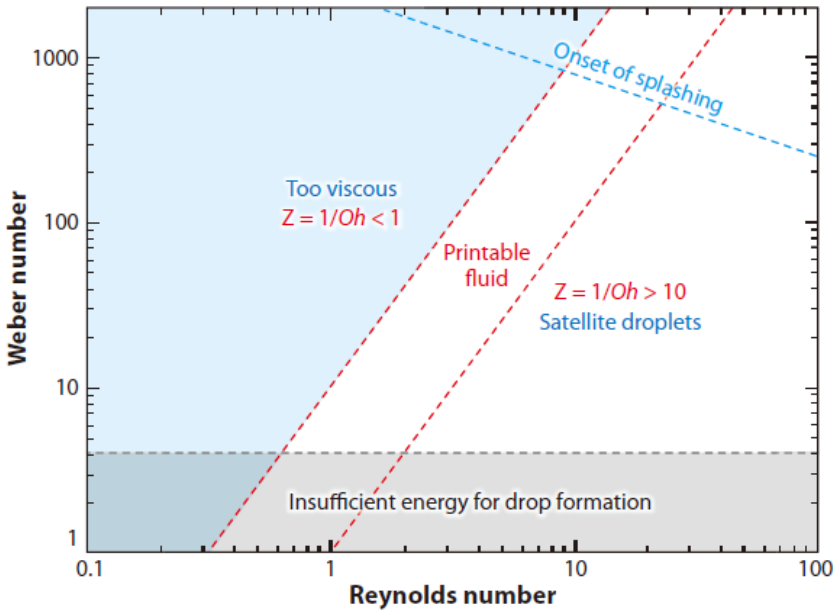

Figure 8. The map defining printable fluid with Re and We as the coordinate system.

1.3 Inkjet application

In recent years there has been considerable interest in, and use of, inkjet printing as a fabrication tool in a number of areas of technology. Inkjet printing is viewed as a versatile manufacturing tool for applications in materials fabrication. The appeal of this technology lies in its being a non-contact, additive patterning and maskless approach. Direct write attribute of inkjet printing allows for deposition of versatile thin films, the designs of which can be changed with ease from batch to batch. Other attractive features of this technology include: reduced material wastage, low cost, and scalability to large manufacturing area.

1.3.1 Applications in Material Science

Because of its ability to deposit liquid phase materials in a precisely controllable manner, inkjet technology has been widely used in various organic electronics device fabrication, such as organic thin-film transistors, light-emitting devices (LEDs), solar cells.

For material science application, a detailed study should be conducted about the droplet/substrate interaction. Kaneda et al. [46] investigated the evaporation rate of polymer solution and its effect on the thin-film shape. When the polystyrene/xylene droplets were ejected onto a lyophobic substrate, the droplets on the substrate resulted in an axisymmetric or nonaxisymmetric ring-like/dot-like film. The film configuration was dominated by the evaporation rate: the slow evaporation rate yielded a dot-like film rather than a ring-like one, and the film symmetry was governed by the local pinning time at the periphery. Lee et al. [47] investigated the characteristics of silver inkjet printing with control of surface energy and substrate temperature. In silver inkjet printing, the hydrophobic fluorocarbon film could reduce the diameter of the printed droplets. When the substrate was kept at room temperature, merging of deposited droplets was observed. Substrate heating was effective in preventing the merging phenomenon among the deposited droplets, and in reducing the width of

printed lines. The merging phenomenon of deposited droplets was also prevented by increasing the UV/O3 treatment time, accompanied by surface energy increase.

Organic thin-film transistors (OTFTs) are widely used in low-end applications, such as RFID tags [48] and display backplanes [49]. An OTFT is a four-layer device with two layers of electrode materials (source, drain and the gate) and one layer each of dielectric and active organic material. Sirringhaus et al. successfully demonstrated the use of an inkjet approach to fabricate channel lengths at sub-100 nm range, which overcomes the switching speed limitation in traditional OTFTs [50-51]. Recently, a more cost-effective approach based upon self-aligning electrodes, resulting in 100 nm channel lengths, was developed [52]. It should be noticed that these examples all use organic-based dielectric materials. Recently, carbon nanotubes have been inkjet printed as the active material for OTFTs [53]. Other inorganic species such as polysilicon [54] and zinc oxide nanoparticles [55] have also been successfully inkjet-printed as active layers in a transistor.

Inkjet printing does not require masks for manufacturing. This property makes inkjet printing a suitable technique for combinatorial studies of various devices, including organic light emitting diodes (OLEDs) [56-57]. Tekin et al. used inkjet printing to examine the influence on the emission properties of six different poly-(phenylene-ethynylene)/PPV based π-conjugated polymers with different side chains and film thicknesses in a parallel manner [58]. In addition, the same group also demonstrated the photoluminescence of inkjet printed inorganic semiconductor nanoparticles [59] (Figure 9). Singh et al. demonstrated bright inkjet printed OLEDs based on Ir-based phosphorescent macromolecules anchored on a polyhedral oligomeric silsesquioxane (POSS) molecular scaffolding [60]. Recently, Haverinen et al. demonstrated electroluminescence from inkjet printed inorganic semiconductor nanoparticles embedded between spin coated hole transport polymer and a thermally evaporated organic small molecule electron transport layer [61].

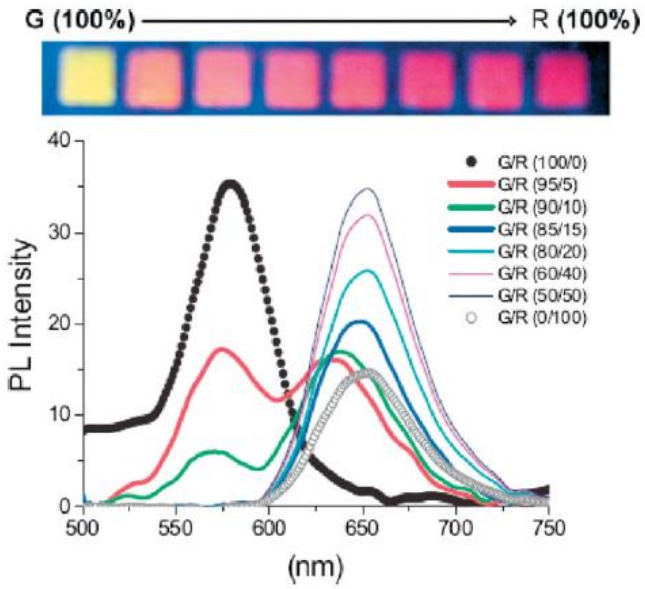

Figure 9. Combinatorial study of printed red and green nanoparticles.

Solar cells offer the promise of harnessing the solar energy. However, solar cells have not yet achieved widespread use owing to the unfavorable cost comparison against fossil fuel-based energy sources. Ever since the initial demonstration of screen printed organic solar cells, printing has been seen to offer the promise of developing industrially scalable cost effective processes [62]. Schubert and coworkers demonstrated the use of bulk heterojunction structures in inkjet printed solar cells [63-64]. Hoth et al. used a blend of P3HT and PCBM in o-dichlorobenzene and mesitylene to demonstrate inkjet printed organic solar cells with a Ca: Ag top cathode on PEDOT: PSS coated ITO [65].

1.3.2 Sensors and Detectors

Sensors play important roles in many applications. Currently, many different types of sensors have been reported to be fabricated using inkjet printing. Crowley and co-workers introduced an ammonia sensor based on amperometric detection by using inkjet printed dodecylbenzene sulfonate (DBSA) - doped PANI nanoparticles on screen printed carbon electrode [66]. Sensor response as a function of film thickness was investigated by printing one to four PANI layers. The sensitivity limit

of this sensor was studied with a variety of different concentrations of ammonium chloride (0-80 μM), resulting in a calculated detection limit of 2.58 μM. Panhuis et al. used coiled conformation biopolymers to distribute SWCNTs and printed transparent composite films on a PET substrate [67]. They found very low conductivity when measured under a nitrogen atmosphere. Surprisingly, they found that the resistance of the composite fell to ~12 MΩ when the film was exposed to ambient conditions. The change in conductivity is attributed to a change in the pathways in the nanotube-biopolymer junctions in presence of water vapor due to the mechanical swelling of the biopolymer matrix. Biesch et al. employed the MEMS (micro-electromechanical system) technology, which involve the deposition of functional layers, to fabricate nanoscale cantilever-based sensors [68]. SAM layers of alkanethiols were deposited on gold-coated cantilever structures, There SAM layers enhance the sensitivity of the cantilevers to ionic concentrations and pH in liquids.

1.3.3 Applications to Bioprinting-Biological

In biology, there is numerous interest in how to precisely position very small droplets of liquid, as such technology is very important for many biological applications, e.g. microdosing, biochemical surface patterning, tissue engineering, and the direct placement of living cells [69]. Inkjet printing is very promising for such applications because of its ability to accurately deposit volumes of solutions in the pL range [70-71]. Bioprinting is defined as the use of printing technology for biological applications, which includes cell based biosensors, tissue engineering, implanted cell-factory devices or external assist devices for organs [72].

Hasenbank et al. demonstrate multi-analyte patterning using a piezoelectric inkjet printing of multiple layers [73]. Newman and co-workers firstly deposited GOD using a piezoelectric printer [74]. Roda et al. [75] showed that enzymes could be deposited by a thermal printer with no significant differences in the enzyme activity. A small amount of sodium dodecyl sulfate (SDS) was added to the enzymatic ink in order to obtain a suitable surface tension. The diameter of the printed spots was 0.2 mm and

the amount of enzyme in each spot was evaluated by means of chemiluminescent detection. Until now, most printed enzymes have been deposited using piezoelectric inkjet printers as it was thought to affect the activity of the enzyme to a less extent [76]. Ilkhanizadeh et al. [77] reported the use of inkjet printing to study the effect of growth factor patterning and gradients on stem cell differentiation. They investigated the influence of three biological molecules, fibroblast growth factor-2 (FGF2), ciliary neurotrophic factor (CNTF) and feotal bovine serum (FBS) differentiation, on the differentiation of rat embryo neural stem cells. Phillippi et al. studied the differentiation of mouse muscle derived stem cells (MDSC) in the presence of printed patterns and concentration gradients of bone morphogenic progein-2 (BMP2). They used fibrin films to immobilize proteins after printing with a piezoelectric DOD system. Studies have demonstrated both the stability of fibrin immobilization and the use of protein patterns and gradients to control and direct populations of cells [78].

Inkjet technology has been widely used in biology, bio-chemistry and other areas, such as biochip [3-7], biosensor [8] and directly deposit living cells, as an important branch of modern tissue engineering [9-10]. Goldmann et al. [11] utilized a standard inkjet printer for the transfer of nucleic acids to solid supports. The author improved the traditional printer, and realized the DNA print when used DNA as the ink. Newman et al. [12] firstly reported a method for HRP printing used piezoelectric inkjet technology. Roda et al. [13] printed HRP onto filter paper used inkjet technology. Besides, inkjet technology has been used for drug screening [14-15]. Boland's group originally reported the use of thermal DOD inkjet for cell deposition [79]. More recent work by this group has printed primary rat embryonic hippocampal and cortical cells [80]. Nakamura and coworkers succeeded in printing bovine vascular endothelial cells using a DOD printer with an electrostatic actuation mechanism [81]. Recently, a thorough investigation of the influence of piezoelectric DOD printing on the survival and viability of a human fibroblast cell line has been reported by Saunders et al. [82] they found that although some cell death may occur as a result of inkjet printing, surviving cells recover rapidly and appear to behave

normally post-printing. In order to produce fully biomimetic structures containing cells, one must be able to fabricate scaffold structures in 3 dimensions on or in which the cells can attach. Boland's group has taken the approach of printing the less viscous $CaCl_2$ solution into a tank of Na alginate solution [83] (Figure 10). The Na alginate will gelled in the presence of Ca^{2+}. In order to generate 3D structure, the tank containing the Na alginate contains a moving table that is initially positioned so that a thin film of <100 μm thickness of the liquid is exposed to the printer. By selectively patterning this film with $Cacl_2$ solution, a defined region of the liquid film is gelled. After this, the platform is lowered a defined distance and a second sequence of printing is used to gel a second layer. This process is repeated untial the final desired structure is achieved (Figure 10). Besides this innovative work, several similar strategies have also been employed to construct 3-D cell-containing structures [84-85].

Inkjet is also a power tool for single cell analysis. Inkjet device has the ability of generating pL level droplets which can be used to package single cells, the compounds in cell just be conserved in a droplet avoiding be diluted by large volume of solution. Thus, the compounds can be more easily detected by MS, CE and other methods. Nakamura et al. [16] realized single cell printing by developing commercial printer, and got single cell array. Schubert and Koltay groups also developed some method for single cells array used inkjet technology [17-18]. Recently, Ellis et al. [19] used inkjet technology to fabricate single cell array and realized single cell MS analysis.

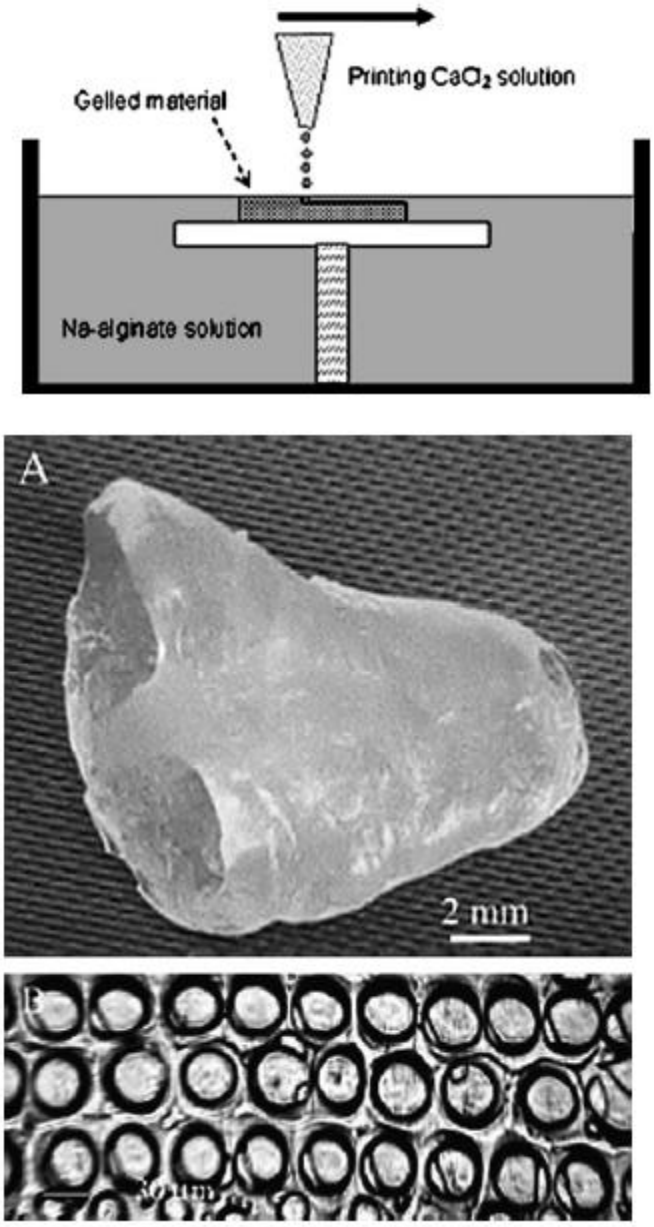

Figure 10: a) the schematic illustration of the printing system for 3-demensional scaffold structures using gelled Na alginate. b) the printed 3D cell-containing structures.

In pharmaceutics, the drug discovery usually involves large scale screen predrugs [86]. Inkjet technology is especially promising in this area since it can easily fabricate high throughput microarray with minimum sample consumption. Arrabito et al. [87] showed that the contactless, low-cost, and rapid drug screening methodology by employing inkjet printing for molecular dispensing in a microarray format. In Figure 11 part A, inkjet printing picoliter volume droplets containing tens of picograms of

molecules (either D-glucose or a mixture of D-glucose/D-glucal) were deposited on a silicon oxide surface where glucose oxidase monolayer were previously immobilized. Upon hitting the solid surface, the dispensed drops form regular rounded spots (Figure 11B). Accordingly, whenever the enzymatic reaction occurs, a red dye complex forms. The more the spot is colored, the higher becomes the grayscale optical contrast of the spot with respect to the background. It is verified that the solid-supported enzymatic surface can be reused for this screening purposes several times by simply rinsing with water.

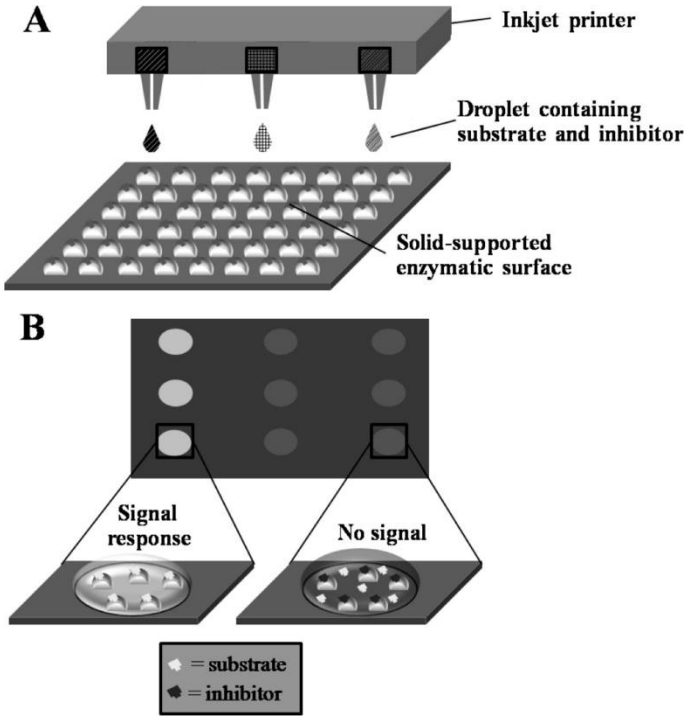

Figure 11. Pictorial sketch of the screening methodology: (A) substrate and inhibitor containing drops dispensed by inkjet printing on the solid-supported enzymatic surface and (B) colorimetric detection for the enzymatic activity. No signal is obtained for a complete inhibition.

Fujita et al. [88] develop super-dense transfected cell microarrays created by a piezoelectric inkjet printer on a glass substrate that had been grafted with poly(ethylene glycol). The field of combinatorial chemistry is starting to utilize drop-on-demand inkjet ejectors to automate the mixing of reagents in different proportions. Through inkjet deposition, each spot has a base nucleotide added and

reacted, then it is washed away prior to the reagent for the next base in the chain being jetted onto the spot. Moreover, drug discovery experiments typically require thousands to hundreds of tests involving novel biologically active agents. Inkjet dispensers that reduce the quantity of fluids use and the time it takes can greatly speed the testing and reduce the cost of the raw materials [89-90].

Inkjet printing is currently at the threshold of becoming a standard fabrication tool, with a wide range of materials science applications [91-92]. The use of inkjet dispensing technology generally provides several advantages over syringe-pump-based liquid handling: accurate and precise aspiration and delivery of nanoliter volumes of reagents; rapid delivery of reagents resulting from non-contact dispensing and rapid valve actuation; and reduced requirements for alignment due to non-contact delivery.

1.4 Outline of this study

The whole thesis flow chart is summarized in Figure 12. In this thesis, I development a multi-channel inkjet sample introduction system and investigate its application to analytical chemistry.

This work mainly consists of two parts of discussion. The part one (chapter 2) is based on the piezoelectric ceramics energy conversion. According to its electromechanical coupling coefficient, we designed a new self-sensing driving circuit for piezoelectric actuator, which combined with abilities of home-made software to change its output frequency, driving voltage and pulse width. A drop-on-demand (DOD) picoliter droplets were easily generated with controllable precision based on the piezoelectric ceramic actuator equipment. In the second part (chapter 3, 4, 5), the DOD-based piezoelectric inkjet is applied to capillary electrophoresis (chapter 3) and chemiluminescence (chapter 4) and immunoassay (chapter 5).

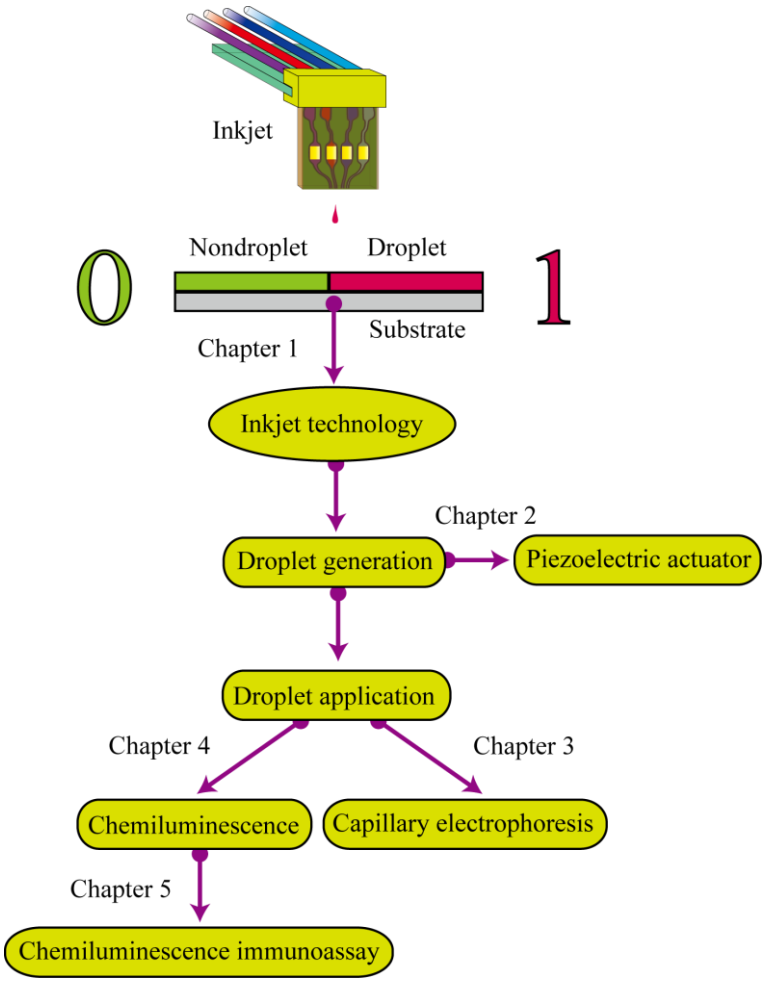

Figure 12. The whole structure of this thesis.

In chapter 3, the picoliter droplets generated by piezoelectric inkjet was applied to capillary electrophoresis (CE) analysis. The DOD picoliter droplets were directly employed for sampling in CE analysis. Finally, Theobromine, Caffeine and Theophiline were then separated by Micellar electrokinetic chromatography using sodium dodecyl sulphate as the micellar phase. Compared to previous methods, the combination of picoliter droplet with CE showed reproducible and reliable analytica results.

In chapter 4, an automatic multi-channel ink-jet chemiluminescence (CL) analysis system has been developed. The four-channel ink-jet device was controlled by a home-made circuit. The whole procedure for CL analysis was automatically completed on a hydrophobic glass side. Horseradish peroxidase (HRP) was selected

as an analyte, and determined by the automatic CL analysis platform. Reaction solutions delivered by different channels were precisely ejected to the same position of the glass slide for the CL analysis. The consumption of reaction solution was reduced to nanoliter level. The whole CL analysis could be completed in less than 4 min, which was benefited from the prompt solution mixing in small size of droplet. Finally, the automatic CL system could also be used for the detection of HRP in HRP-protein conjugates, which showed its practical application in immunoassay.

In chapter 5, a novel chemiluminescence diagnosis system for high-throughput human IgA detection was developed by inkjet nano-injection on a multicapillary glass plate. To proof-of-concept, microhole-based Polydimethylsiloxane sheets were aligned on a multicapillary glass plate to form a microwell array as microreactors for enzyme-linked immunosorbent assay (ELISA). The multicapillary glass plate was utilized as a switch that controlled the holding/passing of the solution. Further, anti-IgA-labeled polystyrene (PS) microbeads was assembled into the microwell array, and an inkjet nano-injection was specially used to distribute the sample and reagent solution for chemiluminescence ELISA, enabling to high-throughput detection of human IgA. Thus, we believe that the inkjet nano-injection for high-throughput chemiluminescence immunoassay on multicapillary glass plate will be promising in disease diagnosis.

Throughout this thesis, I have successfully developed a precise drop-on-demand inkjet sample dispensing system and its applications to analytical chemistry.

Reference

1. P. G. Campbell, L. E. Weiss, Tissue engineering with the aid of inkjet printers, Expert Opin. Biol. Ther., 2007, 7: 1123-1127.
2. A. B. Braunschweig, F. W. Huo and C. A. Mirkin, Molecular printing, Nat. Chem., 2009, 1: 353-358.
3. T. Goldmann, J. S. Gonzalez, DNA-printing: Utilization of a standard inkjet printer for the transfer of nucleic acids to solid supports. Journal of Biochemical and Biophysical Methods, J. Biochem. Biophys, Methods, 2000, 42: 105–110.
4. A. P. Blanchard, R. J. Kaiser, L. E. Hood, High-density oligonucleotide arrays, Biosens. Bioelectron., 1996, 11: 687-690.
5. I. Saaem, K. S. Ma, A. N. Marchi, T. H. LaBean, J. Tian, In situ Synthesis of DNA Microarray on Functionalized Cyclic Olefin Copolymer Substrate. ACS Appl. Mater . Interfaces, 2010, 2: 491-497.
6. J. D. Newman, A. P. F. Turner, G. Marrazza, Ink-jet printing for the fabrication of amperometric glucose biosensors, Anal. Chim. Acta, 1992, 262: 13-17.
7. A. Roda, M. Guardigli, C. Russo, P. Pasini, M. Baraldini, Protein microdeposition using a conventional ink-jet printer. Biotechniques, 2000, 28: 492-496.
8. L. Setti, A. Fraleoni-Morgera, B. Ballarin, A. Filippini, D. Frascaro, C. Piana, An amperometric glucose biosensor prototype fabricated by thermal inkjet printing, Biosens. Bioelectron., 2005, 20: 2019-2026.
9. J. T. Kirk, G. E. Fridley, J. W. Chamberlain, E. D. Christensen, M. Hochberg, D. M. Ratner, Multiplexed inkjet functionalization of silicon photonic biosensors, Lab Chip, 2011, 11: 1372-1377.
10. T. Boland, T. Xu, B. Damon, X. Cui, Application of inkjet printing to tissue engineering, Biotechnol., 2006, 1: 910-917.
11. T. Goldmann, J. S. Gonzalez, DNA-printing: Utilization of a standard inkjet printer for the transfer of nucleic acids to solid supports. J. Biochem. Biophys. Methods, 2000, 42:105-110.

12. J. D. Newman, A. P. F. Turner, G. Marrazza, Ink-jet printing for the fabrication of amperometric glucose biosensors, Anal. Chim. Acta, 1992, 262:13-17.
13. A. Roda, M. Guardigli, C. Russo, P. Pasini, M. Baraldini, Protein microdeposition using a conventional ink-jet printer, Biotechniques, 2000, 28:492-496.
14. A. V. Lemmo, D. J. Rose, T. C. Tisone. Inkjet dispensing technology: Applications in drug discovery, Curr. Opin. Biotechnol., 1998, 9:615-617.
15. G. Arrabito, B. Pignataro, Inkjet printing methodologies for drug screening, Anal. Chem., 2010, 82:3104-3107.
16. M. Nakamura, A. Kobayashi, F. Takagi, A. Watanabe, Y. Hiruma, K. Ohuchi, Y. Iwasaki, M. Horie, I. Morita, S. Takatani, Biocompatible Inkjet Printing Technique for Designed Seeding of Individual Living Cells, Tissue Eng., 2006, 11: 11-12.
17. A. R. Liberski, J. T. Delaney, U. S. Schubert, "One cell-one well": A new approach to inkjet printing single cell microarrays, ACS Comb. Sci., 2010, 13:190-195.
18. A. Yusof, H. Keegan, C. D. Spillane, O. M. Sheils, C. M. Martin, J. J. O'Leary, R. Zengerle, P. Koltay, Inkjet-like printing of single-cells, lab chip, 2011, 11:2447-2454.
19. S. R. Ellis, C. J. Ferris, K. J. Gilmore, T. W. Mitchell, S. J. Blanksby, M. H. Panhuis, Direct lipid profiling of single cells from inkjet printed microarrays, Anal. Chem., 2012, 84: 9679-9683.
20. H. P. Le, Progress and trends in ink-jet printing technology, J. Imaging Sci. Technol., 1998, 42: 49-62.
21. M. R. Keeling, Ink jet printing, Phys. Technol., 1981, 12:196.
22. B. Derby, Inkjet Printing of Functional and Structural Materials: Fluid Property Requirements, Feature Stability, and Resolution, Ann. Rev. Mater. Res., 2010, 40: 395-414.
23. G. D. Martin, S. D. Hoath, I. M. Hutchings, Inkjet printing - the physics of

manipulating liquid jets and drops, J. Phys. Conf. Ser., 2008,105: 1- 14.

24. R. G. Sweet, High frequency recording with electrostatically deflected ink jets, Rev. Sci. Instrum., 1965, 36: 131-136.
25. W. T. Pimbley, H. C. Lee, Satellite droplet formation in a liquid jet, IBM J. Res. Dev., 1977, 21: 21-30.
26. G. L. Filmore, W. L. Buehnet, D. L. West, Drop charging and deflection in an electrostatic ink jet printer, IBM J. Res. Dev., 1984, 21: 37-47.
27. R. G. Sweet, U. S. Patent 3, 1971, 275:576.
28. R. Parashkov, E. Becker, T. Riedl, H. H. Johannes W. Kowalsky, Proc. IEEE, 2005, 93:1321-1329.
29. J. D. Newman, A. P. F. Turner, G. Marrazza, Anal. Chim. Acta, 1992, 262:13-17.
30. S. Magdassi, M. Ben Moshe, Langmuir, 2003, 19: 939-942.
31. T. Xu, J. Jin, C. Gregory, J. J. Hickman, T. Boland, Biomaterials, 2005, 26:93-99.
32. D. Damjanovic, Stress and frequency dependence of the direct piezoelectric effect in ferroelectric ceramics, J. Appl. Phys., 1997, 82:1788-1797.
33. M. S. Hasenbank, T. Edwards, E. Fu, R. Garzon, T. F. Kosar, M. Look, A. M. Hossein, P. Yager, Anal. Chim. Acta, 2008, 611:80 - 88.
34. B. Gans, P. C. Duineveld, U. S. Schubert, Inkjet printing of polymers: state of the art and future developments, Adv. Mater., 2004, 16:203-213.
35. B. Derby, Inkjet Printing of functional and structural materials: fluid property requirement, feature stability and resolution, Annu. Rev. Mater. Res., 2010, 40:395-414.
36. N. Reis, C. Ainsley and B. Derby, Ink-jet delivery of particle suspensions by piezoelectric droplet ejectors, J. Appl. Phys., 2005, 97: 094903.
37. K. A. M. Seerden, N. Reis, J. R. G. Evans, P. S. Grant, J. W. Halloran and B. Derby, Ink-Jet Printing of Wax-Based Alumina Suspensions, J. Am. Ceram. Soc., 2001, 84: 2514- 2520.
38. J. E. Fromm, Numerical-calculation of the fluid-dynamics of drop-on-demand jets, IBM J. Res. Dev., 1984,28: 322-333.

39. N. Reis, B. Derby, Ink jet deposition of ceramic suspensions: modelling and experiments of droplet formation, MRS Symp. Proc., 2000, 624: 65-70.
40. P. C. Duineveld, M. M. de Kok, M. Buechel, A. Sempel, K. A. H. Mutsaers, et al. Ink-jet printing of polymer light-emitting devices. Proc. Conf. Org. Light-Emit. Mater., Devices, 2001, 4464: 59-67.
41. C. D. Stow, M. G. Hadfield, An experimental investigation of fluid-flow resulting from the impact of a water drop with an unyielding dry surface. Proc. R. Soc. London Ser. A, 1981, 373: 419- 441.
42. R. Bhola, S. Chandra, Parameters controlling solidification of molten wax droplets falling on a solid surface. J. Mater. Sci., 1999, 34: 4883-4894.
43. B. Derby, N. Reis, Inkjet printing of highly loaded particulate suspensions, MRS Bull., 2003, 28: 815-518.
44. E. I. Haskal, M. Buechel, J. F. Dijksman, P. C. Duineveld, E. A. Meulenkamp, et al, Ink jet printing of passive-matrix polymer light emitting displays. SID Symp. Dig. Tech. Pap., 2002, 33: 776-779.
45. D. Xu, V. Sanchez-Romaguera, S. Barbosa, W. Travis, et al, Inkjet printing of polymer solutions and the role of chain entanglement, J. Mater. Chem., 2007, 17: 4902-4907.
46. M. Kaneda, H. Ishizuka, Y. Sakai, J. Fukai, S. Yasutake and A. Takahara, AIChE J., 2007, 53: 1100.
47. S. H. Lee, K. Y. Shin, J. Y. Hwang, K. T. Kang, H. S. Kang, J. Micromech. Microeng., 2008, 18: 075014.
48. A. Dodabalapur, organic and polymer transistors for electronics, Mater. Today, 2006, 9: 24-30.
49. J. Jang, Displays develop a new flexibility, Mater. Today 2006, 9: 46-52.
50. H. Sirringhaus, T. Kawase, R. H. Friend, T. Shimoda, M. Inbasekaran, W. Wu, E. P. Woo, High-Resolution Inkjet Printing of All-Polymer Transistor Circuits, Science, 2000, 290: 2123-2126.
51. J. Z. Wang, Z. H. Zheng, H. W. Li, W. T. S. Huck, H. Sirringhaus, Dewetting of

conducting polymer inkjet droplets on patterned surfaces, Nat. Mater., 2004, 3: 171-176.

52. C. W. Sele, T. Werne, R. H. Friend, H. Sirringhaus, Lithography-Free, Self-Aligned Inkjet Printing with Sub-Hundred-Nanometer Resolution, Adv. Mater., 2005, 17: 997-1001.
53. P. Beecher, P. Servati, A. Rozhin, A. Colli, V. Scardaci, S. Pisana, T. Hasan, A. J. Flewitt, J. Robertson, G. W. Hsieh, F. M. Li, A. Nathan, A. C. Ferrari, W. I. Milne, Ink-jet printing of carbon nanotube thin film transistors, J. Appl. Phys., 2007, 102: 043710.
54. T. Shimoda, Y. Matsuki, M. Furusawa, T. Aoki, I. Yudasaka, H. Tanaka, H. Iwasawa, D. Wang, M. Miyasaka, Y. Takeuchi, Solution-processed silicon films and transistors, Nature, 2006, 440:783-786.
55. Y. Y. Noh, X. Cheng, H. Sirringhaus, J. I. Sohn, M. E. Welland, D. J. Kang, Ink-jet printed ZnO nanowire field effect transistors, Appl. Phys. Lett., 2007, 91: 043109.
56. T. X. Sun, G. E. Jabbour, Combinatorial screening and optimization of luminescent materials and organic light-emitting devices, MRS Bull., 2002, 27: 309 -315.
57. Y. Yoshioka, G. E. Jabbour, Inkjet printing of oxidants for patterning of nanometer - thick conducting polymer electrodes, Adv. Mater., 2006, 18: 1307-1312.
58. E. Tekin, H. Wijlaars, E. Holder, D. A. M. Egbe, U. S. Schubert, Film thickness dependency of the emission colors of PPE-PPVs in inkjet printed libraries, J. Mater. Chem. 2006, 16: 4294 - 4298.
59. E. Tekin, P. J. Smith, S. Hoeppener, A. M. J. van den Berg, A. S. Susha, A. L. Rogach, J. Feldmann, U. S. Schubert, Inkjet Printing of Luminescent CdTe Nanocrystal–Polymer Composites, Adv. Funct. Mater., 2007, 17: 23-28.
60. M. Singh, T. Kondou, H. Chae, J. D. Froehlich, S. Li, A. Mochizuki, G. E. Jabbour, Mater. Res. Soc. Fall Meeting 2008, G13.7

61. H. M. Haverinen, R. A. Myllyla¨, G. E. Jabbour, Inkjet printing of light emitting quantum dots, Appl. Phys. Lett., 2009, 94: 073108.
62. S. E. Shaheen, R. Radspinner, N. Peyghambarian, G. E. Jabbour, Fabrication of bulk heterojunction plastic solar cells by screen printing, Appl. Phys. Lett., 2001, 79: 2996.
63. V. Marin, E. Holder, M. M. Wienk, E. Tekin, D. Kozodaev, U. S. Schubert, Ink-Jet Printing of Electron Donor/Acceptor Blends: Towards Bulk Heterojunction Solar Cells, Macromol. Rapid Commun., 2005, 26: 319-324.
64. E. Holder, B. M. W. Langeveld, U. S. Schubert, New Trends in the Use of Transition Metal–Ligand Complexes for Applications in Electroluminescent Devices, Adv. Mater., 2005, 17: 1109-1121.
65. C. N. Hoth, S. A. Choulis, P. Schilinsky, C. J. Brabec, High Photovoltaic Performance of Inkjet Printed Polymer:Fullerene Blends, Adv. Mater. 2007, 19: 3973-3978.
66. K. Crowley, E. O'Malley, A. Morrin, M. R. Smyth, A. J. Killard, An aqueous ammonia sensor based on an inkjet-printed polyaniline nanoparticle-modified electrode, Analyst, 2008, 133: 391-399.
67. M. in het Panhuis, A. Heurtematte, W. R. Small, V. N. Paunov, Inkjet printed water sensitive transparent films from natural gum–carbon nanotube composites, Soft Matter, 2007, 3: 840-843.
68. A. Bietsch, J. Zhang, M. Hegner, H. P. Lang, C. Gerber, Rapid functionalization of cantilever array sensors by inkjet printing, Nanotechnology, 2004, 15: 873.
69. B. Derby, Bioprinting: inkjet printing proteins and hybrid cell-containing materials and structures, J. Materials. Chem., 2008,18: 5717-5721.
70. J. Alper, Bioengineering. Biology and the inkjets, Science, 2004, 305:1895-1895.
71. P. Calvert, Printing Cells, Science, 2007, 318: 208-209.
72. V. Mironov, N. Reis and B. Derby, Review: Bioprinting: A Beginning, Tissue Eng., 2006, 12: 631- 634.
73. M. S. Hasenbank, T. Edwards, E. Fu, R. Garzon, T. F. Kosar, M. Look, A.

Mashadi-Hossein and P. Yager, Anal. Chim. Acta, 2008, 611: 80-88.

74. J. D. Newman, A.P.F. Turner, G. Marrazza, Anal. Chim. Acta, 1992, 262: 13-17.
75. A. Roda, M. Guardigli, C. Russo, P. Pasini, M. Baraldini, Biotechniques, 2000, 28: 492‑496.
76. S. D. Risio, N. Yan, Macromol. Rapid Commun., 2007, 28: 1934-1940.
77. S. Ilkhanizadeh, A. I. Teixeira and O. Hermanson, Inkjet printing of macromolecules on hydrogels to steer neural stem cell differentiation, Biomaterials, 2007, 28: 3936-3943.
78. J. A. Phillippi, E. Miller, L. Weiss,J. Huard, A. Waggoner and P. Campbell, Microenvironments Engineered by Inkjet Bioprinting Spatially Direct Adult Stem Cells Toward Muscle-and Bone-Like Subpopulations, Stem Cells, 2008, 26: 127-134.
79. T. Xu, J. Jin, C. Gregory, J. J. Hickman and T. Boland, Inkjet printing of viable mammalian cells, Biomaterials, 2005, 26: 93–99.
80. T. Xu, C. A. Gregory, P. Molnar, X. Cui, S. Jalota, S. B. Bhaduri and T. Boland, Viability and electrophysiology of neural cell structures generated by the inkjet printing method, Biomaterials, 2006, 27: 3580–3588.
81. M. Nakamura, A. Kobayashi, F. Takagi, A. Watanabe, Y. Hiruma, K. Ohuchi, Y. Iwasaki, M. Horie, I. Morita and S. Takatani, Biocompatible Inkjet Printing Technique for Designed Seeding of Individual Living Cells, Tissue Eng., 2005, 11: 1658–1666.
82. R. E. Saunders, J. E. Gough and B. Derby, Delivery of human fibroblast cells by piezoelectric drop-on-demand inkjet printing, Biomaterials, 2008, 29: 193–203.
83. T. Boland, X. Tao, B. J. Damon, B. Manley, P. Kesari, S. Jalota and S. Bhaduri, Mater. Sci. Eng., C, 2007, 27: 372-376.
84. Y. Nishiyama, M. Nakamura, C. Henmi, K. Yamaguchi, S. Mochizuki, H. Nakagawa and K. Takiura, in Proceedings of the ASME International Conference on Manufac-turing Science and Engineering, American Society for Mechanical Engineers (ASME), New York, NY, USA, 2007, pp 97-102.

85. T. Xu, H. Kincaid, A. Atala and J. J. Yoo, J. Manuf. Sci. Eng., 2008, 130: 021017.
86. D. G. Yu, L. M. Zhu, C. J. Branford-While, X. L. Yang, Three-dimensional printing in pharmaceutics: Promises and problems, Journal of pharmaceutical sciences, 2008, 97:3666-3690.
87. G. Arrabito, B. Pignataro, Anal. Chem., 2010, 82: 3104-3107.
88. S. Fujita, R. Onuki-nagasaki, J. Fukuda, J. Enomoto, S. Yamaguchi, M. Miyake, Lab chip, 2013, 13: 77-80.
89. A. Schober et al., Accurate high-speed liquid handling of very small biological samples, Biotechniques, 1993, 2: 324-329.
90. T. C. Tisone, Dispensing systems for miniaturized diagnostics, IVD Technology, 1998.
91. P. Calvert, Inkjet printing for materials and devices, Chem. Mater., 2001,13: 3299–3305.
92. B. J., de Gans, P. C., Duineveld, U. S., Schubert, Inkjet printing of polymers: state of the art and future developments, Adv. Mater., 2004, 16: 203–123.

Chapter 2

Development of multi-channel inkjet piezoelectric actuator for drop-on-demand droplet generation

1. Introduction

Inkjet has been an attractive technology to deposit various kinds of liquids for many purposes at the past decades [1-4]. The operating principle of inkjet is electromechanical pumping fluids via various actuator. Recently, printing of conductive materials for the fabrication of electronic components and devices becomes an attractive technology in the electronics packaging. Piezoelectric ceramics have been applied universally as energy converting element due to their high piezoelectric coefficient and electromechanical coupling coefficient [5]. A piezoelectrical induced pressure wave can propagate against the surface tension of the fluid, forming a small droplet which is ejected from the nozzle. Under suitable electrical conditions, the ejected fluid develops into a single droplet for quality ink-jetting.

Although piezoelectric inkjet is expensive because of the need to implement micromachining processes and a high voltage driving circuit, piezo-actuated print heads are much more reliable and adaptable in various applications of liquid dispensing systems [6-7]. However, there are some important issues in using piezoelectric actuators for active control both the high electrical voltage and significant power required for these devices and the complexities involved with active control (added hardware, control law design, and implementation).

Herein, a drop-on-demand (DOD) picoliter droplets were easily precise and controllable generated based on the piezoelectric ceramic actuator equipment. Actually, accurate, controllable, and highly repeatable picoliter droplets were successfully produced by the developed system and applied into capillary

electrophoresis (CE), mass spectrum (MS) and chemiluminescence (CL) [8-11].

The mechanism of the process in inkjet was widely studied, including the generation of the pulse, the continuous supplementary of the liquid in the reservoir and the ejection from the nozzle [12]. Piezoelectric ceramics have been used in squeezing the channel in inkjet besides thermal transduction. The ejected nozzle was usually designed between 20-50 μm. However, some solvents were only ejected with proper viscosity, density and surface tension. The Reynolds number (N_{Re}) and the Weber number (N_{We}) were reported to donate at the ejection [13]. The inverse of the Ohnesorge number (Z) was the direct parameter to distinguish whether the droplets could be formed. Fromm reported that stable droplets could be ejected only at $Z > 2$ [14], and transient satellite was observed at $Z > 6$ [15]. Afterwards, Jang et al. redefined the range of Z required for stable droplet generation is $4 < Z < 14$ [12]. Actually, waveform could also influence the droplet ejection besides the structure of the inkjet head and the properties of the solvent. It was reported that double waveforms in one circle will result in the formation of stable droplets and disappearance of satellites [16-17]. Although the mechanism of the effection of pulse on droplet formation was clear [18], the study on the relationship between the width and voltage of a single pulse on droplets was in great demand.

In this chapter, we reported an integrated inkjet printing technology by employing a home-made circuit and software for driving piezoelectric actuator. An accurate, controllable, and highly reproducible picoliter droplet generator was built up for for liquid introduction. Here, a four-channel inkjet microchip based on piezoelectric actuator system supplied by Fuji Electric Co., Ltd. (Tokyo, Japan) was used. The control system can be divided into hardware fabrication and software design and integrated for the droplet generation. The hardware was consisted of two integrated circuit chip board. The mainly parameter of software partition was included output frequency, driving voltage and pulse width.

The effect of single pulse width and voltage on the formation of droplets was studied. Several solvents could be ejected by adjusting the width of the pulse,

including water and acetonitrile. Moreover, the relationship between the voltage and the volume was demonstrated to influence the droplet size. Based on this approach, the volume/mass of droplet can be easily and accurately tuned, which will further facilitate inkjet printing of droplet generation for practical application. We propose that the inkjet printing platform developed can be applied for a variety of practical purposes.

2. Experimental

2.1 Apparatus

The four-channel ink-jet microchip was provided by Fuji Electric Co., Ltd. (Tokyo, Japan). AMS-05K10P/100 DC power was supplied by Max-Electronics Co., Ltd. (Tokyo, Japan). Oscilloscope DSO1002A was purchased from Agilent technologies. VW-9000 : High-speed microscope (camera units: high-speed monochrome VW-600M, macro zoom units: long-distance macro zoom unit VW-Z2 with 4x optical zoom) was purchased from Kyence corporation (Tokyo, Osaka).

2.2 Experimental setup

2.2.1 piezoelectrical characteristic

The structure of the piezoelectric inkjet device which was fabricated for this study is shown in Fig. 1. A piece of piezoelectric ceramic was fixed above the top of the chamber. When a pulse was applied, the piezoelectric ceramic will change the shape in response (inverse piezoelectric effect). The press on the solution chamber, which is generated from the change in shape of piezoelectric ceramic, ejects the solution droplet through the nozzle. The piezoelectric ceramic equivalent circuit is shown in Fig. 2.

$$C = \frac{\varepsilon_{33} A}{\mathrm{t}}$$

Where, C is the static equivalent capacitor (2.5 nF); A is the piezoelectric

ceramic area (2.3 mm x 2.3 mm); t is the piezoelectric ceramic thickness (0.15 mm); ε_{33}: dielectric constant.

Piezoelectric ceramics is not only a simple capacitance but also a micro electromechanical conversion device. Adopting piezoelectric ceramics, mechanical energy can be conversed to electic energy, and power energy also can be conversed to mechanical energy.

Piezoelectric actuator is not only a simple electronic device equivalent to capacitance but also a device realizing the conversion between the electrical energy and mechanical energy. It can be regarded as a plate capacitor C0 (or called a static capacitance) when the piezoelectric quartz crystal is at the static statement. The value of C0 is depending on the geometry size of the wafer and the area of electrode, which usually is about a few or tens of pF. On the other hand, it could be assumed to a inductance L when the quartz crystal is at the vibration statement, whose value of is about several mH or tens of H. The elastic of wafer equivalent to a capacitance C, its value is only 0.01 or 0.2 pF. Moreover, the friction loss of the wafer is equivalent to the resistor R, and its value is about 100 Ω (Usually, R is equal to 0 Ω at ideal situation.).

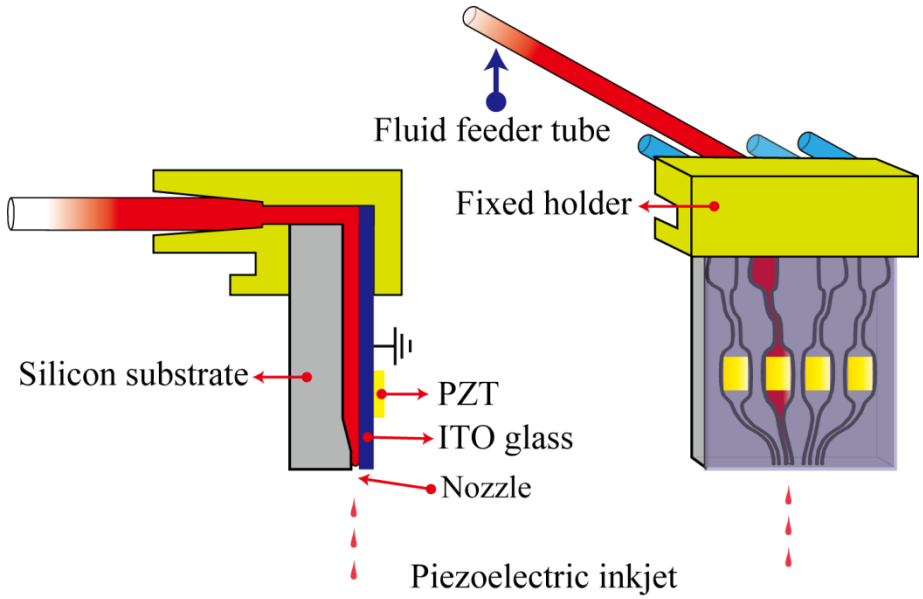

Fig. 1. The structure of the piezoelectrical inkjet device.

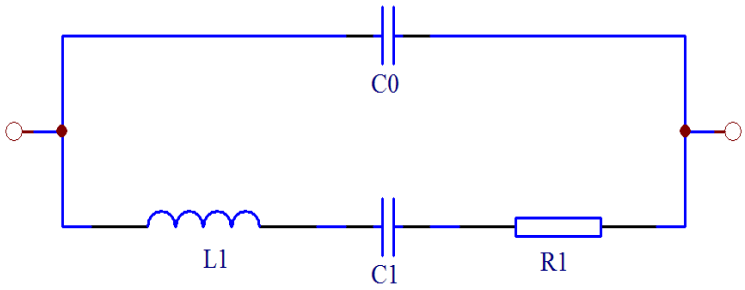

Fig. 2. The equivalent circuit of piezoelectric ceramic.

2.2.2 Piezoelectric actuator hardware design

The structure of the inkjet device used in our experiments is shown in Fig. 3a. A piece of piezoelectric ceramic was fixed on the top of solution chamber. When an electric pulse was applied, the piezoelectric ceramic will change the shape in response (inverse piezoelectric effect). The press on the solution chamber, which is generated from the change in shape of piezoelectric ceramic, ejects the solution through the nozzle, forming a droplet. For inkjet printing of droplet formation, piezoelectric ceramic actuator (driving voltage, driving pulse width and frequency) is crucial for generating uniform and stable droplets. In our experiment, a home-made piezoelectric actuator circuit and related software were used to drive the piezoelectric ceramic (Fig. 3b). Basically, the waveform can be designed on the computer and the signal is passed to the circuit via a USB port. Then the signal is handled on the circuit (RAM chip, FPGA chip) and then amplified through amplification circuit (Q1, Q2 for voltage amplification; Q3, Q4 for current amplification) as shown in Fig. 3c. The amplified signal is then applied and actuated the piezoelectric ceramic. The two resistors R_1, R_4 form a voltage divider that provides the proper potential (bias) to the base. The circuit is designed so that any change in current flow through the transistor alters the potential drop at R_6 and consequently changes the potential. That is an applied voltage to the base to partially restore the original current through the device. The real PCB circuit board picture was shown in Fig. 4. The four channel arbitrary wave generator based on the laboratory-made hardware and software

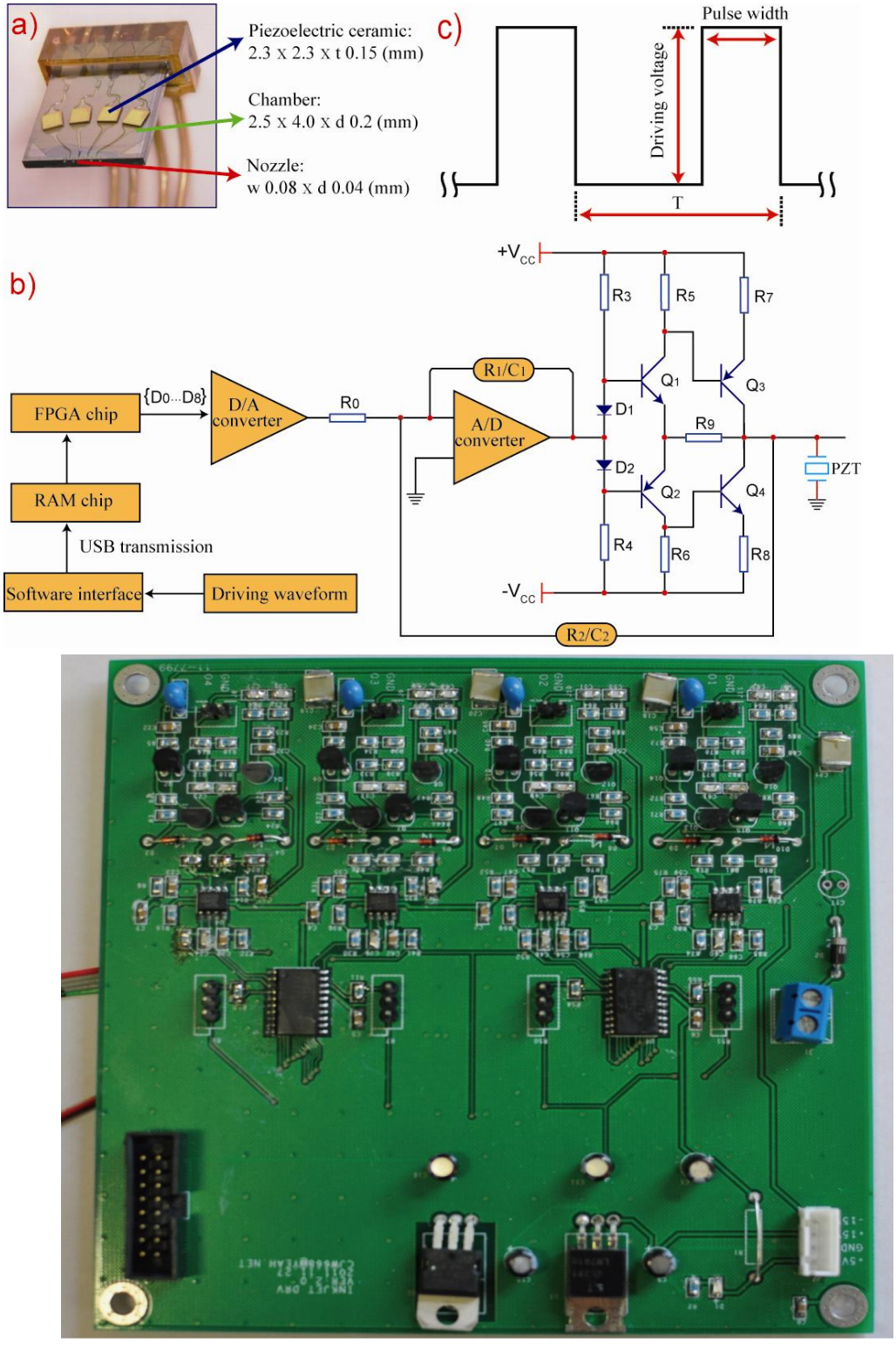

Fig. 3. The picture of four-channel inkjet chip containing piezoelectric ceramic, solution chamber, and nozzle. b) the sketch of the circuit of piezoelectric actuator and related software design, c) Typical driving waveform (square shape) characterizing by driving voltage, pulse width and, d) the picture of piezoelectric actuator module.

2.2.3 Piezoelectric actuator software design

The controller for the piezoelectric ceramic adoptes the TTL .Typically, the driving waveform (square shape) (Fig. 3c) driving the controller is capable of adjusting parameters such as driving voltage, pulse width and frequency through the USB interface. The software interface was compiled by Visual C++ programming language editor. Subsequently, the signal was dealed with by FPGA chip controlling as Fig. 4. shown.

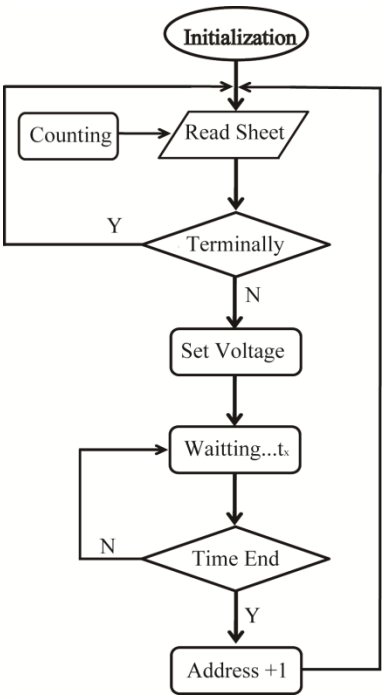

Fig. 4. The flow chart of software program for inkjet droplet generator.

2.2.4 The observation of inkjet ejector droplet formation

The schematic of the experimental setup is depicted in Fig. 5. High-speed microscope VW-9000 machine is employed to observe the droplet formation of inkjet device. The microscope was placed on the holder, whose position and direction can be regulated. The piezoelectric ceramic of inkjet is fabricated based on the bending mode, the nozzle of inkjet was set as the focus of the microscope to monitor the process of droplet formation. The frame rate of the camera was 35000fps and the resolution was 640 × 480 pixels.

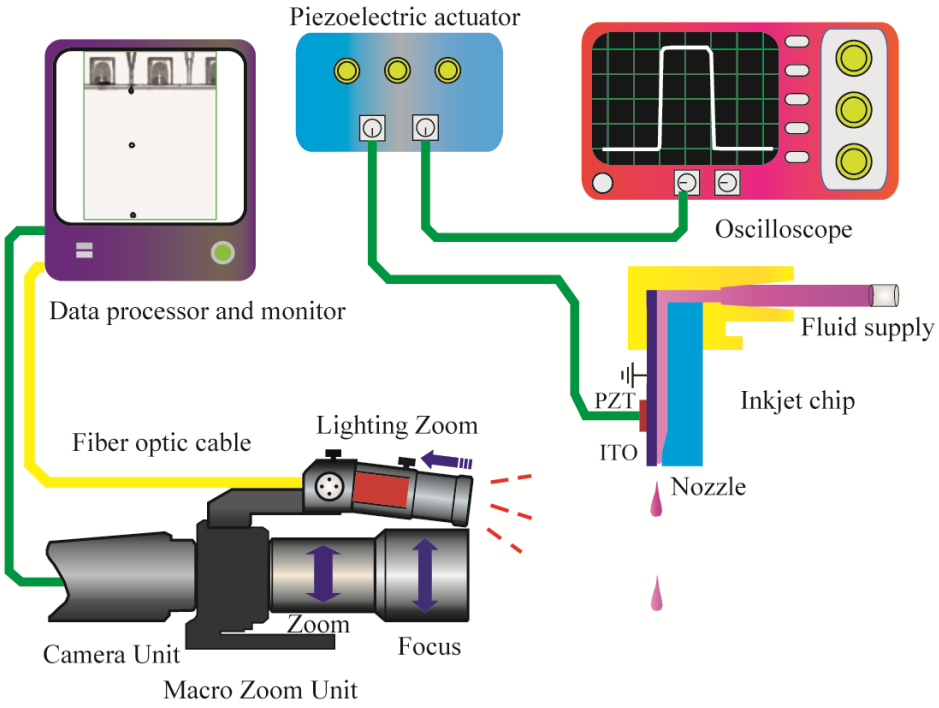

Fig. 5 Experimental setup for the inkjet ejector droplet system driven by a piezoelectric actuator.

3. Results and discussion

3.1 hardware and software design

In the normalization scheme, an electrical model of the load must be developed in order to design an efficient drive circuit. The electrical response of a piezoelectric actuator varies both with the voltage amplifier and with the current amplifier of the output high voltage. It is important to understand variation along both of these parameters, and ensure the driving circuits providing sufficient power to the actuator across the intended operating range. Adopting the setup, the parameters such as driving voltage, driving pulse width, frequency can be easily manipulated and tuned the generated random waves via the laboratory-made software interface shown in Fig. 6a. While, the oscilloscope could monitor the output of the real driving waveform.

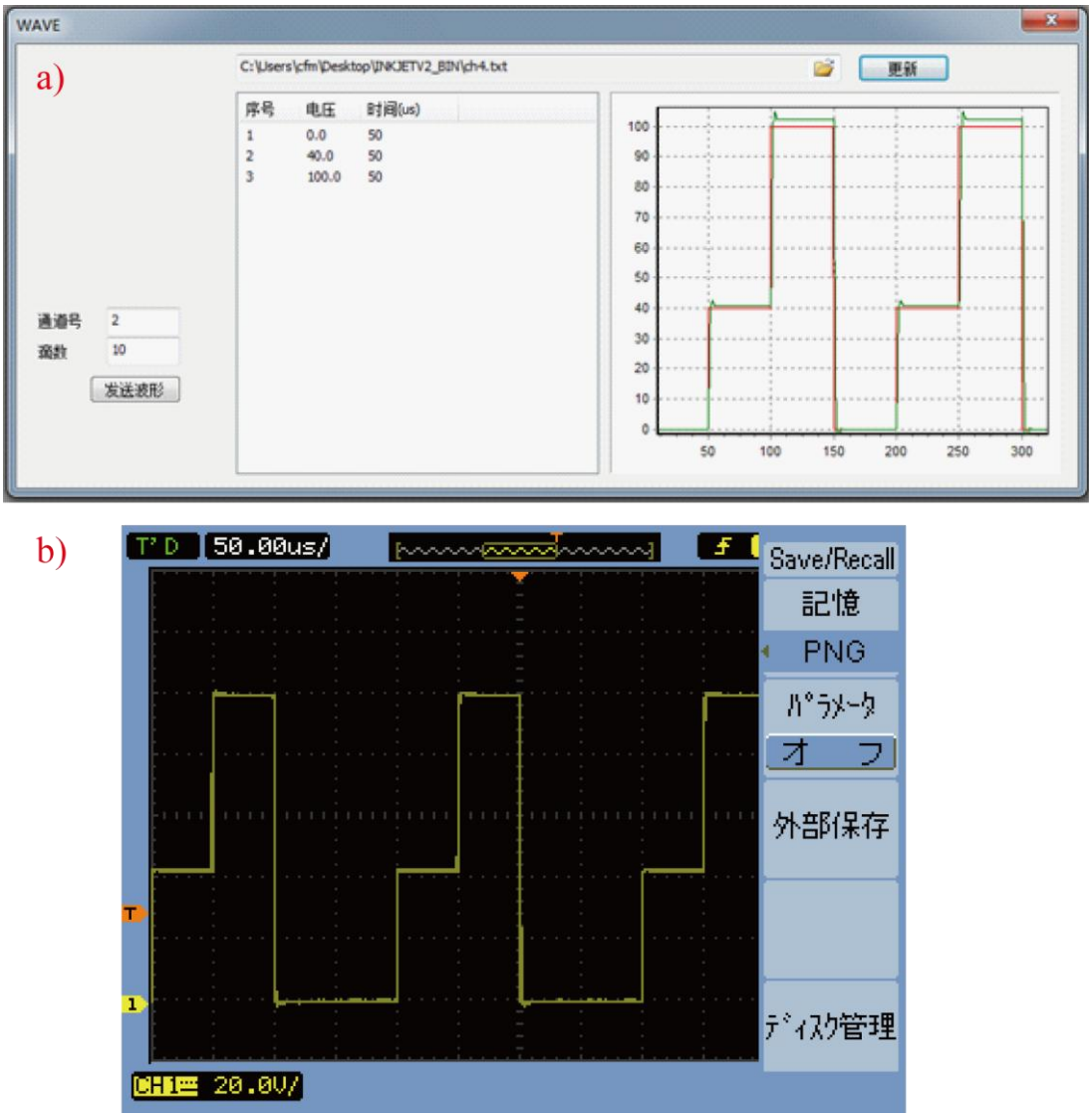

Fig. 6. The interface of the software setup for driving waveform a) and the output waveforms of the home-made circuit was in situ monitored by the oscilloscope b).

3.2 Observation of droplet formation and the output of piezoelectric actuator

In our experiments, a home-made driving circuit combined with the software controlling the piezoelectric actuator was employed to control the ejection of droplets. The parameters of piezoelectric ceramic actuator can be easily manipulated and tuned via ceramic the setup, which will facilitate the control of droplet formation. Here, three conditions related to droplet generation by inkjet printing were observed (in Fig. 7). As shown in Fig. 7a, the droplet generation is not stable (the droplets can't fall in a

straight line) when the driving voltage was set as 44v, and the pulse width was set as 25 μs. With the increase of pulse width to 28 μs, the stable droplet generation can be developed, and the single droplet-on-demand droplet can be obtained (Fig. 7b). With the further increase of pulse width to36 μs, the ejected droplets will split, and the satellite droplets will be formed (Fig. 7c). If the pulse width was kept unchangeable and the driving voltage was tuned, the similar results were also observed (Fig. 7d-e). Therefore, we can conclude that the droplets can neither be formed nor be stably formed when the driving voltage or the pulse width is too low, The reason is probably due to inadequate energy provided by the piezoelectric actuator to overcome the surface tension to form droplets. When these two parameters were in proper ranges, drop-on-demand droplet generation can be obtained. When the driving voltage and the pulse width were too large, the droplet will split up because of the high energy. Thus, the droplet formation could be well-controlled by adjusting the driving voltage and pulse width.

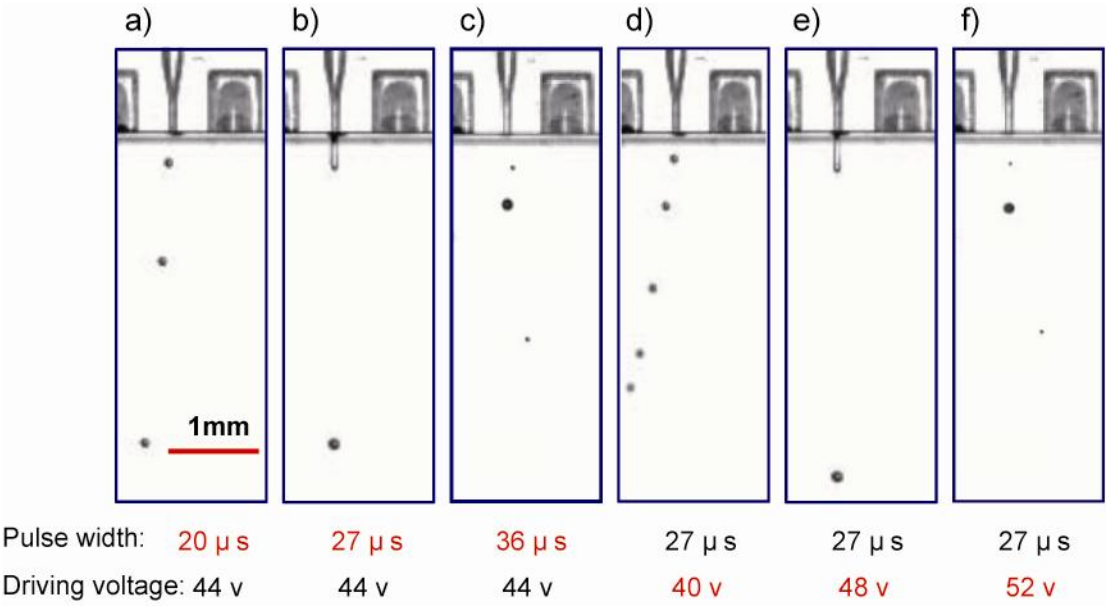

Fig. 7. The droplet generation under different driving waveforms of inkjet (Solution: water, frequency: 1KHz). a)-c) the driving voltage is kept constant and the pulse width is changed. a) droplet generated can't fall in straight line. b) stable drop-on-demand droplet is generated. c) satellite droplets are observed. d)-f) the driving pulse width is unchanged and the voltage is

increased. similar pattern with a)-c) are observed.

3.3 The dynamics of liquid droplet formation

The droplet formation process was monitored through the High-speed microscope VW-9000 machine system as the waveform for the dispensing device was adjusted. We used a single waveform defined by three parameters: baseline voltage, driving voltage, and pulse width. Baseline voltage was set to 0 V is employed to observe the droplet formation of inkjet chip. As shown in Fig. 5, the microscope was placed on the holder, whose position and direction can be regulated. The nozzle part of the ink-jet was set as the focus of the microscope to monitor the process of droplet formation. The frame rate of the camera was 35000fps and the resolution was 256×128 pixels. An idealized depiction of acoustic wave propagation in a DOD dispensing device containing an open-ended microchannel and the PZT positioned near the middle of the chamber. The pressure wave traveling inside the dispenser due to expansion or contraction when the piezoelectric is assumed to be Pressure wave located at the center of the dispenser. The compression pulse from the initial PZT expansion or the contraction waveform meet at the center is in the primary resonance position, and a PZT compression at this time would amplify the pulse resulting in a droplet with maximal velocity. Then, after the maximum pressure wave amplitude at nozzle results in droplet will be ejected.

In piezoelectric inkjet, the piezoelectric ceramic bends in response to the pulse. The deformed ceramic pushes the sample chamber then ejects liquid from the orifice to form droplet. The important physical parameters of printing liquids are viscosity, density, and surface tension. It was reported that the inverse of Ohnesorge number (Z) of the Ohnesorge number (Oh), which is defined as the ration between the reynolds number and a square root of the weber number, is utilized to consider whether a solution can be ejected or not. (Eqn (1)).

$$Z = \frac{1}{Oh} = \frac{N_{\mathrm{Re}}}{\sqrt{N_{We}}} = \frac{va\rho/\eta}{\sqrt{v^2 a\rho/\gamma}} = \frac{\sqrt{d\rho\gamma}}{\eta} \qquad (1)$$

Where ρ is the density of the fluid, γ is the surface tension factor, d is the diameter of the nozzle (equals to 56.6 μm for current inkjet device) and η represents the viscosity.

The above results also indicated that it is possible to generate the stable and drop-on-demand droplets through manipulating the driving voltage and pulse width in appropriate scopes when solutions of different composition has different physical properties. Stable, single, drop-on-demand droplet generation is desirable in a variety of applications for its advantages of uniformity, ease of operation and definite mass and volume. In the experiments, we examined four different solutions (The related Z values were shown in Table 1) adopting our piezoelectric ceramic actuator to perform proper range of driving voltage and pulse width in Fig. 8. With the increase of Z value, the generation of DOD droplet needed big pulse width and high driving voltage. The color areas indicate the ranges that stable, drop-on-demand droplet can be generated. Using our home-made circuit and software, the driving voltage and pulse width can be easily tuned, so that the proper conditions of inkjet printing can be identified for generating stable droplets based on different solutions. Compared to conventional methodology, my ways have made it possible to generate for stable, single, drop-on-demand droplet whatever solution was used. As a result, these techniques would be utilized to wide scopes of solutions to enlarge its applications.

Table 1. physical properties of different solvents under 20℃

solvents	ρ/(Kg/m^3)	η/(mPa·s)	γ/(mN/m)	Z
water	998.23	1.0050	72.88	63.85
20% methanol (v/v)	966.6	1.58	50.4	33.35
ethanol	789.34	1.20	24.11	26.81
50% glycerin(w/w)	1.1263	6.05	69.2	11.02

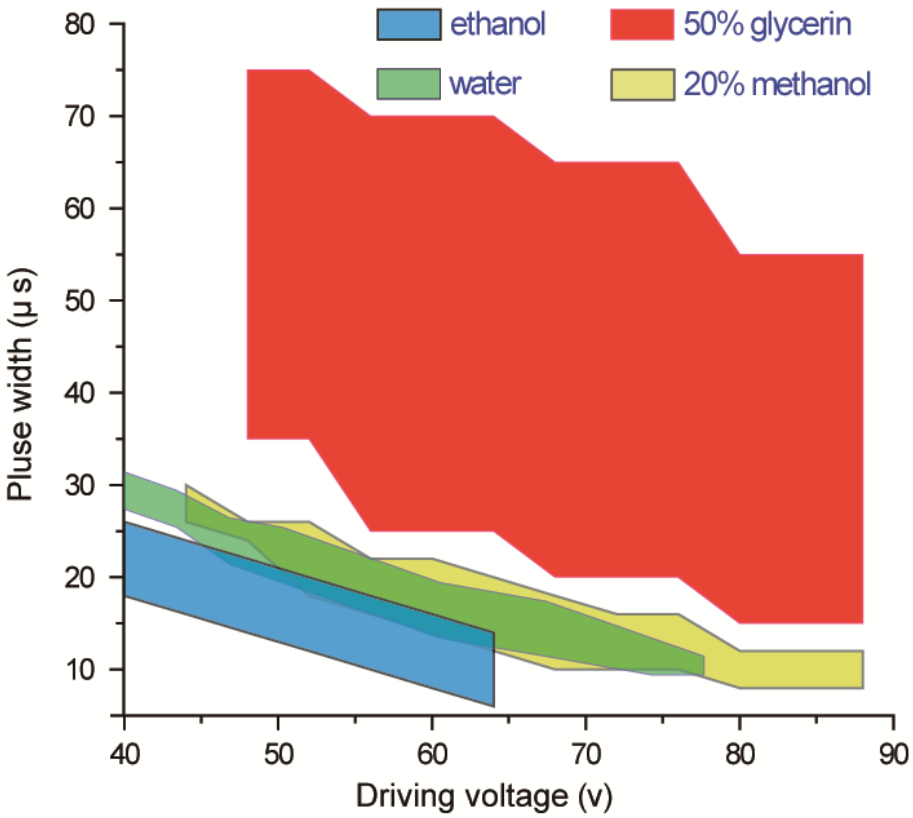

Fig. 8. Stable, uniform, drop-on-demand droplet can be generated for various kinds of solutions. The color areas in the figure represented the proper ranges of driving voltage and pulse width for different solutions.

We have investigated the inter-relationship between inkjet printability and the print fluid's physical properties. By in situ monitoring by high speed camera of jetting dynamics using an imaging system with an interframe time of 36μ s (shown Fig. 10), the droplet formation behavior was characterized in terms of the inverse of the Ohnesorge number which is related to the viscosity, surface tension, and density of the fluid. The piezoelectric actuator inappropriate for inkjet printing driving waveform, the fluids with Z values were also because of their inability to form a single droplet. These low viscosity fluids had easy droplet ejection without significant viscous dissipation. Large oscillatory kinetic energy and high surface tension detached the retreating filament from the rapidly falling primary droplet, forming undesired satellites. A suitable inkjet printing driving waveform range will indicate whether or not a fluid can be stably and accurately printed by inkjet printing, and that

the lower limit is determined by the point at which a satellite forms instead of single droplet. In this study, we redefine the printable range of Z by in situ monitoring of droplet formation dynamics for various fluids having different driving waveform, I found that the lower Z value which is more a range of the pulse width. We can determine the printable driving voltage and pulse width range by considering characteristics of printability such as single droplet formability, the minimum stand-off distance (i.e., the distance from the nozzle tip to the substrate), positional accuracy, and maximum allowable jetting frequency. These can be used to reduce the number of experiments needed to determine the optimal inkjet printing conditions for each fluid.

3.4 Manipulation of droplet volume

The volume of droplet can be easily controlled by manipulating the wave forms of driving voltage. As the droplets were generated by inkjet printing, the volume/mass of the droplets were measured when it was driven by different driving voltage and pulse width (Fig. 9). It should be noted that for the measurement of small-volume droplet, special consideration of evaporation should be taken into to obtain accurate mass/volume. As shown in Fig. 9, the volume of droplet has a good linear increase in response to the rise of driving voltage, which gives a linear fit of $y=6.83x-166.07$, (y is the volume of one droplet, x represents the driving voltage) with $R^2=0.997$. If the driving voltage is unchanged, the volume of droplet will be increased with the increased pulse width. Therefore, by manipulating the wave form of inkjet piezoelectric actuator and changing the driving voltage and pulse width through our home-made circuit and software, we can easily, accurately control the volume/mass of droplet, which will further facilitate inkjet printing of droplet generation for practical application.

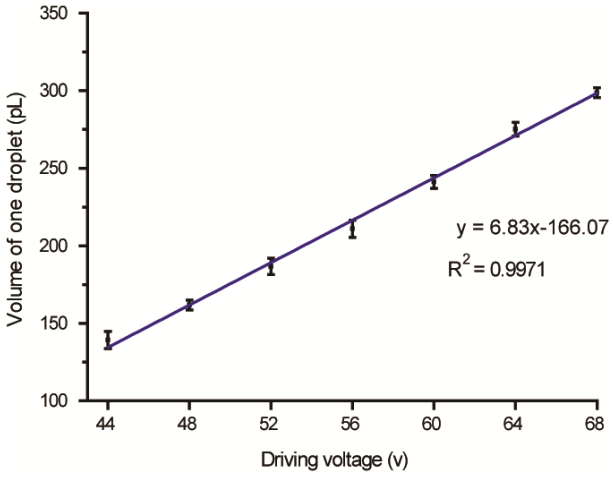

Fig. 9. Droplet volume increases linearly with the addition of driving voltage. (solution: 10% methanol (v/v), pulse width:18 μs, frequency: 1 KHz, each data point in the graph was measured for 10 repeated times).

3.5 Measurement of droplet velocity

To visualize the droplet formation, the high-speed microscope VW-9000 machine was employed to obtain a sequence of image during droplet formation (Fig. 10). Based on the information indicated in Fig. 10, we can calculate the velocity of DOD droplet ejection through the nozzle.

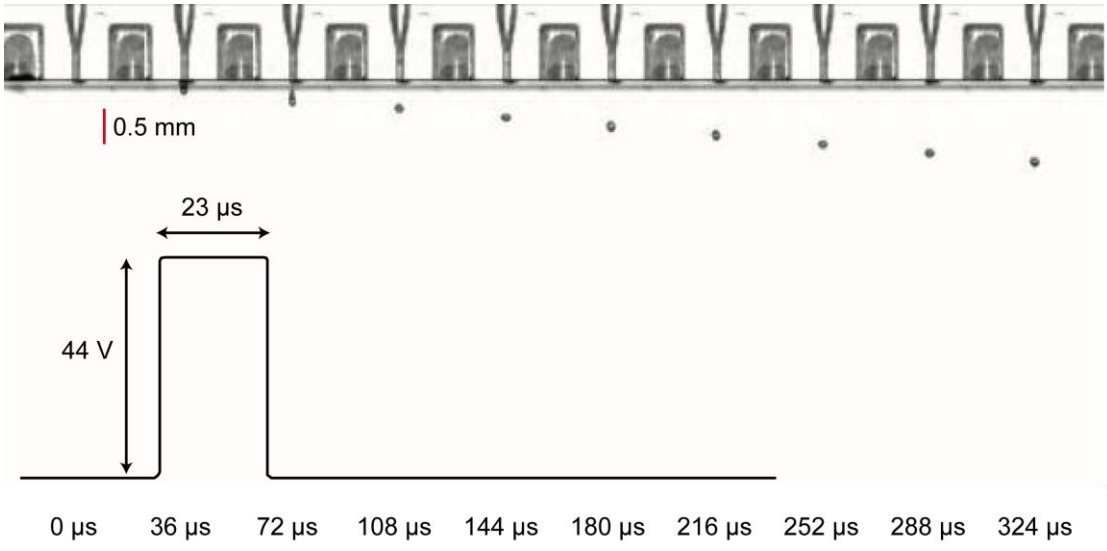

Fig. 10. Measurement of ejection droplet velocity, solution: water. Driving waveform frequency:1 KHz.

Conclusions

In summary, a control system was designed and established for the four channel inkjet piezoelectric actuator. The high accuracy and reproducible picoliter droplet was produced by the proposed system. The proposed four channel inkjet piezoelectric actuator system was desired to the application to the follow-up research work, including capillary electrophoresis (chapter 3) and chemiluminescence (chapter 4 and chapter 5).

Reference

[1] P. Calvert, Chem. Mater., 2001, 13, 3299-3305.

[2] B. J., de Gans, P. C., Duineveld, U. S., Schubert, Adv. Mater., 2004, 16, 203–123.

[3] J. H. Oh, S. Y. Lim, J. Micromech. Microeng., 2010, 20, 015030 (9pp).

[4] K. Y. Shin, S. H. Lee, J. H. Oh, J. Micromech. Microeng., 2011, 21, 045012 (11pp).

[5] R. J. Wood, E. Steltz, R. S. Fearing, Sensors and Actuators A: Physical, 2005, 119, 476 - 488.

[6] M. Karpelson, G.-Y. Wei, R. J. Wood, sensors and actuators A: Physical, 2012, 176, 78-89.

[7] K. Suresh, G. Uma, M. Umapathy, journal of intelligent material systems and structures, 2012, 25, 587-593.

[8] Zeng, H. L; Weng, Y; Ikeda, S; Nakagawa, Y; Nakajima, H; Uchiyama, K. Anal. Chem. 2012, 84, 10537-10542.

[9] Chen, F. M; Zhang, Y. D; Nakagawa, Y; Zeng, H. L; Luo. C; Nakajima, H; Uchiyama, K; Lin, J-.M. Talanta, 2013, 107, 111-117.

[10] Luo, C; Ma, Y; Li, H. F; Chem, F. M; Uchiyama, K; Lin, J.-M. J. Mass Spectrom. 2013, 48, 321-328.

[11] Chen, F. M; Lin, Z; Zheng, Y. Z; Zeng, H. L; Nakajima, H; Uchiyama, K; Lin. J.-M. Anal. Chim. Acta, 2012, 739, 77-82.

[12] D. Jang, D. Kim, J. Moon, Langmuir, 2009, 25, 2629-2635.

[13] V. Bergeron, D. Bonn, J.Y. Martin, L. Vovelle, Nature, 2000, 405, 772-775.

[14] J.E. Fromm, IBM J. Res. Dev., 1984, 28, 322-333.

[15] P. Shin, J. Sung, M.H. Lee, Microelectron. Reliab., 2011, 51, 797-804.

[16] H.M. Dong, W.W. Carr, J.F. Morris, Phys. Fluids, 2006, 18.

[17] H.Y. Gan, X.C. Shan, T. Eriksson, B.K. Lok, Y.C. Lam, J. Micromech. Microeng., 2009, 19.

[18] R.M. Verkouteren, J.R. Verkouteren, Langmuir, 2011, 27, 9644-9653.

Chapter 3

A piezoelectric drop-on-demand generator for accurate samples in capillary electrophoresis

1. Introduction

In the past decade, microdroplet techniques are of great interest in research due to its rapid mass/heat transfer, reduced sample consumption and ultra-high throughputs [1-4]. Microdroplets have been widely applied in various areas, such as synthesis microreactors [5], sample injection in analytical methods [6,7], and microarray-based dispensing technique [8]. Moreover, precision-controllable nanoliter-droplets are recognized as an excellent pathway for biological studies [9,10], especially in single-cell analysis and drug screening [11,12]. For these reasons, numerous strategies have been developed for droplet formation and manipulation. Microfluidic-created shear field on integrated microchip is extensively utilized for high-throughput droplet formation [13-18]. Alternatively, electrowetting-based digital microfluidics allows the formation of sub-microliter droplets and controllable manipulation [19-21]. Other mechanisms including electrospray [22], surface tension [23] are also used for droplet generation, all of which provide new possibility for the wide application of droplet-based systems.

Ink-jet printing is a novel and powerful technology that can produce precisely controllable droplet with specified volume and velocity, potentially expanding in drug screening [24], tissue engineering [25] and electronics manufacturing [26]. Compared to other methods, the ink-jet-based droplet generation is especailly attractive because the droplet contents can be easily analyzed by various methods since it can be compatibly connected with analytical techniques, such as nanoliter microarray based chemiluminescent detection [27], capillary electrophoresis (CE) [28], and mass spectrometry (MS) [29]. The mechanism of the ink-jet process has been well studied

[30]. Factors such as the properties of the solution (viscosity, density and surface tension), the characteristic of driving waveform and the ink-jet head structure has been found to affect the ink-jet process seriously [31-34].

Capillary electrophoresis is a powerful method for both qualitatively and quantitatively analyzing sample rapidly and precisely. Coupling the ink-jet droplet generation with capillary electrophoresis, not only provides an approach to chemically analyze the contents of droplet; but also can provide a novel method for the sampling. The ink-jet printing droplet has been previously coupled with capillary elecphoresis [35], where an acoustic levitator is used to achieve analyte enrichment. This work is pioneering, however, a detailed study about the control of droplet volume for sampling in electrophoresis; the separation performance of droplet contents and the quantitative relationship is still in great demand. Our group previously reported the application of ink-jet-printing as an accurate sampling method for capillary electrophoresis [28].

In this work, a systematic characterization of this system, especially the droplet generation control and the quantitative relationship of ink-jet-based sampling was performed. A home-made circuit and software for driving the piezoelectric actuator were described. The waveform (the driving voltage and the pulse width) was precisely controlled for stable, drop-on-demand droplet formation. Various solutions (methanol/water, caffeine/water and protein/water and etc.) were dispensed as single on-demand droplet by adjusting the driving waveform within appropriate ranges. The relationship between the voltage, width of pulse and the volume of droplets was also investigated. Droplets containing theobromine, caffeine and theophiline were separated by capillary electrophoresis using sodium dodecyl sulphate (SDS) as the micellar phase. Quantitative relationship between the injection volumes and signal responses were obtained for these three substances, respectively.

2. Materials and methods

2.1 Apparatus

The ink-jet microchip was provided by Fuji Electric Co., Ltd. (Tokyo, Japan). VW-9000 High-speed microscope (camera units: high-speed monochrome VW-600M, macro zoom units: long-distance macro zoom unit VW-Z2 with 4x optical zoom) was from Kyence Corporation (Tokyo, Osaka). The balance BP2111D was provided by Sartorius (Goettingen, Germany). The UV detector (Model: CE-971UV) for capillary electrophoresis was from JASCO (Tokyo, Japan). All aqueous solutions were prepared by ultrapure water which was purified by Millipore-Q device (Millipore Japan Co., Tokyo, Japan).

2.2 Reagents

Ethanol, glycerol, methanol, theobromine, caffeine, theophiline were purchased from Wako Pure Chemical Industries Ltd. (Tokyo, Japan). Extran MA01 was purchased from Merck (Darmstadt, Germany). NaOH and HCl from Kanto Kagaku (Tokyo, Japan). All aqueous solutions were prepared by ultrapure water which was purified by Millipore-Q device (Millipore Japan Co., Tokyo, Japan). The polystyrene microspheres of carboxylate-modified (i.d.: 40 nm, 4%) was purchased from Duke Scientific coorporation (Pala Alto, CA, USA). All buffers were filtered through a 0.45 μm membrane filter before using.

2.3 Pretreatment and assembly of ink-jet chip

The pretreatment of ink-jet chip was performed according to the instructions provided by the supplier, and was described previously [27]. Basically, the ink-jet microchip (See Fig. 1) microchannel was filled with a 20% (w/w) Extran MA 01 solution for 30 min to clean the channel and make the channel hydrophilic. Then the channels were washed with ultrapure water. After that, sample solutions were introduced into the channels of the ink-jet microchip through capillary tubes (Drummond, 75 mm hematocrit tube, 0.1 mL). The piezoelectric ceramics on the

ink-jet was connected with the control circuit.

2.4 Image Capturing

The high-speed microscope VW-9000 machine is employed to observe the droplet formation of ink-jet chip. As shown in Fig. 1, the microscope was placed on the holder, whose position and direction can be regulated. The nozzle part of the ink-jet was set as the focus of the microscope to monitor the process of droplet formation. The frame rate of the camera was 35000fps and the resolution was 256×128 pixels.

2.5 Measurement of volume/mass of droplet

It should be noted that for measurement of small-volume droplet, special consideration of evaporation should be taken into to obtain accurate mass/volume data. In the experiment, the measurement of volume/mass of droplet was performed according to a method reported previously [36]. Basically, the mass of 10 000 droplets were monitored on an accurate balance automatically at a time interval of 10s. Then another 10 000 droplets were ejected and the mass was recorded. The accurate mass of the droplet was calculated from the mass increase which incorporated the consideration of the loss caused by evaporation.

2.6 Ink-jet-based droplet formation for sample injection in capillary electrophoresis

The ink-jet printing of droplet formation is used for sample injection of capillary electrophoresis. The capillary inlet was placed in the upward, the nozzle of ink-jet is aligned with the inlet of capillary tube under the monitor of microscope as shown in Fig. 1. The ink-jet is fixed on a XY-stage with frames. The position precision of XY-stage used in our experiment is less than 0.5μm. Therefore by adjusting the XY-stage handfully, the nozzle of ink-jet is moved just on top of the capillary tube that the droplet generated can fall directly into the capillary tube. Fig. 1 shows the

whole experimental setup which includes the ink-jet printing system, the observation system and the capillary electrophoresis system. For each electrophoresis sample injection, the inlet of capillary was moved up out of the buffer reservoir, with 2 cm higher than the outlet of capillary. The ink-jet nozzle is just on top of the inlet of capillary with a distance of 0.1 cm. The droplets generated directly fall into the capillary inlet. When all the droplets were entering the capillary, the capillary was moved down about 2 cm into the buffer reservoir. Then high voltage is applied for capillary separation.

Capillary separation was performed at the room temperature 20±0.5℃ and relative humidity 39±1% RH. The buffer solution: 50mM glycine-NaOH buffer, pH 9.5, sample: caffeine, theobromine, theophilline dissolved by the buffer solution; high voltage: 10kV, capillary: ID: 50μm, length：effective Length:43cm. Absorbance wave length: 254nm, driving waveform: pulse width: 27μs, driving voltage: 44V, frequency: 1KHz.

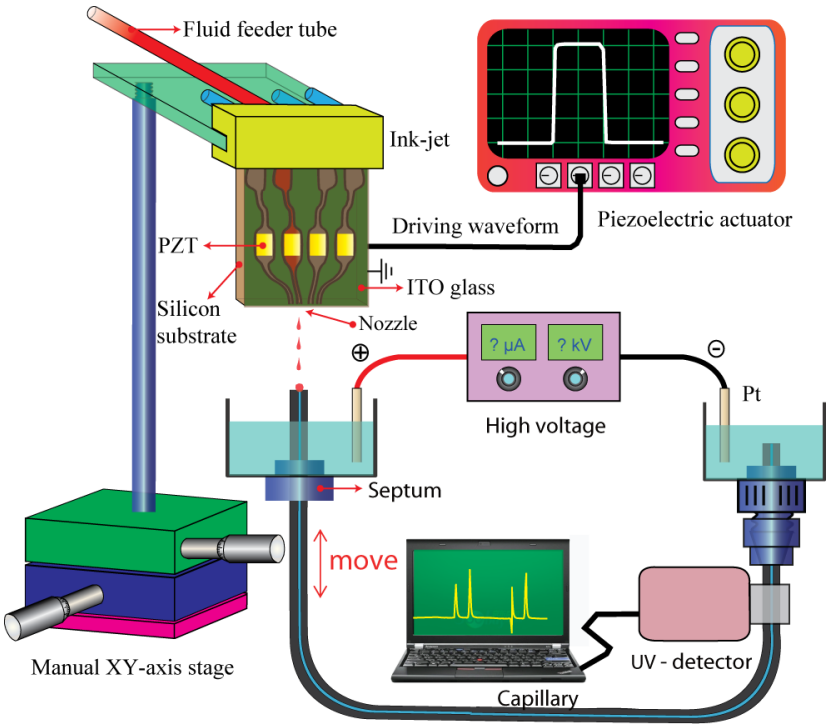

Fig. 1. Schmatic illustration of whole experimental setup. Ink-jet printing of droplet generation, high-speed micro observation system, capillary electrophoresis system are presented in the figure.

3. Results and discussion

3.1 Ink-jet printing of droplet formation

Ink-jet-based droplet formation has been widely used for a variety of applications. In conventional, commercialized ink-jet printing instruments, and actuator parameter is always fixed because only some certain solutions can be ejected. Under this condition, the inverse (Z) of the Ohnesorge number (Oh), which is defined as the ratio between the reynolds number and a square root of the weber number, is utilized to consider whether a solution can be ejected or not. However, this limitation constrains the applicability of ink-jet printing for various purposes. In our experiments, a home-made driving circuit combined with a software to control the piezoelectric actuator was employed to control the ejection of droplets. With this experimental setup, the parameters of actuator can be easily manipulated and tuned, which will facilitate the control of droplet formation.

The above results also indicated that it is possible to generate the stable and drop-on-demand droplets via manipulating the driving voltage and pulse width into appropriate scopes from solutions of different composition that have different physical properties. Stable, single, drop-on-demand droplet generation is desirable in a variety of applications for its advantages of uniformity, ease of operation and definite mass and volume. In the experiments, we examined nine different solutions with our method and a proper range of driving voltage and pulse width was identified for respective solution (see Fig. 3). As shown in Fig. 3, the color areas indicate the ranges that stable, drop-on-demand droplet can be generated. By using our home-made circuit and software, the driving voltage and pulse width can be easily tuned that proper conditions of ink-jet printing can be identified for generating stable droplets from different solutions. Compared to conventional methodology, which can only use certain solutions, our approach has made it possible to use various solutions for stable, single, drop-on-demand ink-jet droplet formation. These results indicate that our technique is very promising because the wide scopes of solutions used for

ink-jet printing can enlarge the its application for various purposes.

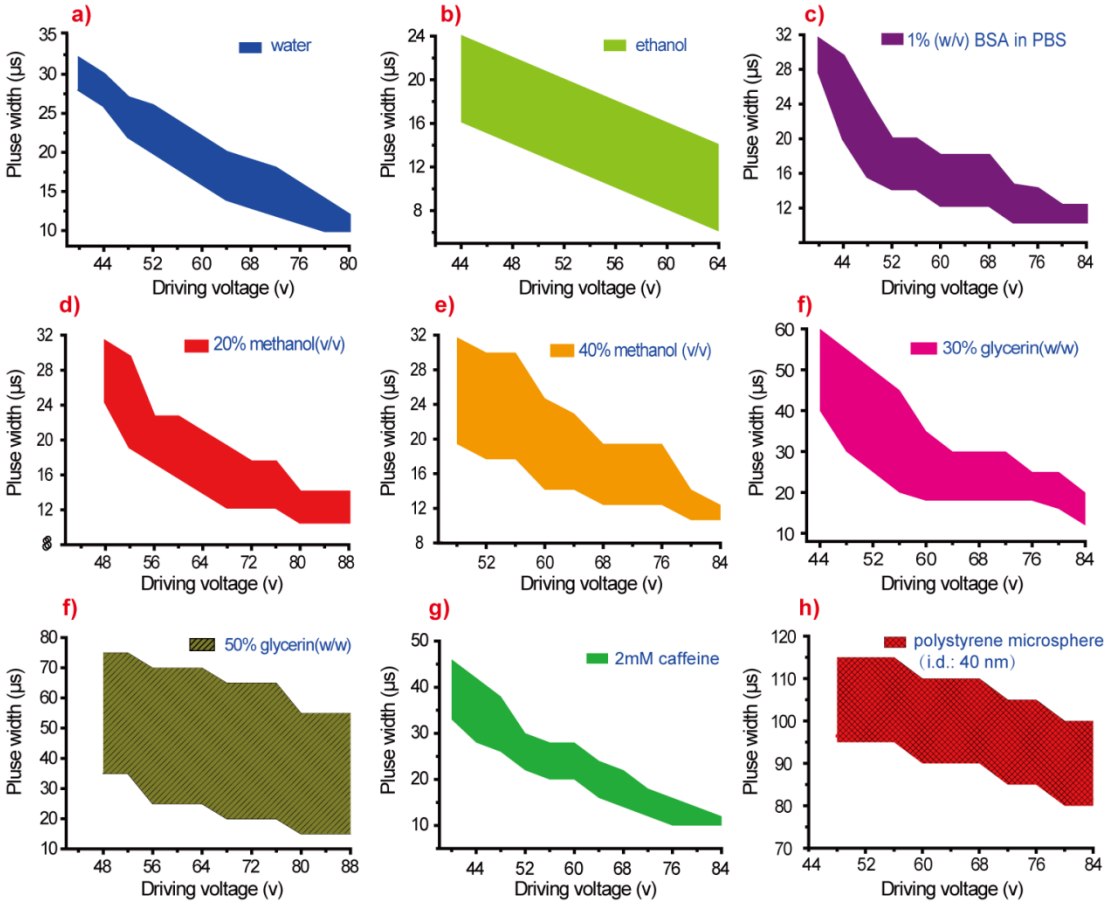

Fig. 3. Generation of the stable, uniform and drop-on-demand droplet for different kinds of solutions under different driving voltage and pulse width. The color area in each figure represents the proper ranges of driving voltage and pulse width for respective solutions.

3.2 Manipulation of droplet volume

With our designed system, the volume of droplet can also be easily controlled by manipulating the waveforms of driving actuator. As shown in Fig. 4a, the volume/mass of the droplets were of good linear relationship with different driving voltage when the droplets were generated by ink-jet printing. The linear relationship between the volume of droplet and the rise of driving voltage is as following,

$$y=6.83x-166.07 \quad (1)$$

where y is the volume of one droplet, x represents the driving voltage, with R^2=0.9971.

On the other hand, when the driving voltage is fixed, the volume of droplet will be increasing with the addition of pulse width (Fig. 4b) with the linear relationship:

$$y=7.58x-1.11 \qquad (2)$$

with R^2=0.9989.Therefore, by manipulating the wave form of ink-jet piezoelectric actuator, changing the driving voltage and pulse width through our home-made circuit and software, we can easily, accurately control the volume/mass of droplet, which will further facilitate ink-jet printing of droplet generation for practical application.

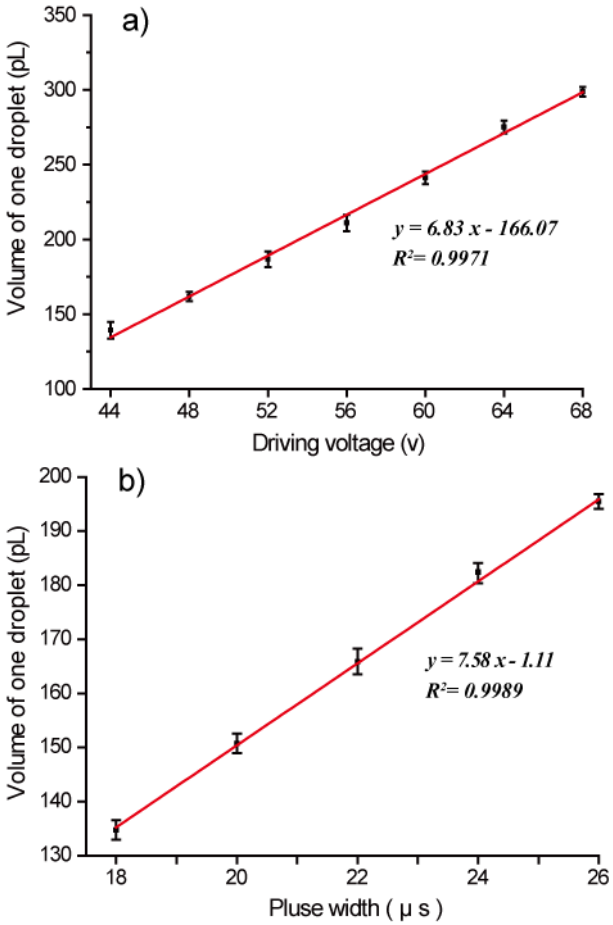

Fig. 4 The linear relationship between droplet volume and driving waveform. a) the droplet volume versus the driving voltage. b) the droplet versus the pulse width. For both conditions, very good linear relationship were obtained. Solution: 10% methanol (v/v), Pulse width: 18μs, Frequency: 1 KHz. Each data point in the graph was measured for 10 repeated times).

3.3 Application as sample injector for capillary electrophoresis

Traditional capillary electrophoresis injection modes such as siphon injection, pressure injection, vacuum injection and electrokinetic injection suffered from the injection discrimination effect and the deviation of sample volume between each injection. Besides, these methods can't give out the absolute, accurate injection volume [37-39]. Our laboratory previously developed a capillary electrophoresis system using ink-jet-printing as sampling method. Ink-jet printing can generate highly stable and controllable nanoliter drop-on-demand droplet, thus is ideal for precise and accurate sample injection in electrophoresis. In a previous study, the injection process was thoroughly investigated and the analytical performance of this new electrophoresis system was compared with traditional systems. The whole experimental setup was shown in Fig. 1. The inlet of capillary tube was aligned with the nozzle of inkjet under microscope through adjusting xy-stage. The droplets generated by inkjet printing were then directly infused into the capillary tube and finished the process of sample injection. As stated before, the volume of droplets can be adjusted through changing the driving voltage and pulse width in proper scopes. For electrophoresis injection, the sample volume was also controlled by the number of droplets for each injection. Fig. 5a shows the electrophoresis graph of samples composed of different number of droplets, which is determined by the number of pulses applied on the piezoelectric actuator of the inkjet. In Fig.6a, different number of droplets (1, 5, 10, 50, 100) were injected into the capillary for electrophoresis. The the signal intensity was increasing with the increased injection volume. Fig. 5b shows the linear fitting of the peak area of each injection corresponding to the number of droplets injected, with the fitting line of $y=2.11x+3.98$, where y is the signal intensity, and x is the number of droplet. This result was reasonable because the droplet generated by inkjet printing under our experimental condition was uniform and stable. All the contents in the droplet were accurately loaded into the capillary tube, thus the signal response should be consist with the quantity of injection volumes.

These results indicated that the inkjet-based droplet generation can be used to

sample injection for practical electrophoresis application. Besides, the volume of the droplet used in this experiment is calculated to be 194 pL (RSD=1.3%, n=10) with methods described before. Considering the concentration of the solution is known (2 mM caffeine), the absolute quantity of sample can be obtained. Based on these results, we propose that with the inkjet printing of droplet generation for electrophoresis injection, a lot of parameters, including droplet volume, the concentration of the solution, the instrumental responding factor for certain substance can be determined.

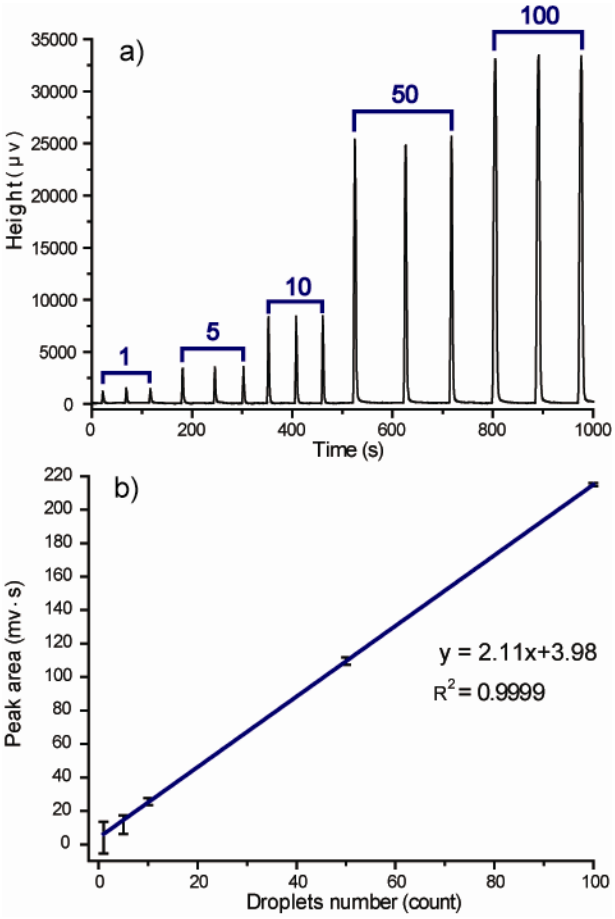

Fig. 5 a) The electrophoresis graph of samples composed of different number of droplets(1, 5, 10, 50, 100 repsectively). b) The linear fitting of peak area versus the number of droplets. (For each data point, 10 times of repeated experiments were measured)

In the work, a systematic characterization of quantitative relationship of ink-jet-based sampling for electrophoresis was performed. With our designed ink-jet system, the microdroplet can be easily, precisely generated and controlled from

various solutions. This serves as an essential quality control for ink-jet sampling method. As shown in Fig. 1. The inlet of capillary tube was aligned with the nozzle of ink-jet under microscope through adjusting XY-stage. The droplets generated by ink-jet printing was then directly infused into the capillary tube and finished the process of sample injection. As a model scheme, solutions composing of theobromine, caffeine, theophiline are used for droplet generation and separated by micellary capillary using sodium dodecyl sulphate (SDS) as the micellar phase.

With the utilization of ink-jet for sampling in electrophoresis, the injection volume can also be manipulated by changing the driving waveform or the number of pulses. In the experiments, we investigated the electrophoresis performance of the different injection volume by controlling the number of droplets for each injection. Fig. 6a shows the electrophoresis graphs of samples composed of different number of droplets (2, 5, 10, 20, 40) injected into the capillary for electrophoresis. Fig. 6b shows the linear fitting of peak area of different substances corresponding to the number of droplets injected. As shown in Figs. 6a and 6b, these three substances were successfully separated under our condition. And the intensity of respective substance increases linearly with the addition of injection volume. In the experiment, we also control the injection volume constant with fixed number of droplets (40) and with the increased concentration of analytes, the respective signals also increase linearly as shown in Table 1. These results indicate the high reliability and accuracy of the ink-jet based electrophoresis method.

Such high accuracy and reliability were reasonable because the droplet generated by ink-jet printing under our experimental condition was uniform and stable. All the contents in the droplet were accurately loaded into the capillary tube, thus the signal response should be consist with the quantity of injection volumes. These results indicated that the ink-jet-based droplet generation can be used to sample injection for practical electrophoresis application. Besides, the volume of the droplet used in this experiment can be calculated to be 179 pL (RSD=1.2%, n=10) with methods described before, Considering the concentration of the solution is known (4 mM

caffeine, 2 mM theobromine, 4 mM theophiline), absolute quantity of sample can be obtained. Based on these results, we propose that with the ink-jet printing of droplet generation for electrophoresis injection, a lot of parameters, including droplet volume, the concentration of the solution, the instrumental responding factor for certain substance can be determined. The separation and analysis of some biological and environmental samples are continuously studying in our two collaboratories.

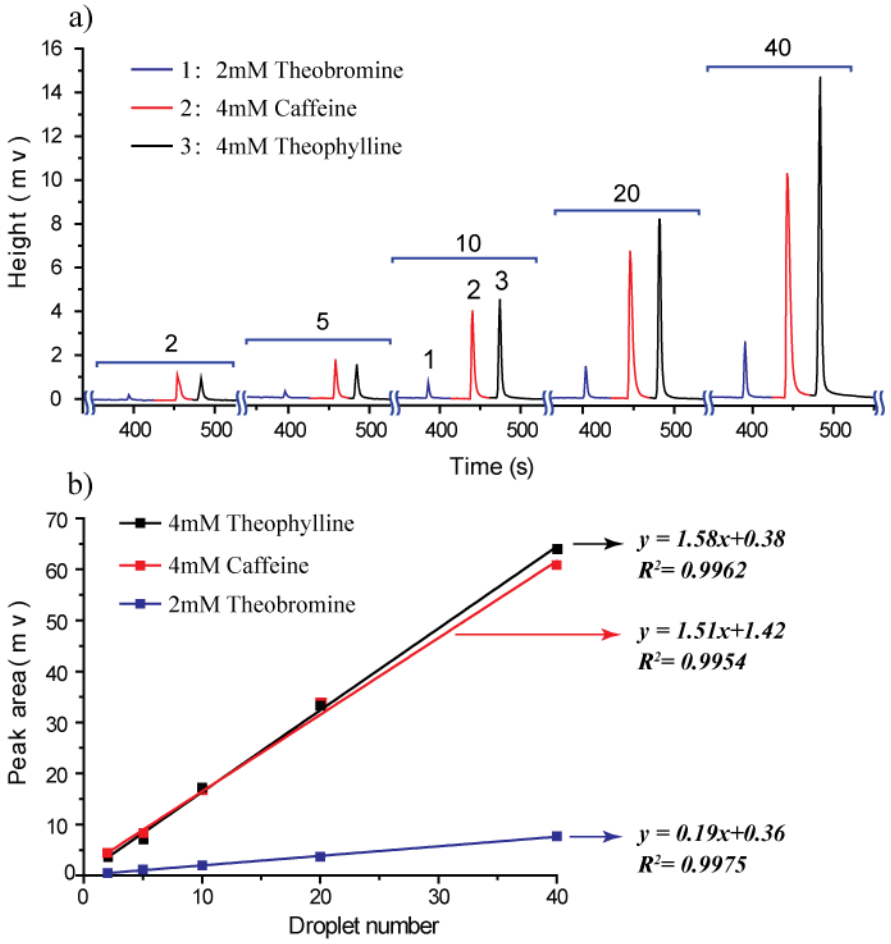

Fig. 6. The correspondence of droplets number to the signal intensity of capillary electrophoresis. a) The electrophoresis graph of samples composed of different number of droplets (2, 5, 10, 20, 40 repsectively). b) The linear fitting of peak area versus the number of droplets. (For each data point, 10 times of repeated experiments were measured).

Table 1. The performace of capillary electrophoresis for different concentration of

solutions injected by ink-jet printing. Samples composed of different concentration of solutions with fixed volume (40 droplets).

Analyte	t_r/ min	RSD of t_r / % (n=10)	RSD of peak area / %(n=10)	Linearity-dose curve	Detection limit / (mM/L)
Theobromine	6.55	0.2	0.83	y=3.93 x – 0.11 R^2=0.9983	0.08
Caffeine	7.55	1.2	1.22	y=17.12 x – 2.88 R^2=0.9993	0.02
Theophilline	8.38	2.1	0.78	y=33.91 x – 2.81 R^2=0.9985	0.06

4. Conclusion

In this work, ink-jet printing for uniform, stable, drop-on-demand droplet formation was developed and investigated. The utility of home-made circuit board and software, which enables us to tune the driving waveform of ink-jet chip conveniently. The solutions that can be ejected are enlarged extensively and the formed droplets can be manipulated easily and precisely. Finally, this highly precise picoliter droplet generator is employed for sampling of capillary electrophoresis which is advantageous over conventional injection methods in that the actual volume of sampling can be obtained. We propose that the combination of picoliter droplet generator with capillary electrophoresis will be applicable for real sample separation and analysis. Besides, the ink-jet printing platform developed can be applied for a variety of other practical purposes.

References

[1] L. Mazutis, J.-C. Baret, P. Treacy, Y. Skhiri, A. F. Araghi, M. Ryckelynck, V. Taly, A. D. Griffiths, Lab Chip, 2009, 9, 2902-2908.

[2] D. T. Chiu, R. M. Lorenz, G. D. M. Jeffries, Anal. Chem., 2009, 81, 5111-5118.

[3] S.-Y. Teh, R. Lin, L.-H. Hung, A. P. Lee, Lab Chip, 2008, 8, 198-220.

[4] X. C. I. Solvas, M. Srisa-Art, A. J. Demello, J. B. Edel, Anal. Chem., 2010, 82, 3950-3956.

[5] H. Song, D. L. Chen, R. F. Ismagilov, Angew. Chem. Int. Edit., 2006, 45, 7336-7356.

[6] S. Liu, P. K. Dasgupta, Anal. Chem., 1995, 67, 2042-2049.

[7] M. Abdelgawad, M. W. L. Watson, A. R. Wheeler, Lab Chip, 2009, 9, 1046-1051.

[8] D. N.Gosalia, S. L. Diamond, Proc. Natl. Acad. Sci., U.S.A. 2003, 100, 8721-8726.

[9] P. Mary, A. Chen, I. Chen, A. R. Abate, D. A. Weitz, Lab Chip, 2011, 11, 2066-2070.

[10] A. C. Hatch, J. S. Fisher, A. R. Tovar, A. T. Hsieh, R. Lin, S. L. Pentoney, D. L. Yang,A. P. Lee, Lab Chip, 2011, 11, 3838-3845.

[11] S. Koster, F. E. Angile, H. Duan, J. J.Agresti, A. Wintner, C. Schmitz, A. C. Rowat, C.A. Merten, D. Pisignano, A. D. Griffiths, D. A.Weitz, Lab Chip, 2008, 8, 1110-1115.

[12] A. Schmid, H. Kortmann, P. S. Dittrich, L. M. Blank, Curr. Opin. Biotech., 2010, 21, 12-20.

[13] M. Joanicot, A. Ajdari, Science, 2005, 309, 887-888.

[14] V. V. Zuev, B. Steinhoff, S. Bronnikov, H. Kothe, I. Alig, Polymer, 2012, 53, 755-760.

[15] T. Horie, K. Nakatsune, T. Matsumoto, K. Tateishi,Ohmura, N. Chem. Eng. Process., 2011, 50, 1-8.

[16] K. B. Migler, Phys. Rev. Lett., 2011, 86, 1023-1026.

[17] T. Thorsen, R. W. Roberts, F. H. Arnold, S. R. Quake, Phys. Rev. Lett., 2001, 86, 4163-4166.

[18] T. G. Mason, J. Bibette, Phys. Rev. Lett., 1996, 77, 3481-3484.

[19] R.B. Fair, Microfluid. Nanofluid., 2007, 3, 245-281.

[20] M. G. Pollack, A. D. Shenderov, R. B. Fair, Lab Chip, 2002, 2, 96-101.

[21] A. R. Wheeler, Science, 2008, 322, 539-540.

[22] J. U. Park, J. H. Lee, U. Paik, Y. Lu, J. A. Rogers, Nano Letters, 2008, 8, 4210-4216.

[23] J. Liu, J.-M. Lin, D. J. Knopp, Micromech. Microeng, 2008, 18, 095014.

[24] G. Arrabito, B. Pignataro, Anal. Chem., 2010, 82, 3104-3107.

[25] K. Pataky, T. Braschler, A. Negro, P. Renaud, M. P. Lutolf, J. Brugger, Adv. Mater. , 2012, 24, 391-396.

[26] B. -J. de Gans, P. C. Duineveld, U. S. Schubert, Adv. Mater., 2004, 16, 203-213.

[27] F. Chen, Z. Lin, Y. Zheng, H. Zeng, H. Nakajima, K. Uchiyama, J.-M. Lin, Anal. Chim. Acta, 2012, 739, 77-82.

[28] H. Zeng, Y. Weng, S. Ikeda, Y. Nakagawa, H. Nakajima, K. Uchiyama, Anal. Chem., 2012, 84, 10537−10542.

[29] L. Chen, M.Yuan, H. Li, F. Chen, K. Uchiyama, J.-M. Lin, J. Mass Spectrom., 2013, 48, 321-328.

[30] D. Jang, D. Kim, J. Moon, Langmuir, 2009, 25, 2629-2635.

[31] V. Bergeron, D. Bonn, J. Y. Martin, L.Vovelle, Nature, 2000, 405, 772-775.

[32] P. Shin, J. Sung, M. H. Lee, Microelectron. Reliab, 2011, 51, 797-804.

[33] H. M. Dong, W. W. Carr, J. F. Morris, Phys. Fluids., 2006, 18, 072102.

[34] H. Y. Gan, X. Shan, T. Eriksson, B. K. Lok, Y. C. Lam, J. Micromech. Microeng, 2009, 19, 055010.

[35] M. Petersson, J. Nilsson, L. Wallman, T. Laurell, J. Johansson, S. Nilsson, J. Chromatogr., B, 1998, 714, 39-46.

[36] R. M. Verkouteren, J. R. Verkouteren, Anal. Chem., 2009, 81, 8577-8584.

[37] X. Huang, M. J. Gordon, R. N. Zare, Anal. Chem., 1988, 60, 375-377.

[38] D. J. Rose, Jr., J. W. Jorgenson, Anal. Chem., 1988, 60, 642-648.

[39] E. V. Dose, G. Guiochon, Anal. Chem., 1992, 64, 123-128.

Chapter 4

Development of an automatic multi-channel ink-jet ejection chemiluminescence system and its application to the determination of horseradish peroxidase

1. Introduction

Chemiluminescence (CL) is an excellent analytical method, and has been extensively developed in bio-analytical assay because of its high sensitivity, wide linear range, and low scattering light interference [1]. Besides this, it was easily operated and automated when combined with flow-injection analysis (FIA) [2]. In the past decade, Flow injection analysis with chemiluminescence detection (FIA-CL) has been widely used in clinical medicine, food analysis and environmental testing [3-5]. However, the FIA-CL technologies suffered some disadvantages: large sample-consumption and manually sampling [6]. With the development of automatic and miniaturized analysis systems, micro total analysis systems (μ-TAS) have attracted great interest due to advantages in portability and speed of analysis [7, 8]. There is high demand in developing automatic controllable devices that could eject a very small amount of liquid with contactless, low-cost, and high reproducibility.

The ink-jet device was recognized as a very important industrial technology that can precisely control the velocity and volume at defined microarray spots [9]. It has attracted great interest in various fields for dispensing nano- and pico-liter levels of liquid on the surface of a wide variety of substrates [10-12]. These ultra-small droplets could be automatically dispensed by ink-jet and reached the reaction location precisely through the nozzle [13]. Currently, ink-jet printing technologies have been demonstrated to be suitable for simultaneous multiple analytes sensing with thousands of detection zones using microliter volumes of samples [14, 15]. Ink-jet was also

successfully used in analytical chemistry, such as an ultra small sample injection instrument for capillary electrophoresis [16], gas chromatography [17], mass spectrometers [18, 19] and immunochemical sensor [20, 21]. The application of ink-jet printing in micro-scale analysis could not only satisfy ultra-rapid and low reagent consumption for the high-throughput analysis, but also typically facilitate more precise sample injection and automatically control instrumental tools. Based on these features, the inkjet technology could be comparable with flow-injection analysis with unique advantages, such as easy operation and automatic control. Therefore, the ink-jet printing technology showed great potential in CL analysis, and could be of great significance in automatically sampling with low sample consumption.

Horseradish peroxidase (HRP) is a very important enzyme reagent that has highly efficient catalysis ability on the decomposition of peroxide [22]. It has been widely used as a probe in immunoassay for the quantification of antigen or antibody [23]. Many analytical strategies have been developed to detect HRP, such as colorimetric solution assay, electrical method, fluorescence spectrum, as well as CL analysis [24, 25]. For example, orthophenylene diamine, 2, 2′-azinobis 3-ethylbenzothiazoline-6-sulfonic acid or tetramethylbenzidine could react with HRP to produce substance with ultraviolet-visible absorption or electrical signal [26, 27]. The absorption analysis for HRP was extremely limited by its low sensitivity. The fluorescent analysis for HRP with greatly improved sensitivity was suffered from high background interruption [28]. Therefore, CL can be an excellent method for HRP detection due to its high sensitivity. Here, luminol became an effective CL substrate for HRP because of its high CL signal intensity [29].

In this work, an automatic multi-channel ink-jet ejection CL system has been successfully developed and used to detect HRP with high sensitivity and reproducibility. Different from flow injection method and manual pipette CL method, the ink-jet device was used as the sample ejection device for the determination of trace amount of HRP, which facilitated rapid and automated analysis. Furthermore, the ink-jet could precisely control the sample injection in small volume and the CL

reaction could be completed in short time. Hence, the automatic multi-channel ink-jet ejection CL system has great potential in automatic on-site CL dynamic investigation and bio-analysis.

2. Materials and methods

2.1 Apparatus

The four-channel ink-jet microchip was provided by Fuji Electric Co., Ltd. (Tokyo, Japan). AMS-05K10P/100 DC power was supplied by Max-Electronics Co., Ltd. (Tokyo, Japan). The electromotive x-y stage MMU-60X was purchased from Chuo Precision Industrial Co., Ltd. (Tokyo, Japan). 75MM hematocrit tube was purchased from funakoshi, Ltd (Tokyo, Japan). The CL signal was recorded by a BPCL ultra-weak CL analyzer (Institute of Biophysics, Chinese Academy of Science, Beijing, China). BHP9504 micro-plate luminescence analyzer was from Beijing Hamamatsu Technology Co., Ltd. (Beijing, China). All aqueous solutions were prepared by ultrapure water which was purified by Millipore-Q device (Millipore Japan Co., Tokyo, Japan).

2.2 Reagents

3-Aminophthalhydrazide (luminol) was purchased from Acros Organics (Pittsburgh, U.S.A.). Dimethyl sulfoxide (DMSO) and Extran MA01 used for the cleaning of the ink-jet microchip were from Merck (Darmstadt, Germany). 4-Iodophenol (PIP) was obtained from Alfa Aesar Co., Ltd. (Tianjin, China). H_2O_2, $NaH_2PO_4 \cdot 2H_2O$, $Na_2HPO_4 \cdot 12H_2O$, hydrochloric acid were purchased from Beijing Chemical Reagent Co., Ltd. (Beijing, China). Tris (hydroxymethyl) aminomethane was from Roche. Diagnostics (Schweiz). Tridecafluoro-1, 1, 2, 2-tetrahydrooctyl trichlorosilane was from Sigma (St. Louis, MO). Bovine serum albumin (BSA), HRP conjugated and HRP were both from Bioss. Co., Ltd. (Beijing, China). All buffers

were filtered through a 0.45 μm membrane filter before using.

2.3 The pretreatment of substrate and ink-jet microchip

The glass slides (30 mm × 30 mm, Matsunami Glass Ind., Ltd., Osaka, Japan) for automatic CL analysis were cleaned by piranha solution (H_2SO_4 : 30% H_2O_2=3:1, v/v) and pure water respectively. Then, the pre-cleaned glass slides were silanized by exposure into tridecafluoro-1, 1, 2, 2-tetrahydrooctyl trichlorosilane vapor for 2 h.

The 4-channel ink-jet microchip with 995 μm of interval between channels was used in our experiment. Firstly, the ink-jet microchip microchannel was filled with a 20% (w/w) Extran MA 01 alkaline solution for 30 min to avoid bubble formation, Then the channels were washed by Milli-Q water, and filled with sample solutions for use, after that, sample solutions were introduced into the channels of the ink-jet microchip with capillary tubes (Drummond, 75MM Hematocrit Tube, 1mL).

2.4 Ejection CL detection system for multi-channel ink-jet microchip

To realize automatic CL microarray analysis, the ink-jet injection technique was used to eject the sample solutions automatically (Fig. 1) and the photograph of the instrument(Fig. S1).

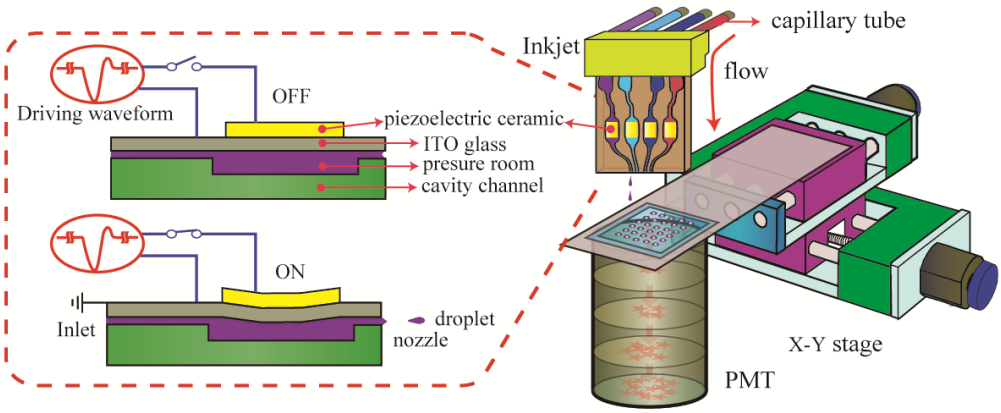

Fig. 1. Schematic diagram of the automatic ink-jet CL detection system and the principle of the ink-jet microchip.

Based on the bend mode of the piezoelectric ceramic that was tightly stuck on the loading chamber of ink-jet microchip, the ejection of droplets from multi-channel ink-jet was controlled by software. The pulsed power voltage was utilized to press the extrusion chamber via the piezoelectric device. Solutions were firstly loaded in the individual channels by the corresponding capillary tubes, then were dispensed by different nozzles onto the same position on the microarray glass slides.

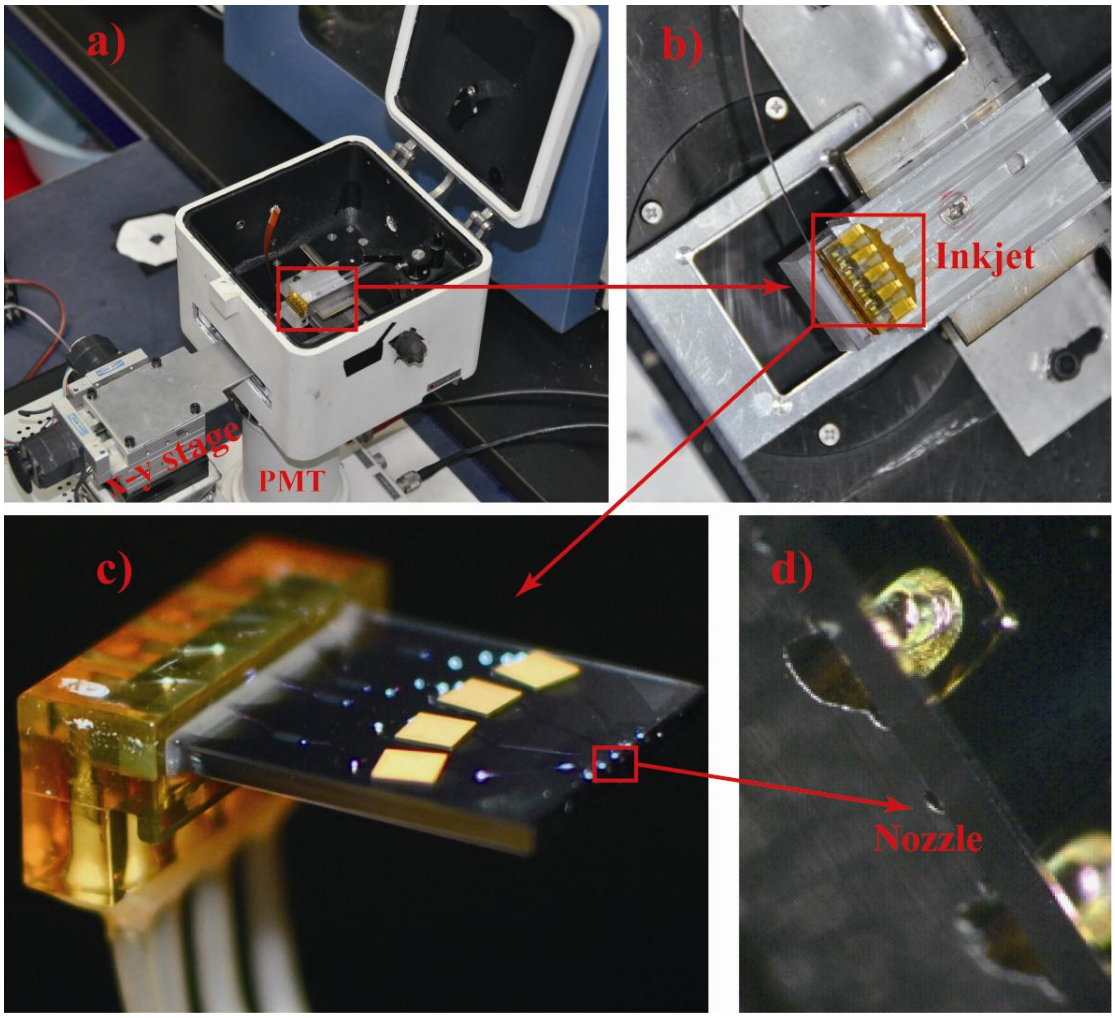

Fig. S1. The photograph of a) the instrument containing the inkjet, x-y stage for the glass slide moving, and PMT; b) the exact position of inkjet; and c) the amplified inkjet; d) the nozzle of the inkjet.

Here, the exactly ejecting positions on the glass slide were automatically controlled by an electromotive x-y stage via the laboratory-made software systems.

The precision of electromotive x-y stage was ±0.5 μm/step. The multichannel ink-jet ejection process was shown in Fig. 2. When the droplet was ejected on the glass slides, the photomultiplier (PMT) was used as detector to detection the CL signal at the same time. By adjusting the ejecting position of the reaction solution droplets, the CL signal of parallel microarray of CL reaction dots can be effectively recorded one by one. Finally, the data can be easily read by the laboratory-made software.

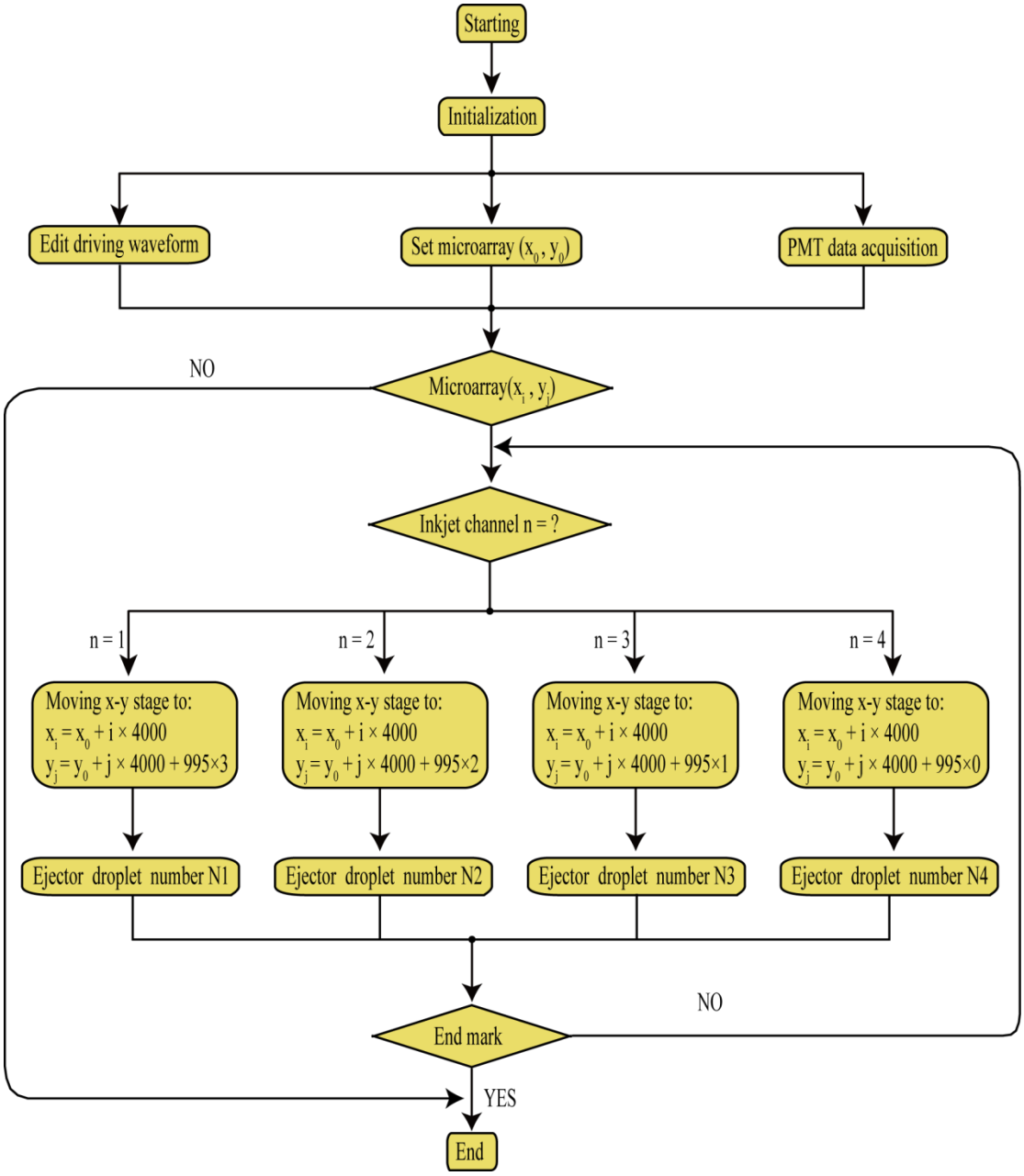

Fig. 2. Logic controlling block of the automatic ink-jet CL detection system.

2.5 Automatic CL analysis

In order to perform the CL analysis via the droplet microarray experiments, different solutions was loaded into channels by the corresponding capillary tubes. Then, H_2O_2, luminol, HRP and PIP solutions were ejected onto the glass for CL reaction. The sample droplets were accurately ejected on the same point to complete the mixing and detecting. This process was automatically controlled by the electromotive x-y stage. The CL signal was collected and amplified by PMT. The collected analog signal was performed by ultra-low input bias current operational amplifier and converted into digital signal by high precise A/D conversion chip. Finally, the digital signal was collected by a micro-processor and transferred through the USB interface to the software interface.

2.6 Detection of BSA-HRP

BSA-HRP was used as the target analyst to perform the practical test. In our experiments, 1.0 mg/mL of BSA-HRP was diluted with the Tris-HCl buffer (pH=8.5) to different concentions. Then, the BSA-HRP solutions was detected by the automatic ink-jet CL analysis. For comparison, the diluted BSA-HRP solutions introduced by pipetting were also determined by BHP9504 micro-plate luminescence analyser. In brief, BSA-HRP solutions with different concentration were pipetted into the microplate. Then the mixture of relative luminol solution and H_2O_2 solution was added into the microplate. The CL from each well on the microplate was recorded by BHP9504 micro-plate luminescence analyser. All the operation conditions of control test of BSA-HRP were the same as the above method for automatic ink-jet CL analysis shown in 2.5. Experiments were repeated more than three times.

3. Results and discussion

3.1 The volume of ejected droplet

To automatically control the ejection of the droplets, we designed a driving circuit combined with a home-made software to automatically control the

piezoelectric ceramic, which was settled on the ITO glass to press the micro-channels and perform the droplets ejection. The driving circuit included four independent driven modules, which can be separated and arbitrarily controlled via editing the driving frequency, driving voltage, and the drive waveform through the software. By changing and modulating the time (t) and voltage (V) of the supplied driving waveform (Fig. 3a), the volume and number of ejected droplets can be controlled. Based on the expansion principle of piezoelectric ceramic, the driving waveform was consisted with three periods of voltage, the relative driving time could be called as t_1, t_2 and t_3. To achieve the optimal driving waveform for the stable and uniform droplets, t_2 and t_3 were set at 80 μs and 20 μs respectively. Glycerin aqueous solution was selected as the test solution to investigate the ejection of droplets. 2×10^6 droplets of glycerin solution were ejected and weighted. The humidity should be kept greater than 40% to reduce the evaporation of droplets at the room temperature. We found that the volume of every droplet increased with the drive voltage (Fig. 3b). At the same time, with the increasing of concentration of glycerin solutions, the ejected volume of every droplet was decreased. When the concentration of glycerin solution reached 30% (w/w), and the driving voltage was less than 50 V, the inkjet chip couldn't eject any droplets. This was attributed to the increased viscosity of the high concentration of the glycerin solution. The RSDs in the whole ejection experiment were less than 3.5% (Table 1).

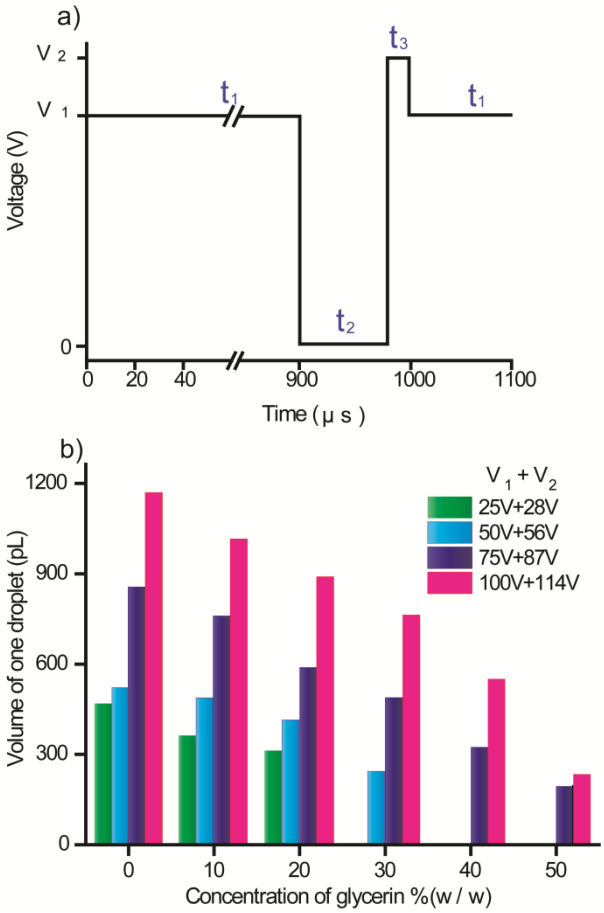

Fig. 3. Driving waveform of ink-jet microchip (a) and the volume of one droplet of glycerin solution in different concentrations driven by different voltages (b).

Regarding the ejection of the reaction solutions in automatic CL analysis, we ejected 2×10^6 droplets of reaction solutions with certain concentrations by ink-jet and weighted them. The RSDs of each solution with different concentrations were within 2.1% (n=8). The reason is that all the reaction solutions were diluted by the tris-HCl buffer, so the viscosity of the reaction solutions was controllable. Therefore, we assumed the deviation induced by viscosity in the volume of droplets of reaction solutions could not influence the precision of the automatic CL detection.

Table 1. the volume and RSD of each droplet of glycerin solution at different concentrations

Driving voltage	V1:75 V, V2: 87V		V1:100 V, V2: 114 V	
Glycerin conc.[wt%]	Volume of one droplet [pL]	RSD [%] n=10	Volume of one droplet [pL]	RSD [%] n=10
0	856	1.8	1170	2.1
10	780	2.7	1016	1.8
20	585	2.9	890	0.9
30	489	2.1	763	1.7
40	324	3.5	550	1.4
50	194	0.8	234	2.2

3.2 Ejection order of reaction solutions

Automatic luminol-H_2O_2-HRP CL analysis system platform was utilized and optimized in the present work. The solutions of luminol, H_2O_2 and HRP were ejected through three different channels located in one ink-jet microchip. The droplets ejected by the ink-jet device were mixed and reacted on the glass slide. Since the emission of CL was affected by the mixing state of the reaction solutions, different ejection order of solutions were investigated. The experimental results showed the strongest intensity and highest signal to noise ratio was monitored by injecting HRP solution into the mixture of H_2O_2 solution and luminol solution (Fig. 4). Hence, this ejection mode was utilized in the following experiments.

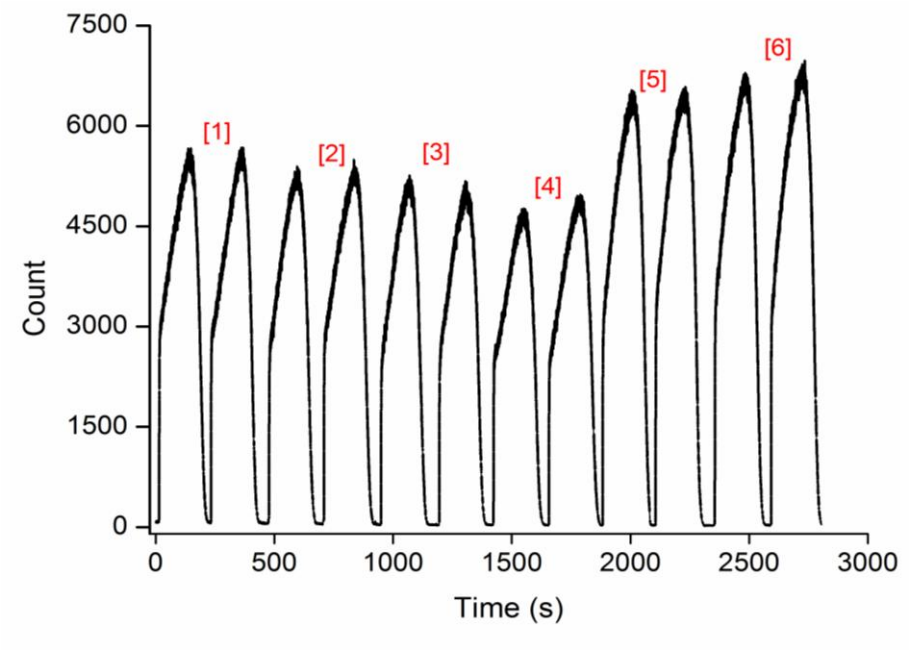

Fig. 4. Injection order of reaction reaction solutions: Each channel respectively ejcted 50droplet, [1]: Inject H_2O_2 to the mixture of luminol-HRP; [2]: luminol- H_2O_2- HRP; [3]: HRP - H_2O_2- luminol; [4]: HRP -luminol- H_2O_2; [5]: H_2O_2-HRP- luminol; [6]: H_2O_2- luminol - HRP .

3.3 Effect of the number of droplets on the CL intensity

The number of ejected droplets through each channel played an important role for the CL intensity. We have investigated the CL intensity by changing the number of ejected droplets from each channel (Fig. 5), with three reaction solutions keeping at the same number of droplets. When the number of droplets of three solutions were smaller than 50, the CL intensity was weak. With the increasing of the number of the droplet, CL lasted for longer time and much more reaction solutions were required. Therefore, 50 droplets of the each reaction solutions were adopted for the automatic CL determination.

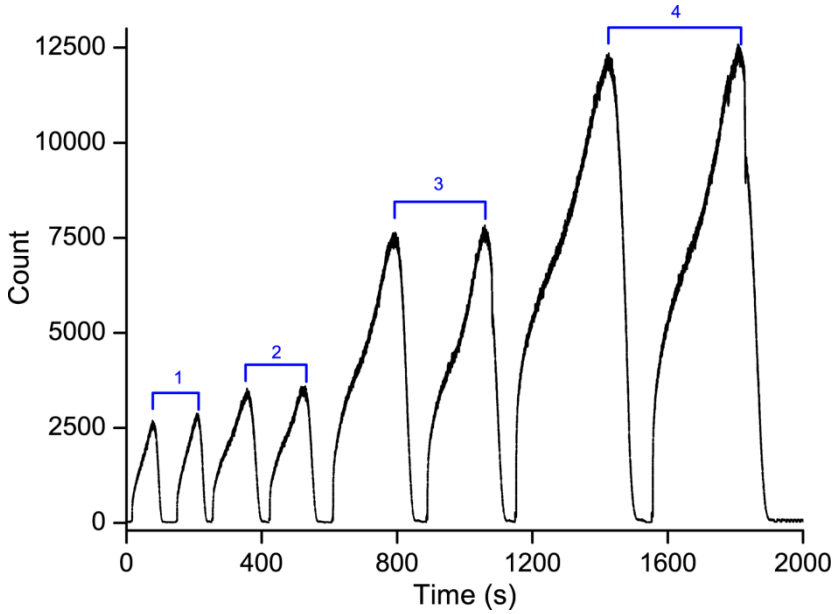

Fig. 5. Influence of the number of droplets on the CL intensity. The ordinal number of 1 to 4 in the figure stands for the number of droplets of 10, 20, 50 and 100, respectively. All reagents were dissolved in Tris-HCl buffer (0.1 M, pH 8.5), in presence of 10 μg/mL HRP, 0.4 mM PIP, 1mM H_2O_2 and 0.05 mM luminol. The voltage for the PMT was set at 1.1 kV; the signal-collecting interval was set as 0.1 s.

Table 2. Compare to the theoretical value of diffusion time and actual value.

Average	Actual value	Theoretical value
T_1=90s	$\frac{T_2}{T_1}=1.67$	$\frac{T_{d2}}{T_{d1}}=1.59$
T_2=150s	$\frac{T_3}{T_1}=2.88$	$\frac{T_{d2}}{T_{d1}}=2.92$
T_3=259s	$\frac{T_4}{T_1}=4.34$	$\frac{T_{d4}}{T_{d1}}=4.64$
T_4=391s		

3.4 Kinetic curve of the luminol-H_2O_2-HRP CL system

During the automatic CL analysis, 50 droplets of three reaction solutions were

ejected from each channel. The total volume of 50 droplets of solution was calculated as 49 nL. The CL reaction could be completed within 225 s in the automatic CL analysis platform (Fig. 6a). For comparison, 50 μL of luminol, H_2O_2 and HRP solutions were injected into a glass cuvette by pipette. It was found that 10,000 s of reaction time was needed for the CL reaction (Fig. 6b). It was obvious that the ink-jet automatic CL analysis platform was not only beneficial in the rapid determination but also for its low reagent consumption.

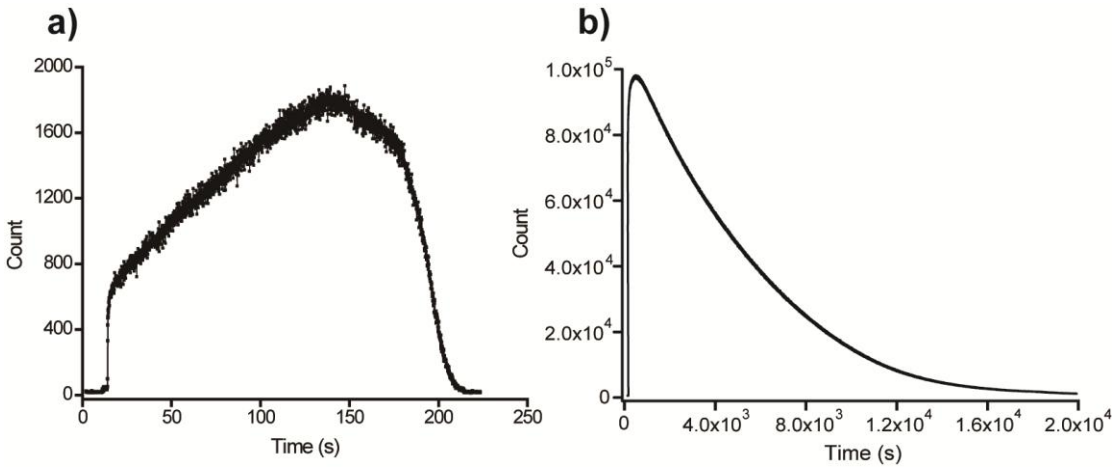

Fig. 6. The CL kinetic curves for the luminol-H_2O_2-HRP system with ink-jet injection (a) and conventional pipette injection (b).

3.5 Optimization of reaction conditions

The CL intensity of the luminol-H_2O_2-HRP system on glass slide microarray was increased with the concentration of HRP solution when the concentration of luminol and H_2O_2 solution were in certain range. Hence, the CL system could be developed for the determination of HRP. In order to get the best detection conditions for HRP, the effects of pH value, concentration of luminol solution, H_2O_2 and PIP solution have been investigated in details.

Tris-HCl buffer solution with pH value in the range of 7.0-9.5 was used as the reaction buffer for the CL analysis. When pH value was lower than 9.0, the CL intensity increased with pH (Fig. 7a). The CL intensity went down with the increasing

of pH value above 9.0. Although the strongest intensity was obtained at pH 9.0, the RSD value was arised under the pH value and the whole detection system was less stable. Hence, the Tris-HCl solution at pH 8.5 was selected as the buffer solution in the following experiments.

In the absence of HRP, H_2O_2 could also intrigue the CL emission from the luminol in alkaline media. Hence, the CL emission from the luminol- H_2O_2 system in presence and absence of HRP should be both investigated to obtain the optimal signal to noise ratio. As shown in Fig. 7b, we could see that the CL intensity (with or without HRP) increased with the concentration of luminol solution in the range of 5-25 μM and exhibited a little change with the concentration of luminol solution higher than 25 μM. If the concentration of luminol solution increased up to 50 μM, the CL intensity became stable, and good signal to noisel rate could be obtained. Therefore, luminol with concentration of 50 μM was selected in the subsequent investigation.

The CL intensity increased with the concentration of H_2O_2 solution in the range of 0 -1.0 mM (Fig. 7c). When the concentration of H_2O_2 solution was higher than 1.0 mM the CL intensity almost had no change.

PIP was added into the luminol- H_2O_2-HRP CL system as the signal enhancer to get the lower detection limit. From the Fig. 7d, PIP solution with a concentration of 0.4 mM provided the highest CL intensity. Hence, it was selected as the optimal concentration.

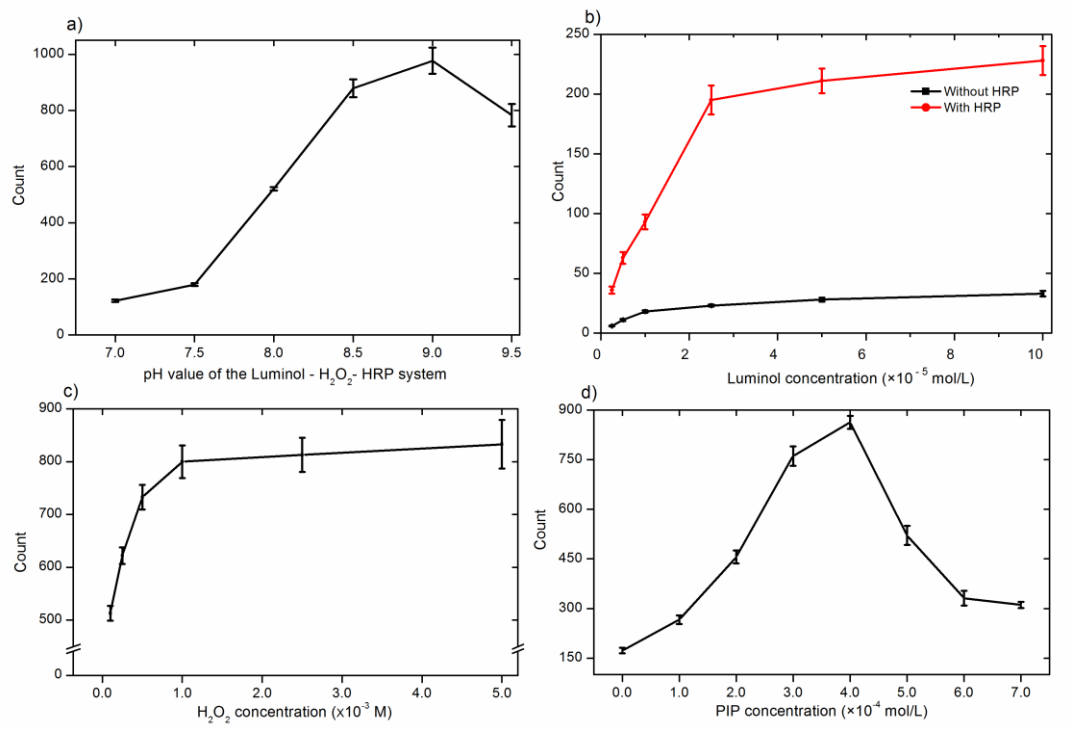

Fig. 7. Effects of concentration of luminol (a), pH value (b), concentration of H_2O_2(c), concentration of PIP(d) on the CL intensity. The voltage for PMT was set at 1.1 kV; the signal-collecting interval was set as 0.1 s.

3.6 Methodology evaluation

Under the optimized conditions, the CL signals of serial concentrations of HRP solution was shown in Fig. 8. We got a good linear relationship between CL intensity and HRP concentration in the range of 0.01 - 0.05 μg/mL with a correlation coefficient of 0.9954. And the relative standard deviation (RSD) values (n=10) of the CL analysis were 4.0%, 3.2% and 3.8%, when the concentration of HRP solutions were 0.049, 0.19 and 0.42 μg/mL, resepectively. The limit of detection (LOD) for HRP was 0.005 μg/mL (S/N=3) .

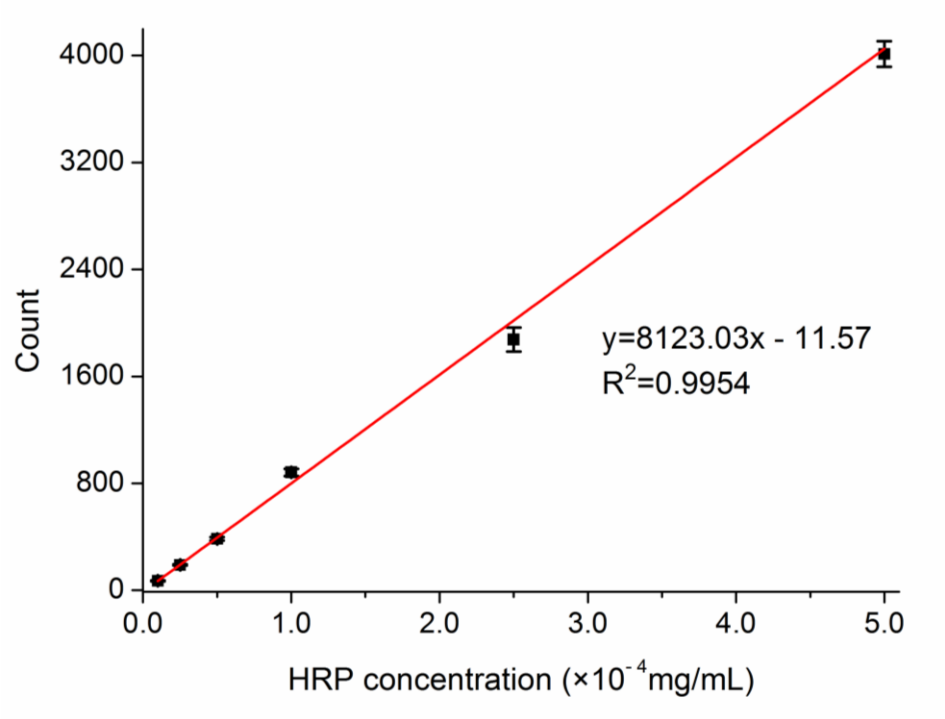

Fig. 8. Dynamic curve of HRP in the range from 0.01-1.0 μg/mL.

The proposed method could also be applied to the determination of BSA-HRP conjugate. The BSA-HRP conjugate was diluted by the Tris-HCl buffer (pH=8.5) in different ratio (1:10000 and 1:20000). Then the concentration of BSA-HRP in solution was detected by the automatic ink-jet CL analysis platform. The detected concentration of the two diluted solution was 0.17 and 0.38 μg/mL. For comparison, the concentration of the BSA-HRP in the diluted BSA-HRP was also determined by BHP9504 micro-plate luminescence analyzer using pipetting introduction. The detected concentration for diluted solution is 0.20 and 0.36 μg/mL, respectively. The two results were matched with each other very well. Therefore, the automatic CL analysis platform could be an alternative of the traditional pipetting method.

The proposed method could detect HRP in its protein conjugate, which indicates that it could also be developed as a CL platform for HRP based immunoassay. The multi-channel ink-jet ejection CL system could automatically control the solution volume as well as the solution injecting time, which has great potentials in automatic on-site CL dynamic investigation and provides new tools for the CL mechanism

research. Sample in nanoliter was enough for one-round determination, which is beneficial for toxic sample or trace bio-sample analysis.

5. Conclusion

We integrated the ink-jet microchip with a home-designed drive circuit and computer controlled system to set up a simple, automatical CL analysis platform for bioanalysis. The consumption of CL reaction solutions was in nanoliter level, which exhibited great potential in green chemistry. Finally, the automatic CL analysis platform has been succesfully used for the CL detection of HRP and its protein conjugate. Compared with the conventional pipetting CL detection, the automatic inkjet microchip CL analysis technique has many advantages, such as low sample-consumption, short reaction-time and high reproducibility, which could be the alternative of the conventional CL analytical technology.

Reference

[1] J.-M. Lin, Ed., Chemiluminescence-Basic principles and applications, Chemical Industry Press, Beijing, 2004.

[2] E. H. Hansen, M. Miró, Trends Anal. Chem., 2007, 26, 18-26.

[3] P. Fletcher, K. N. Andrew, A.C. Calokerinos, S. Forbes, P. J. Worsfold, Luminescence, 2001, 16, 1-23.

[4] D. W. King, W. J. Cooper, S. A. Rusak, B.M. Peake, J. J. Kiddle, D. W. O'Sullivan, M. L. Melamed, C. R. Morgan, S. M. Theberge, Anal. Chem., 2007, 79, 4169-4176.

[5] M. Liu, Z. Lin, J.-M. Lin, Anal. Chim. Acta, 2010, 670, 1-10.

[6] L. Zhao, L. Sun, X. Chu, Trends Anal. Chem., 2009, 28, 404-415.

[7] S. Rubio, D. Perez-Bendito, Anal. Chem., 2009, 81, 4601-4622.

[8] Y. Chen, J. Pawliszyn, Anal. Chem., 2006, 78, 5222-5226.

[9] Y. Kudo, T. Nakahara, T. Nakagama, N. Seino, M. Shinoda, K. Uchiyama, Anal. Sci., 2007, 23, 91-95.

[10] K. Uchiyama, H. Nakajima, T. Hobo, Anal. Bioachem., 2004, 379, 375-382.

[11] R.M. Verkouteren, J. R. Verkouteren, Anal. Chem., 2009, 81, 8577-8584.

[12] B.K. Singh, A.C. Hillier, Anal. Chem., 2007, 79, 5124-5132.

[13] T. Nishiyama, F. Endo, H. Eguchi, J. Tsunokawa, T. Nakagama, N. Seino, M. Shinoda, T. Shimosaka, T. Hobo, K. Uchiyama, Chem. Lett., 2006, 35, 272-273.

[14] W. Martinez, S. T. Phillips, G. M. Whitesides, Proc. Natl. Acad. Sci. USA, 2008, 105, 19606 -19611.

[15] H. W. Ma, Y. Z. Wu, X. L. Yang, X. Liu, J. N. He, L. Fu, J. Wang, H. K. Xu, Y. Shi, R. Q. Zhong, Anal. Chem., 2010, 82, 6338-6342.

[16] M. W. Vannatta, C. D. Whitmore, N. J. Dovichi, Electrophoresis, 2009, 30, 4071 -4074.

[17] H.-L. Zeng, N. Seino, T. Nakagama, Y. B. Kikuchi, H. Nagano, K. Uchiyama, J. Chromatogr. A, 2009, 1216, 3337-3342.

[18] T. Laurell, J. Nilsson, G. Markovarga, Anal. Chem., 2005, 77, 264-272.

[19] S. Ekstrom, P. Onnerfjord, J. Nilsson, M. Bengtsson, T. Laurell, G. Marko-Varga,

Anal. Chem., 2000, 72, 286-293.

[20] K. J. Abe, K. R. Kotera, K. J. Suzuki, D. Cittrio, Anal. Bioanal. Chem., 2010, 398, 885-893.

[21] G. Arrabito, B. Pignatoro, Anal. Chem., 2010, 82, 3104-3107.

[22] J. Xua, F. Shang, J. H. T. Luong, K. M. Razeeba, J. D. Glennon, Biosen. Bioelectron., 2010, 25, 1313-1318.

[23] X. Yang, Y. Guo, A. Wang, Anal. Chim. Acta, 2010, 666, 91-96.

[24] E. Baldich, F. j. d. Campo, F. X. Munoz, Biosens. Bioelectron., 2009, 25, 920-926.

[25] S. S. Zhang, J. Yang, J. H. Lin, Biochem., 2008, 72, 47-52.

[26] G. Soman, X.Y. Yang, H. G. Jiang, S. Giardina, G. Mitra. J. Immunol. Methods., 2011, 373, 181-191.

[27] A. Frey, B. Meckelein, D. Externest, M. A. Schmidt. J. Immunol. Methods., 2000, 233, 47-56.

[28] M. J. Zhou, Z. J. Diwu, N. Panchunk-voloshina, R. P. Haugland, Anal. Biochem., 1997, 253, 162-168.

[29] K. Akimoto, Y. Shinmen, M. Sumida, S. Asami, T. Amachi, H. Yoshizumi, Y. Saeki, S. Shimizu, H. Yamada, Anal. Biochem., 1990, 189, 182-185.

Chapter 5

Inkjet Nano-injection for high-thoughput Chemiluminescence Immunoassay on Multicapillary Glass Plate

INTRODUCTION

Recently, immunoassays are increasingly emerged as one of the most important bioanalytical techniques in clinical diagnosis and environmental testing [1-2]. Typically, immunoassays are particularly efficient diagnostic methods for infectious diseases. For example, to prevent the pandemic spread of infectious diseases, compact and touch less diagnosis or screening methods are greatly desired for on-site investigation in the field. Immunoassay methods, including chemiluminescence immunoassays (CLIA) [3-5], enzyme-linked immunosorbent assays (ELISA) [6-10], fluoroimmunoassays (FIA) [11-14], and radioimmunoassays (RIA) [15-16], have been widely used in the clinical diagnosis.

Nowadays, CLIA is recognized as a powerful tool for disease diagnosis owing to its several advantages, such as high sensitivity, rapid analysis, and easy automatization [17]. Recently, there is of great interest in developing high-throughput methods for analyzing a large number of samples. Thus, many efforts were devoted to improving the throughput of immunoassays. For example, Zhao et al. developed a novel method of micro-plate magnetic chemiluminescence enzyme immunoassay for rapid and high-throughput analysis of 17β-estradiol in water samples [18]. Ge et al. established a 3D origami-based CL immune device that printed an immunoassay on a sheet of paper via wax printing. The printed immunoassay was used as a multiplexed CL immunoassay for point-of-care diagnostics by simple and procedural operations.[4] Wang et al. established a simple competitive ELISA for rapid measure of secretory immunoglobulin A (s-IgA) in saliva [19]. Liu et al. report a paper analytical device based on the SlipChip concept [20]. However, these methods still required many steps

and high reagent consumption. Thus, it is vital to develop new platform which perform not only the capability of high throughput but also the reagent consumption and easy operation. CLIA commonly utilizes microbeads, as well as micro channels containing magnetic beads [21], or specially designed micro channels containing other types of beads [22]. Immunoassay reagents are usually very expensive, and thus, it is vital to develop micro-volume reactions. However, with such small volumes, it is difficult to change the solution and wash to separate bonded and free antibody (or antigen) (B/F separation). Some researchers developed methods for B/F separation, but the reported platforms are difficult to establish or not easy to operate [23-24].

Inkjet technology can be easily used for liquid injection at the nanoliter to picoliter level. This technology will enable us to exactly control the speed and volume of ejected samples. Many researchers used the inkjet technology for common analytical technologies, such as paper-based fluidic device [25-26], capillary electrophoresis (CE) [27-28], and mass spectrometry (MS) [29]. Chen et al. successfully applied a multi-channel inkjet for CL analysis. The consumption of CL solutions in this method was cut down at the nanoliter level, and the CL analysis has been successfully used for the CL detection of HRP and its protein conjugate [30]. Zeng et al. reported a highly accurate sample injection system for capillary electrophoresis (CE) based on an inkjet microchip capable of reproducing exact introduction volumes at the picoliter level [27]. Luo et al. presented the association of inkjet and electrospray ionization MS to detect picoliter droplets. The liquid volume and the position of the liquid on the tip was precisely controlled to form ultrafine droplets for successive ionization of the analyte [29]. Here, we describe the development of rapid and high-throughput disease diagnosis by combining CLIA and inkjet technology.

In the present work, we developed a high-throughput CLIA method for IgA analysis by combining inkjet technology with multicapillary plate. Home-made inkjet waveform driving device was used to generate picoliter droplets for solution injection [28]. Besides, we used multicapillary glass plate as the container of the reaction,

which supply the advantages of high throughput and easy washing. We successfully detected different concentrations of IgA to get the standard curve, and the IgA concentration in saliva was quantitatively determined. The established platform has the advantages of high-throughput, high speed, high sensitivity and automation.

EXPERIMENTAL SECTION

Reagents and Materials

Human IgA ELISA kit (Affinity purified goat anti-human IgA (1^{st} Ab), human reference serum with the IgA concentration at 1.2 mg/mL, and HRP-conjugated goat anti-human IgA (2^{nd} Ab-HRP)) was obtained from Bethyl Laboratories (Montgomery, TX, USA). SuperSignal ELISA Pico Chemiluminescent Substrate [Luminol/enhancer solution and peroxide (H_2O_2) solution] was purchased from Thermo Scientific (Rockford, USA). Bovine serum albumin (BSA) was obtained from Merck (Calbiochem, German). Phosphate buffer solution (PBS: 0.01 M, pH 7.4) was prepared from 0.01 M NaH_2PO_4 solution, and its pH value was adjusted to 7.4 using 0.01 M Na_2HPO_4 solution. Sample/Conjugate diluent: Tris buffer (50 mM, pH 8.0) included 0.14 M NaCl and 0.05% Tween 20. Na_2HPO_4, NaH_2PO_4, and Tris(hydroxymethyl) amino methane were purchased from Wako Pure Chemical Industries Ltd. (Tokyo, Japan). Extran MA01 was purchased from Merck (Darmstadt, Germany). 2-(*N*-morpholino)ethanesulfonic acid (MES free acid) was purchased from US Biological (Swampscott, MA, USA). NaCl, $NaHCO_3$, Na_2CO_3, H_3BO_3, 2-amionethanol, acetone, NaOH, and HCl were from Kanto Chemical Co. Inc. (Tokyo, Japan). The Polybead® carboxylate 20.0-micron microbeads (2.5% solids-latex) were purchased from Polysciences, Inc. (Warrington, PA). *N*-(3-dimethylaminopropyl)-*N′*-ethylcarbodiimide hydrochloride (EDC) and casein from bovine milk were purchased from Sigma-Aldrich. The neutral detergent used for cleaning of the multicapillary glass was obtained from Tomisc (Tokyo, Japan). Chloroform was purchased from NacalaiTesque, Inc. (Kyoto, Japan). Filter paper was obtained from Blaine test paper® (Advantec Co., Tokyo, Japan).

All buffers used in the experiment were filtered through a 0.45-μm membrane filter (4700, Nihon Millipore). The PDMS kit was obtained from Dow Corning Toray (Tokyo, Japan). The SU-8 3050 was obtained from Nippon Kayaku (Tokyo, Japan). All aqueous solutions were prepared by ultrapure water that had been purified using a Millipore-Q system (Millipore Japan Co., Tokyo, Japan).

Apparatus

The inkjet device was provided by Fuji Electric Co., Ltd. (Tokyo, Japan). A VW-9000 high-speed microscope was obtained from Kyence Corporation, (Osaka, Japan) and it was employed to observe the droplet ejected by the inkjet. A BP2111D micro-balance was obtained from Sartorius (Goettingen, Germany). Photomultiplier (PMT) H10722 and the multicapillary plate with arrayed micro through-holes (33 mm diameter for whole area, 27 mm for capillary area, 1 mm thickness, 10 μm capillary i.d.) were obtained from Hamamatsu Photonics (Hamamatsu, Japan). The electromotive x-y stage MMU-60X was purchased from Chuo Precision Industrial Co., Ltd. (Tokyo, Japan). The 75-mm hematocrit tube was purchased from Funakoshi, Co. (Tokyo, Japan). The 96-well plate reader was from Spectra Fluor Tecan (Kawasaki, Japan). Adobe Illustrator CS4 was used to generate the photo-mask pattern and was obtained from Adobe Systems Incorporated (San Jose, CA, USA).

Design of the CLIA system

The design of the platform is shown in Figure 1. The inkjet device was pretreated according to the method described elsewhere [28]. We used home-made hardware and software for the CLIA inkjet nano-injection system. Driving waveform applied to the piezoelectric device on inkjet was controlled by the home-made amplifier (voltage; 0~100V, pulse width; 0~255 μs). The exact position of the inkjet on the microwell were automatically controlled by an electromotive x-y stage via the home-made software. Firstly, the 1^{st} Ab was chemically immobilized on the surface of carboxylated microbeads [31], and then, the microbeads were blocked with 1%

BSA in 0.01 M PBS buffer (pH 7.4). Further, the microbeads were diluted 10-fold and resuspended in 0.01 M PBS buffer. For the sample assay, the 1st Ab-PS microbeads suspension was dispensed to the microwells by a pipette. A filter paper was used to remove the solution in the microwell by touching the bottom of multicapillary plate for solution passing. The platform could complete the entire procedure of CLIA, including injection/dilution for human IgA, dilution buffer, 2nd Ab-HRP, and CL substrate solution. Series of concentrations for standard human IgA was generated on-chip by controlling the ratio of droplet numbers from different inkjet channels (One channel loaded human IgA solution, and the other channel loaded dilutiing buffer). Similarly, the 2nd Ab-HRP was also diluted on-chip as the same manner(See supporting information video 1 for droplets mixture). Free human IgA, 2nd Ab-HRP and other proteins were washed away with washing buffer by touching the bottom of multicapillary glass using filter paper after incubation. Finally, CL substrate solutions were ejected to the microwells from the another channel for CL signal detection.

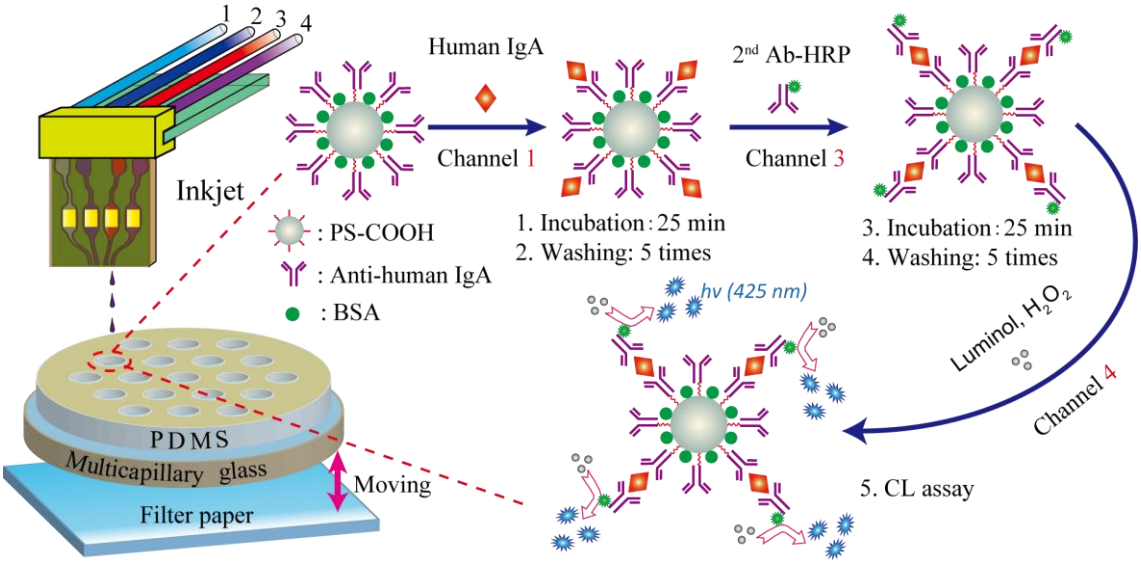

Figure 1. Schematic illustration of the sandwich CLIA for human IgA detection in the microwells on the multicapillary glass plate.

PDMS Fabrication and Multicapillary Glass Plate Treatment

Details of the fabrication procedure of PDMS sheet with microwells array was shown in Figure 2 in supporting information.

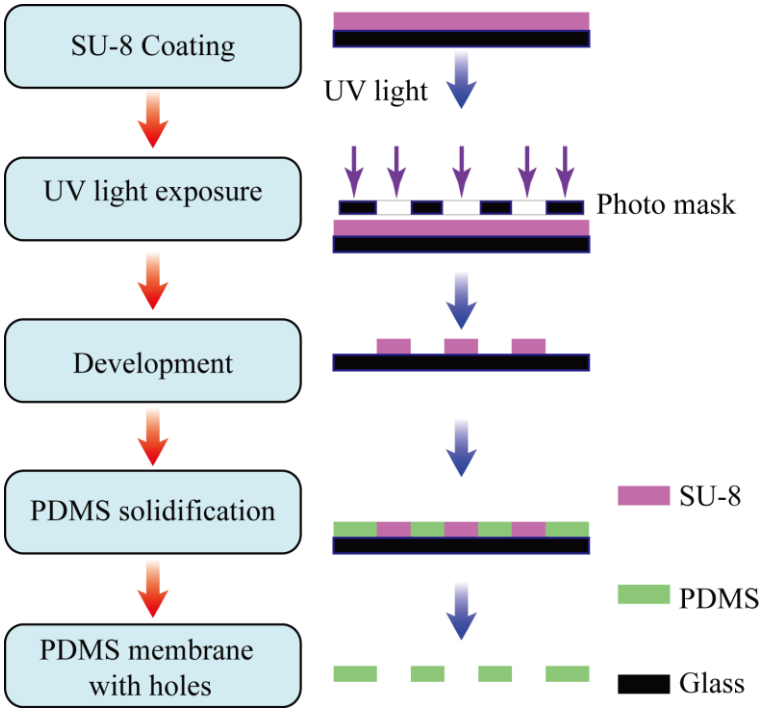

Figure 2. Process of the PDMS microwell array fabrication.

Briefly, the photomask for the PDMS microwell array (19 wells, i.d. 1.5 mm, Figure 3a and 3b) was designed by Adobe Illustrator CS. Then, a piece of glass with spin-coated negative photoresist (SU-8) was covered by the photomask and exposed to UV light to translate the design onto the photoresist. Finally, the photoresist was developed using the SU-8 developer to generate an array of convex and cyclical pillars on the glass slide, which was the template for the PDMS sheet with microwells. PDMS prepolymer and curing agent were mixed at a mass ratio of 10: 0.5 and poured onto the template described above after vacuum degassing. The PDMS on the template was cured at 65℃ for 1.0 h. Then, the PDMS replica was peeled off from the template, which generated in a PDMS sheet with an array of microwells with a height of approximately 1.2 mm and a diameter of approximately 1.5 mm (Figure 3d).

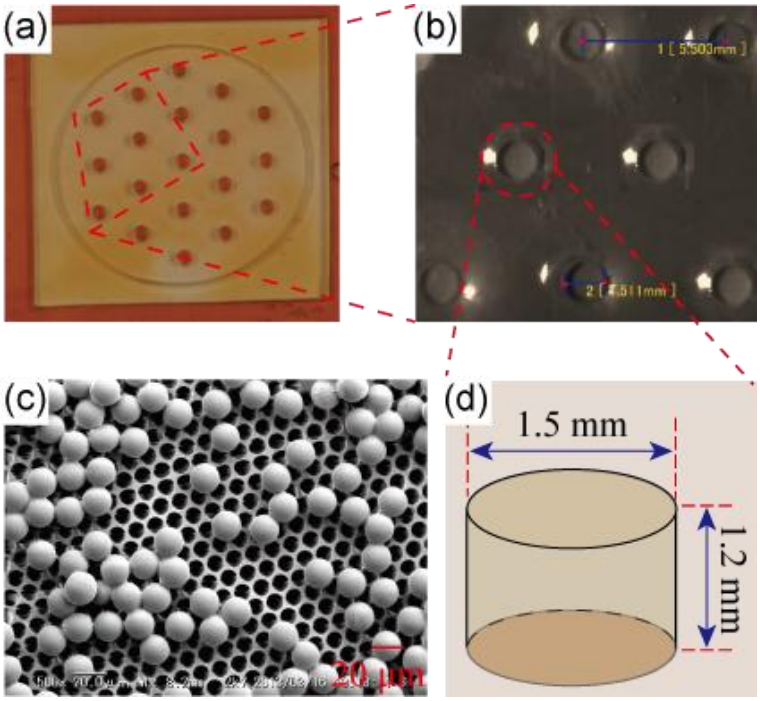

Figure 3. Design of the array of microwells: （a) photomask template, （b) picture of completed PDMS sheet with microwells, （c) the SEM imaging of the PS microbeads on the multicapillary glass plate , （d) size of each microwell.

To the following immunoassays, the multicapillary glass plate was immersed into a neutral detergent under gentle shaking overnight to remove the absorbed impurities and then successively immersed into ultrapure water, acetone, chloroform, acetone, and ultrapure water for ultrasonic cleaning for 15 min, respectively. After the plate was immersed in to the freshly prepared H_2SO_4 (98%): H_2O_2 (30%) = 3:1(v/v) for 30 min, and then it was sonicated in ultrapure water for 15 min. To make the capillary surface hydrophilic, it was incubated in 0.1 M NaOH for 15 min and then water for 15 min under gentle shaking. Finally, the cleaned multicapillary plate was dried under nitrogen stream and then was baked in an oven at 65℃ for 20 min. The multicapillary plate was then incubated in 1% BSA in 50 mM Tris buffer (pH 8.0) at 4℃ for overnight to block the surface. Before use, it was washed with 0.1% Tween-20 in 50 mM Tris-HCl buffer (pH 8.0) followed by drying with nitrogen stream. It was baked in the oven at 65℃ for 20 min, then assembled with the pre-cleaned PDMS sheet, and attached onto the top surface of the multicapillary glass

plate to form the microwell array.

Preparation of goat 1st Ab-PS microbeads conjugates

Carboxy group modified PS microbeads were washed according to the standard method presented in the manufacturer's guidance. Then, the microbeads were resuspended in 0.1 M MES buffer and then mixed with 2% EDC in equal volumes for 3-4 hours at room temperature followed by centrifugation for 5-6 min. Then the supernatant was removed and discarded. This process was repeated several times. After the resultant microbeads were re-suspended in 0.2 M borate buffer, 5

0 μg IgA was added and then they were mixed gently overnight at room temperature on an end-to-end mixer. Followed by washing, the amount of 1st Ab added in less than the amount in the supernatant represents the amount bound to the microbeads. The 1st Ab-PS microbeads were blocked with 0.25 M ethanolamine for unreacted sites and 1% BSA solution in 0.2 M borate buffer for any remaining non-specific protein bonding sites. The 1st Ab-PS microbeads (2.5%, w/v) suspension was finally resuspended in 0.01 M PBS (pH 7.4) storage buffer for later experiments.

Optimization of the Platform and Real Sample Detection

The procedures of the sandwich CLIA is shown in Figure 4. Based upon the platform, we optimized a serial of conditions including the accuracy of injection volumes of sample from each channel of the inkjet, multicapillary glass plate blocking solution, incubation time and RH box for the CLIA system, the amount of 1st Ab-PS microbeads, the concentration of 2nd Ab-HRP, CL substrate droplet number and determination of human IgA concentration in saliva was carried out under the optimized conditions.

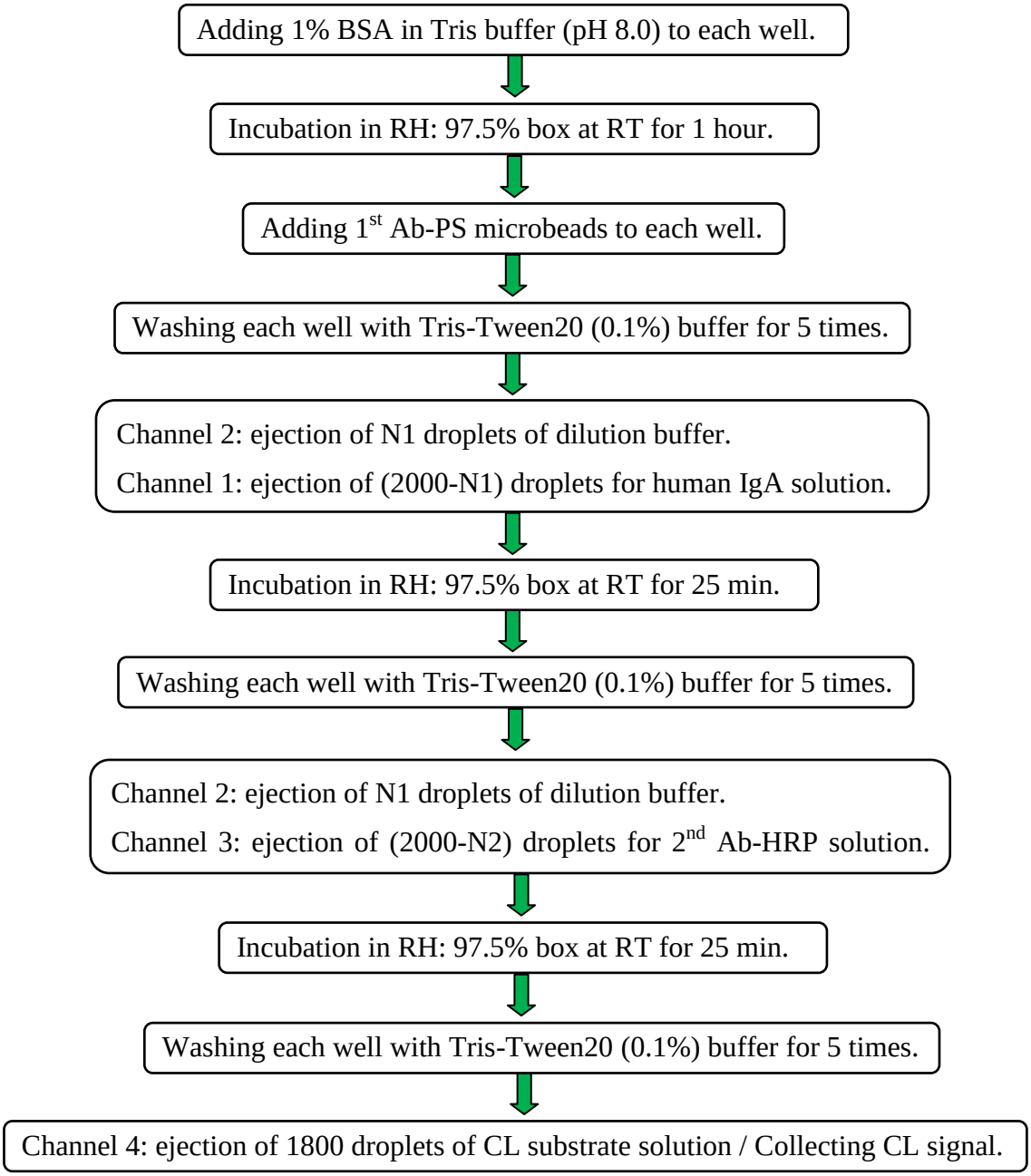

Figure 4: Schematic illustration of the sandwich CLIA for human IgA detection process in a multicapillary glass plate containing a well array constructed using inkjet injection.

Results and Discussion.

Control holding/passing solution on multicapillary glass

The inner diameter of the capillary on the multicapillary glass plate is approximately 10 μm, which is smaller than the diameter of the microbeads; therefore,

the microbeads cannot pass through the multicapillary glass plate. Initially, the solution will not flow out of the bottom of the capillaries in the multicapillary glass plate because of the Laplace pressure by a sufficiently small capillary radius (r). The interface between the solution and air forms a meniscus at the bottom of capillary. The meniscus holds the solution by the Laplace pressure, ($\Delta p = \frac{2\gamma}{R}$ R : curvature radius of the meniscus), which is based upon the surface tension (γ) at the bottom of the capillaries. When the liquid meniscus reached to balance (as shown in Figure 5e dotted lines), the liquid gravity force (G) would be balanced by the Laplace pressure ($G = \Delta p$) to hold the solution. Once the absorbent (filter paper) was placed at the bottom of the multicapillary glass plate, the solution would contact the absorbent fibers. Thus, the Laplace pressure disappeared. The solution would contact the absorbent fibers. Thus, the Laplace pressure disappeared. The solution in the capillary just be acted by the G and the absorbing force (Fa) shown in Figure 5d. Under this situation, the solution was absorbed and thus flushed out of the capillaries. Thus, it is convenient to use the multicapillary glass plate as a platform for the B/F separation.

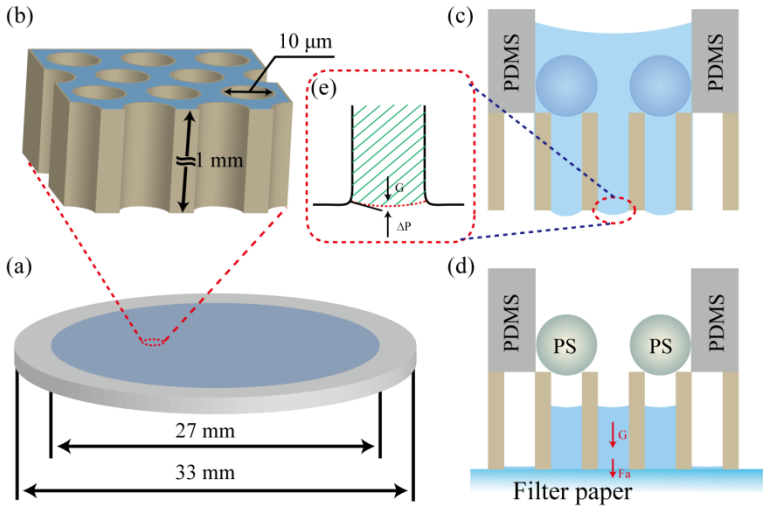

Figure 5. Appearance (a) and structure (b) of the multicapillary glass plate, and capillaries in the multicapillary glass plate for holding (c) and passing (d) the solution and the capillary force controlled mechanism (e).

Optimization of blocking buffer for the multicapillary glass plate and driving waveform for inkjet

In order to decrease background signal arising from nonspecific adsorption of the multicapillary glass plate, several kinds of blocking solutions were investigated. Four kinds of blocking solutions, including 1% BSA in PBS (pH 7.4), 1% BSA in Tris buffer (pH 8.0), 1% casein in PBS (pH 7.4) and 1% casein in Tris buffer (pH 8.0) were tested. First, blocking buffer solutions were added to the microwells on multicapillary plate. Then incubated for 1 h in RH: 97.3 % box at room temperature (RT). After washing with washing buffer, 2nd Ab-HRP was added and incubated for 20 min. After 5 times washing, CL substrate solutions were added and CL intensities were measured. From the results of the blocking investigation (Figure 6), the comparison among the blocking solutions showed different efficiency in decreasing the background. It was found that the smallest background signal was obtained by using 1% BSA in Tris buffer (pH 8.0). Thus, it was chosen for the following experiments.

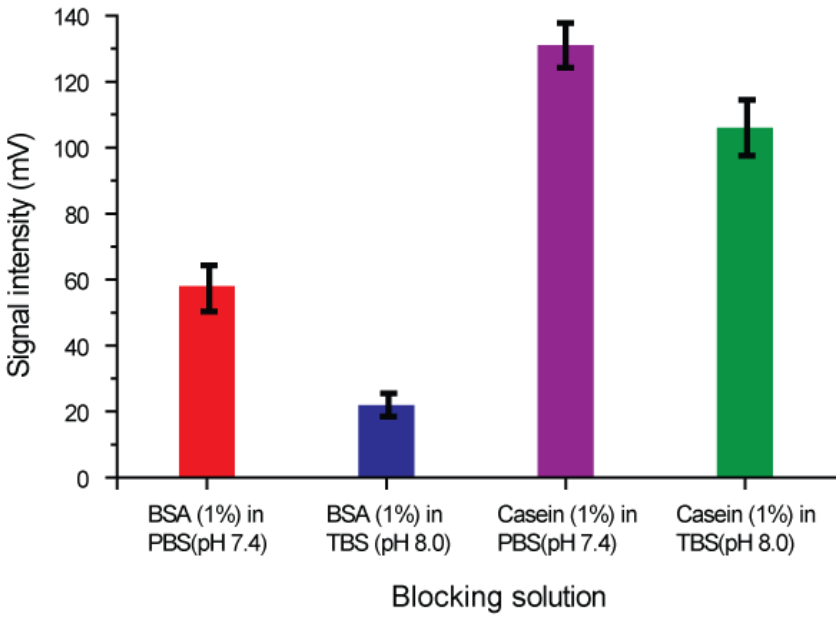

Figure 6. Optimization of the multicapillary glass plate blocking solution.

Based upon the investigation of the driving waveform applied to the

piezo-electric ceramic on inkjetinkjet, the optimal conditions of the driving waveform and pulse width for inkjet were listed in Table 1. Under optimal condition, the volume of each droplet for human IgA, dilute solution, 2nd Ab-HRP and substrate solution was 396 pL, 397 pL, 393 pL and 686 pL, respectively.

Table 1. Optimization of the inkjet driving waveform and volumes of droplets.

Channel	Sample	Driving waveform	Volume (pL) / droplet	RSD%(n=10)
Channel 1	Human IgA (1μg mL^{-1})	56 V, 32 μs	396	2.3
Channel 2	Dilute solution	30 V, 30 μs	397	1.1
Channel 3	2^{nd} Ab-HRP (1μg mL^{-1})	60 V, 30 μs	393	0.9
Channel 4	Luminol : H_2O_2 = 1:1(v/v)	60 V, 32 μs	686	2.9

Investigation of evaporation

Evaporation of the sample and solution is a very important problem in low-volume CLIA methods, so it is vital to make this effect clear in our experiments. We investigated this issue by carrying out the incubation for IgA assays under different relative humilities (RH) box (for example: 6.4%, 43.2%, 97.3%) at RT. The relationships between CLIA system incubation time and signal intensity under different RH condition are shown in Figure 7. The results show that under the low RH, the solution in the holes would dry off when the incubation time was longer than 10 min. As a result, large RSDs (7.9% - 21.6%) were observed. Thus, it would be difficult to control the switching of passing/holding by filter paper under low RH conditions. However, when we placed the plate in a higher RH box (97.3%), the solution in the microwells would not obviously evaporate even after 2 h. Based on the results, the CL signal intensity increased in the range of 0-25 min, and then reached a plateau from 25 to 35 min when the incubation was carried out under the 97.3% RH. In other words, 25 min of incubation time was sufficient to reach to equilibrium between antibody and antigen reaction. Therefore, we selected optimal incubation

conditions for the CLIA system as: 25 min in higher RH box (97.3%).

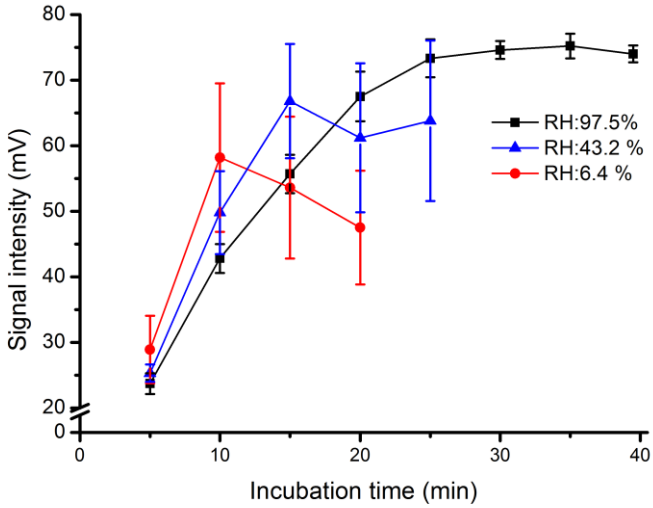

Figure 7. Relationship between CL intensity and incubation times at different RH box (the same incubation times for 2nd Ab-HRP was set at each point). The volume of the 1st Ab-PS microbeads (0.25%, w/v) suspension was 18 μL, the concentration of 2nd Ab-HRP was 0.1 μg mL^{-1}, human IgA was 125 ng mL^{-1}, the droplets number of the CL substrate was 1800.

Optimization of the volume of 1st Ab-PS microbeads

In order to perform automatic, as well as a highly sensitive and rapid analysis, we optimized the volume of the 1st Ab-PS microbeads suspension applied to each micorwell. Firstly, we diluted the original 1st Ab-PS microbeads suspension (2.5%, w/v) 10-fold with 0.01M PBS buffer (pH 7.4). Then, a certain volume of the 1st Ab-PS microbeads suspension (3-33 μL) was dispensed to each micorwell by pipette followed by the measurement of IgA by the procedure (shown in Figure 4). Concomitant increase of the CL signal intensity was observed with the increase of the volume of 1st Ab-PS microbeads suspension in the range of 3 - 24μL and it shows a plateau over 24μL (shown in Figure 8). We selected optimal conditions of 24 μL as the volume of the 1st Ab-PS microbeads suspension (0.25%, w/v), which corresponded to microbeads number of 13,648±572 (n=10)/well.

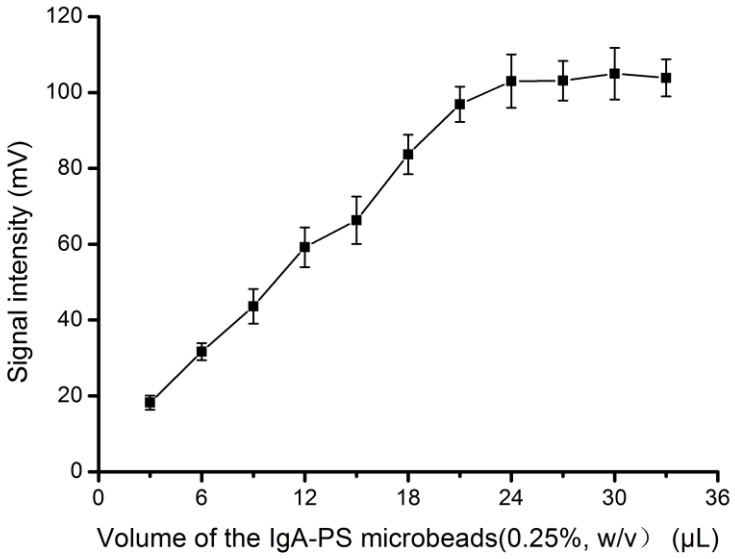

Figure 8. Relationship between CL intensity and the volume of the 1st Ab-PS microbeads suspension (0.25%). The concentration of 2nd Ab-HRP was 0.1 μg mL^{-1}, human IgA was 125 ng mL^{-1}, 2000 droplets as the number of droplets of the CL substrate.

Effect of the concentration of 2nd Ab-HRP on the CL signal intensity

Effect of the concentration of 2nd Ab-HRP on the signal intensities was also examined. At first, control serum containing 1.0 μg mL^{-1} of human IgA was loaded to the inkjet channel 1, then the 50 mM Tris-buffer (pH 8.0) (dilute solution) was loaded to the inkjet channel 2 for the dilution for series of IgA and 2nd Ab-HRP concentration by controlling the droplet number ratio from different inkjet channels. And then 2nd Ab-HRP solution (1μg mL^{-1}) and CL substrate solution were loaded into the inkjet channel 3 and channel 4, respectively. The CLIA on the system was carried out according to the procedure shown in Figure 4. Figure 9 shows the effects of the 2nd Ab-HRP concentration (0.1, 0.2, 0.5, 1.0 μg mL^{-1}) on the IgA measurement. When the concentration of the 2nd Ab-HRP increased, larger signal intensities of the background were also observed. Meanwhile, the lower concentration of the 2nd Ab-HRP gave smaller background signal intensities. It should be taken into account that the distance between the neighboring micorwell would be considered because of the cross-talking in the chemiluminescence method, especially for the high-throughput detection. So

we selected 0.5 μg mL^{-1} of 2nd Ab-HRP in terms of the signal intensity and throughput of measurement. Finally, the calibration curve (The blue one in Figure 9.)was obtained in Figure 9 using series of human IgA concentrations generated by inkjet under established conditions (The volume of 1st Ab-PS microbeads solution was 24 μL, and the droplets number of CL substrate solution was 1800). The calibration curve was linear in the range of 1.0 - 31.25 ng mL^{-1}, and the fitting formula was Y=67.96X+141.56 (R^2=0.9912, where X; human IgA concentration, Y; singal intensity).

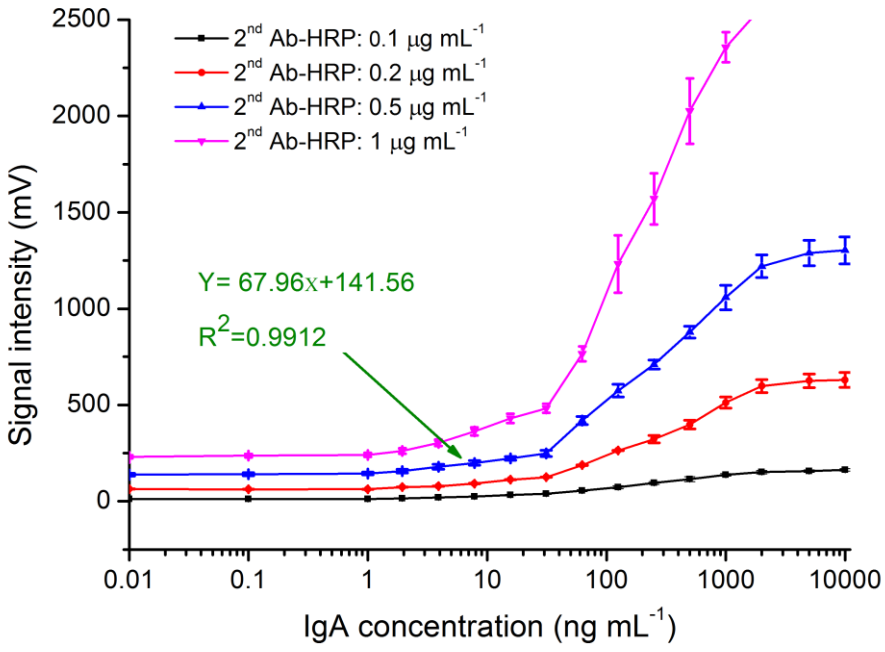

Figure 9. Relationship between CL intensity and concentration of human IgA at 4 different concentrations of 2nd Ab-HRP.

Optimization of CL substrate volume

Figure 10 shows the effects of CL substrate volume on the CLIA signal intensity. CL intensity increased with increasing CL substrate droplets number up to 1800. Based on the results, we selected optimal conditions as follows: 1800 droplets as the number of droplets of the CL substrate.

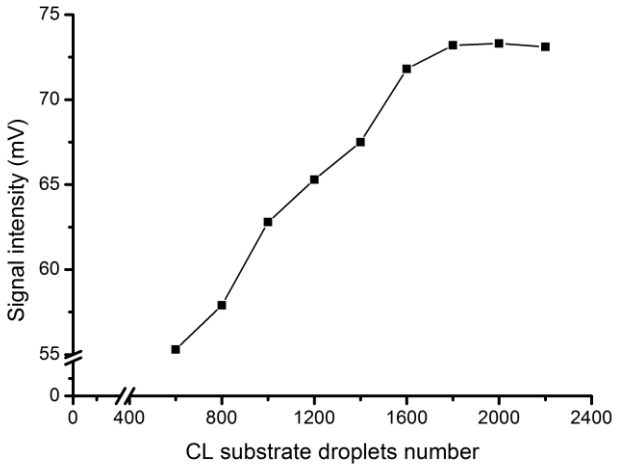

Figure 10. Relationship between CL intensity and droplet number of CL substrate (Luminol: H_2O_2 = 1:1)

Under the optimized conditions, the CLIA for human IgA measurement was carried out according to the established method using inkjet device. As shown in the figure 9, a good relationship between the signal intensity and the IgA concentration was finally obtained. Limit of detection (blank ± 3 SD) as low as 0.1 ng mL^{-1} was achieved for human IgA. In a comparison with a traditional 96-well plate, we achieved a lower LOD, a 50% decrease in analysis time, and 126 times less reagent consumption, as shown in Table 1. The proposed method could be considered as more sensitive for the detection of IgA with the potential in automatic and minimized on-site detections [19, 22, 32].

Table 1. Comparison of the assay of human IgA in the multicapillary glass plate with the microwell array and in the 96-well plate.

Methods	Incubation time (min)		Total assay time (min)	Sample volume (μL)	LOD (ng mL^{-1})
	Human IgA	2^{nd} Ab-HRP			
Multicapillary plate	25	25	<60	0.79	0.10
96-well plate	60	60	>140	100	0.86

Real Sample Detection

We determined the concentration of the human IgA in saliva that had been diluted 1,0000-fold (sample from a volunteer) using the presented method. The concentration of human IgA in the diluted saliva samples were between 181.4 to 213.1 ng mL^{-1} with the RSD below 5.1% shown in Table 2, which were very similar to the analytical results obtained by using the 96-well plate. The established platform had the advantages of high speed and low reagent consumption. Because of the use of inkjet technology, the platform also had the advantage of potential automation and compaction.

Table 2. Determination of human IgA in saliva by the multicapillary glass plate with the microwells array and by the 96-well plate.

Sample	Dilution ratio	Multicapillary plate		96-well plate	
		Calculated Conc. (ng mL^{-1})	RSD % (n=5)	Calculated Conc. (ng mL^{-1})	RSD % (n=5)
S1	1:10000	181.4	3.6	172.3	2.9
S2	1:10000	189.3	5.1	176.6	4.2
S3	1:10000	213.1	4.3	201.9	4.6

CONCLUSIONS

We determined the concentration of the human IgA in saliva that had been diluted 1,0000-fold (sample from a volunteer) using the presented method. The concentration of human IgA in the diluted saliva samples were between 181.4 to 213.1 ng mL^{-1} with the RSD below 5.1% shown in Table 2, which were very similar to the analytical

results obtained by using the 96-well plate. The established platform had the advantages of high speed and low reagent consumption. Because of the use of inkjet technology, the platform also had the advantage of potential automation and compaction.

References

(1) Yang, M. H; Kostov, Y; Bruck, H. A; Rasooly, A. *Anal. Chem*. **2008**, 80, 8532-8537.

(2) Urdea, M; Penny, L. A; Olmsted, S. S; Giovanni, M. Y; Kaspar, P; Shepherd, A; Wilson, P; Dahl, C. A; Bochsbaum, S; Moeller, G; Burgess, D. C. H. *Nature*, **2006**, 444, 73-79.

(3) Liu, F; Li, Y. M; Song, C. J; Dong, B. Q; Liu, Z. J; Zhang, K; Li, H. T; Sun, Y. J; Wei, Y. Y; Yang, A. G; Yang, K; Jin, B. Q. *Anal. Chem*. **2010**, 82, 7758-7765.

(4) Ge, L; Wang, S. M; Song, X. R; Ge, S. G; Yu, J. H. *Lab Chip*, **2012**, 12, 3150-3158.

(5) Liu, Y.-M; Mei, L; Liu, L.-J; Peng, L.-F; Chen, Y.-H; Ren, S.-W. *Anal. Chem*. **2011**, 83, 1137-1143.

(6) Ye, F. G; Shi, M; Huang, Y; Zhao, S. L. *Clin. Chim. Acta*. **2010**, 411, 1058-1062.

(7) Rissin, D. M; Kan, C. W; Campbell, T. G; Howes, S. C; Fournier, D. R; Song, L; Piech, T; Patel, P. P; Chang, L; Rivnak, A. J; Ferrel, E. P; Randall, J. D; Provuncher, G. K; Walt, D. R; Duffy, D. C. *Nat. Biotechnol*. **2010**, 28, 595-599.

(8) Apilux, A; Ukita, Y; Chikae, M; Chailapakul, O; Takamura, Y. *Lab Chip*, **2013**, 13, 126-135.

(9) Yanagisawa, N; Dutta, D. *Anal. Chem*. **2012**, 84, 7029-7036.

(10) Dixit, C. K; Vashist, S. K; O'Neill, F. T; O; Reilly, B; Craith, B. M; O'Kennedy, R. *Anal.Chem*. **2010**, 82, 7049-7052.

(11) Kokko, T; Kokko, L; Lovgren, T; Soukka, T. *Anal.Chem*. **2007**, 79,

5935-5940.

(12) Kuningas, K; Ukonaho, T; Pakkila, H; Rantanen, T; Rosenberg, J; Lovgren, T; Soukka, T. *Anal.Chem*. **2006**, 78, 4690-4696.

(13) Wang, Y. Y; Liu, B. *Biosens. Bioelectron*. **2009**, 24, 3293-3298.

(14) Shen, W. Z; Li, M. Z; Xu, L; Wang, S. T; Jiang, L; Song, Y. L; Zhu, D. B. *Biosens. Bioelectron*. **2011**, 26, 2165-2170.

(15) Karir, T; Hassan, P. A; Kulshreshtha, S. K; Samuel, G; Sivaprasad, N; Meera, V. *Anal.Chem*. **2006**, 78, 3577-3582.

(16) Schaefer, O; Bohlmann, R; Schleuning, W.-D; Schulze-Forster, K; Humpel, M. *J. Agric. Food Chem*. **2005**, 53, 2881-2889.

(17) Xin, T.-B; Liang, S.-X; Wang, X; Li, H. F; Lin, J.-M. *Anal. Chim. Acta*. **2008**, 627, 277-284.

(18) Zhao, L. X; Lin, J.-M. *J. Biotechnol*. **2005**, 118, 177-186.

(19) Wang, D; Zhou, J.-Q; Zhao, M.-P. *Talanta*, **2010**, 82, 432-436.

(20) Liu, H; Li, X; Crook, R. M. *Anal. Chem*. **2013**, 85, 4263–4267.

(21) Choi, J.-W; Ahn, C. H; Bhansali, S; Henderson, H. T. *Sens. Actuator, B*. **2000**, 68, 34-39.

(22) Sato, K; Tokeshi, M; Odake, T; Kimura, H; Ooi, T; Nakao, M; Kitamori, T. *Anal.Chem*. **2000**, 72, 1144-1147.

(23) Kai, J; Puntambekar, A; Santiago, N; Lee, S. H; Sehy, D. W; Moore, V; Han. J; Ahn, C. H. *Lab Chip*, **2012**, 12, 4257-4262

(24) Siuti, P; Retterer, S. T; Choi, C.-K; Doktycz, M. J. *Anal.Chem*. **2012**, 84,

1092-1097.

(25) Lin C. C; Kuo C. W; Pao L. H. *Anal. Bioanal. Chem*., **2010**, 398, 885.

(26) Abe, K; Suzuki, K; Citterio, D. *Anal.Chem*. **2008**, 80, 6928-6934.

(27) Zeng, H. L; Weng, Y; Ikeda, S; Nakagawa, Y; Nakajima, H; Uchiyama, K. *Anal. Chem*. **2012**, 84, 10537-10542.

(28) Chen, F. M; Zhang, Y. D; Nakagawa, Y; Zeng, H. L; Luo. C; Nakajima, H; Uchiyama, K; Lin, J-.M. *Talanta*, **2013**, 107, 111-117.

(29) Luo, C; Ma, Y; Li, H. F; Chen, F. M; Uchiyama, K; Lin, J.-M. *J. Mass Spectrom*. **2013**, 48, 321-328.

(30) Chen, F. M; Lin, Z; Zheng, Y. Z; Zeng, H. L; Nakajima, H; Uchiyama, K; Lin. J.-M. *Anal. Chim. Acta*. **2012**, 739, 77-82.

(31) Liang, J; Wang, Y; Liu, B. *RSC Adv*. **2012**, 2, 3878-3884.

(32) Zhou, Y; Zhang, Y. H; Lau, C. W; Lu, J. Z. *Anal. Chem*. **2006**, 78, 5920-5924.

Chapter 6

Conclusion

In this thesis, we developed a new inkjet system and then applied it on immumoassay and capillary injetction. The main results were showed as follow:

In chapter 1, I designed a new home-made driving circuit for piezoelectric actuator, which combined with home-made software to changes its output frequency, driving voltage and pulse width. A drop-on-demand (DOD) picoliter droplet was generated in precision-controllable manner by use of the driving system.

In chapter 2, We propose a piezoelectric droplet generator for injection of well-defined amounts of sample in capillary electrophoresis. We demonstrate stable, precise and drop-on-demand droplet formation for various solutions, with precise control of waveform driving piezoelectric crystal inside the ink-jet head. By tuning the waveform, we can also manipulate the droplet size and delivery frequency. This injector was used in sampling for capillary electrophoresis. As a state-of-the-art application, the analysis of the obromine, caffeine and the ophiline using micellar electro kinetic Chromatography was developed. The volume of sample (single droplet) analyzed in this experiment was 179 pL (RSD%, n=10). The detection limits for caffeine, theobromine, and the ophiline are 0.02, 0.08 and 0.06mM/L, respectively. Compared with conventional methods, the combination of picoliter droplet dispenser with capillary electrophoresis allows precise and accurate sampling, as well as for reduced sample consumption, which will prove to be an efficient to oline quantitative separation and analysis.

In chapter 3, An automatic multi-channel ink-jet for chemiluminescence (CL) analysis was developed. The four-channel ink-jet device was controlled by a home-made circuit. Differing from the classic flow injection CL, the whole procedure for CL analysis was automatically completed on a hydrophobic glass side. CL reaction of luminal and hydrogen peroxide for the determination of horseradish peroxidase (HRP) was selected as an application to automatic CL analysis platform. All solutions delivered by different channels were precisely ejected to the same

position of the glass slide for the CL analysis. The consumption of reaction solution was reduced to nanoliter level. The whole CL analysis could be completed in less than 4 min, which was benefited from the prompt solution mixing in small size of droplet. The CL intensity increased linearly with HRP concentration in the range from 0.01 to 0.5μg/mL. The limit of detection (LOD) (S/N = 3) was 0.005 g mL−1. Finally, the automatic CL system could also be used for the detection of HRP in HRP–protein conjugates, which showed its practical application in immunoassay.

In chapter 4, We report a novel chemiluminescence diagnosis system for high-throughput human IgA detection by inkjet nano-injection on a multicapillary glass plate. To proof-of-concept, microhole-based Polydimethylsiloxane (PDMS) sheets were aligned on a multicapillary glass plate to form a microwell array as microreactors for enzyme-linked immunosorbent assay (ELISA). The multicapillary glass plate was utilized as a switch that controlled the holding/passing of the solution. Further, anti-IgA-labeled polystyrene (PS) microbeads was assembled into the microwell array, and an inkjet nano-injection was specially used to distribute the sample and reagent solution for chemiluminescence ELISA, enabling to high-throughput detection of human IgA. As a result, the performance of human IgA tests revealed a wider range for the calibration curve and a lower limit of detection (LOD) of 0.1 ng mL^{-1} than the ELISA by a standard 96-well plate. The analysis time and reagent consumption were significantly decreased to a great extent. The IgA concentration in saliva samples were determined between 181.4 to 213.1 ng mL^{-1} (after 1000-fold dilution) by the developed ELISA system. Thus, we believe that the inkjet nano-injection for high-throughput chemiluminescence immunoassay on multicapillary glass plate will be promising in disease diagnosis.

Throughout this thesis, I have successfully developed a precise drop-on-demand inkjet sample dispensing system and its applications to analytical chemistry.

List of Publication

(1) Fengming Chen, Zhen Lin, Yongzan Zheng, Hulie Zeng, Hizuru Nakajima, Katsumi Uchiyama, Jin-Ming Lin, Development of an automatic multi-channel ink-jet ejection chemiluminescence system and its application to the determination of horseradish peroxidase, Analytica Chimica Acta, 2012, 739, 77-82. (SCI)

(2) Fengming Chen, Yandong Zhang, Yuri Nakagawa, Chen Luo, Hulie Zeng, Katsumi Uchiyama, Jin-Ming Lin, A piezoelectric drop-on-demand generator for accurate samples in capillary electrophoresis, Talanta, 2013, 107, 111-117. (SCI)

(3) Fengming Chen**,** Sifeng Mao, Hulie Zeng, Shuhua Xue, Jianmin Yang, Hizuru Nakajima, and Jin-Ming Lin, Katsumi Uchiyama, Inkjet Nano-injection for high-thoughput Chemiluminescence Immunoassay on Multicapillary Glass Plate, Analytical Chemistry, 2013, 85, 7413−7418. (SCI)

(4) Chen Luo, Yuan Ma, Haifang Li, Fengming Chen, Katsumi Uchiyama and Jin-Ming Lin, Generation of picoliter droplets of liquid for electrospray ionization with piezoelectric inkjet, Journal of Mass Spectrometry, 2013, 48, 321-328. (SCI)

(5) Ying Wang, Hulie Zeng, Yuri Nakagawa, Saori, Ikeda, Fengming Chen, Hizuru Nakajima, Separation and determination of dopamine and epinephrine in serum by capillary electrophoresis with inkjet introduction system, Chromatography, 2013, 34, 33-40.

Acknowledgment

First and foremost, this thesis has been accomplished under the direction of Professor Katsumi Uchiyama, I would like to extend my sincerest gratitude to whose instructive advice and guidance throughout my thesis has been invaluable. At the same time, I would like to express my gratitude to all those who helped me during the writing of this thesis. High tribute shall be paid to Dr. Hulie Zeng, whose profound knowledge of English triggers my love for this beautiful language and whose earnest attitude tells me how to write this thesis and learn English. I am also express thanks to deeply indebted to Professor Yang Ming, Associate Professor Nakajima sensei and Kato sensei for serving as a second reader to review my doctor thesis.

I am also would like to express my heartfelt gratitude to Tsinghua University Professor Jin-ming Lin laboratory, who have instructed and helped me a lot in the past six years. I also owe my sincere gratitude to Professor Lin laboratory other students (Zhen Lin, Qiushui Chen, Yandong Zhang, Fei Chen and Sifeng Mao) in experiment and revised research paper for their direct and indirect help to me.

The author also would like to express thanks to Shu-hua Xue, Jian-ming Yang, Ying Wang, Ying Rang, Yuri Nakagawa, Kazuhiro Morioka, Saori Ikeda, Akihito Konenaga and so on, whose gave me their help and time in listening to me and helping me work out my problems during the difficult experiment of the thesis. Their support and willingness to help will always be appreciated.

Third, I must thank very much to the scholarship supplied for the author from the High-Tech Research Program by Tokyo metropolitan government for their generous funding, which removed financial concern from my decision to embark on this journey. Some faculty members in international center have been very kind enough to extend their help on my daily life to promise I can complete my research smoothly and all of my Japanese friends for their kindly helps during I studied in japan are gratefully acknowledged.

Fengming Chen

Department of Applied Chemistry,

Graduate School of Urban Environmental Sciences,

Tokyo Metropolitan University

Hachioji, Tokyo 192-0397, Japan